ELEMENTA
Science of the Anthropocene

Tarasick, D, et al. 2019. Tropospheric Ozone Assessment Report: Tropospheric ozone from 1877 to 2016, observed levels, trends and uncertainties. *Elem Sci Anth,* 7: 39. DOI: https://doi.org/10.1525/elementa.376

REVIEW

Tropospheric Ozone Assessment Report: Tropospheric ozone from 1877 to 2016, observed levels, trends and uncertainties

David Tarasick[*], Ian E. Galbally[†,‡], Owen R. Cooper[§,‖], Martin G. Schultz[¶], Gerard Ancellet[**], Thierry Leblanc[††], Timothy J. Wallington[‡‡], Jerry Ziemke[§§], Xiong Liu[‖‖], Martin Steinbacher[¶¶], Johannes Staehelin[***], Corinne Vigouroux[†††], James W. Hannigan[‡‡‡], Omaira García[§§§], Gilles Foret[‖‖‖], Prodromos Zanis[¶¶¶], Elizabeth Weatherhead[§,‖], Irina Petropavlovskikh[§,‖], Helen Worden[‡‡‡], Mohammed Osman[****,††††,‡‡‡‡], Jane Liu[§§§§,‖‖‖‖], Kai-Lan Chang[§,‖], Audrey Gaudel[§,‖], Meiyun Lin[¶¶¶¶,*****], Maria Granados-Muñoz[†††††], Anne M. Thompson[§§], Samuel J. Oltmans[‡‡‡‡‡], Juan Cuesta[‖‖‖], Gaelle Dufour[‖‖‖], Valerie Thouret[§§§§§], Birgit Hassler[‖‖‖‖‖], Thomas Trickl[¶¶¶¶¶] and Jessica L. Neu[******]

From the earliest observations of ozone in the lower atmosphere in the 19th century, both measurement methods and the portion of the globe observed have evolved and changed. These methods have different uncertainties and biases, and the data records differ with respect to coverage (space and time), information content, and representativeness. In this study, various ozone measurement methods and ozone datasets are reviewed and selected for inclusion in the historical record of background ozone levels, based on relationship of the measurement technique to the modern UV absorption standard, absence of interfering pollutants, representativeness of the well-mixed boundary layer and expert judgement of their credibility. There are significant uncertainties with the 19th and early 20th-century measurements related to interference of other gases. Spectroscopic methods applied before 1960 have likely underestimated ozone by as much as 11% at the surface and by about 24% in the free troposphere, due to the use of differing ozone absorption coefficients.

There is no unambiguous evidence in the measurement record back to 1896 that typical mid-latitude background surface ozone values were below about 20 nmol mol^{-1}, but there is robust evidence for increases in the temperate and polar regions of the northern hemisphere of 30–70%, with large uncertainty, between the period of historic observations, 1896–1975, and the modern period (1990–2014). Independent historical observations from balloons and aircraft indicate similar changes in the free troposphere. Changes in the southern hemisphere are much less. Regional representativeness of the available observations remains a potential source of large errors, which are difficult to quantify.

The great majority of validation and intercomparison studies of free tropospheric ozone measurement methods use ECC ozonesondes as reference. Compared to UV-absorption measurements they show a modest (~1–5% ±5%) high bias in the troposphere, but no evidence of a change with time. Umkehr, lidar, and FTIR methods all show modest low biases relative to ECCs, and so, using ECC sondes as a transfer standard, all appear to agree to within one standard deviation with the modern UV-absorption standard. Other sonde types show an increase of 5–20% in sensitivity to tropospheric ozone from 1970–1995.

Biases and standard deviations of satellite retrieval comparisons are often 2–3 times larger than those of other free tropospheric measurements. The lack of information on temporal changes of bias for satellite measurements of tropospheric ozone is an area of concern for long-term trend studies.

Keywords: Ozone; Troposphere; Measurements; Trends; Historical; Climate

1. Introduction

Tropospheric ozone is a greenhouse gas and pollutant detrimental to human health and plant growth (Monks et al., 2015; WMO Reactive Gases Bulletin, 2018). Large changes after 1990 in the global distribution of the anthropogenic emissions that produce ozone have been reported, including reductions in North America and Europe and increases in Asia (Richter et al., 2005; Granier et al., 2011; Russell et al., 2012; Hilboll et al., 2013; Cooper et al., 2014; Zhang et al., 2016). This rapid shift, coupled with limited ozone monitoring in developing nations, has left scientists unable to answer the most basic questions: Which regions of the world have the greatest human and plant exposure to ozone pollution? How is ozone changing in nations with strong emission controls? To what extent is ozone increasing in the developing world? How can the atmospheric sciences community facilitate access to the ozone metrics necessary for quantifying ozone's impact on climate, human health and crop/ecosystem productivity?

To answer these questions, the International Global Atmospheric Chemistry Project (IGAC) developed the *Tropospheric Ozone Assessment Report (TOAR): Global metrics for climate change, human health and crop/ecosystem research* (www.igacproject.org/activities/TOAR). Initiated in 2014, TOAR's mission is to provide the research community with an up-to-date scientific assessment of tropospheric ozone's global distribution and trends from the surface to the tropopause. TOAR's primary goals are, 1) Produce the first tropospheric ozone assessment report based on the peer-reviewed literature and new analyses, and 2) Generate easily accessible, documented data on ozone exposure metrics at thousands of measurement sites around the world (Lefohn et al., 2018). Through the TOAR surface ozone database (Schultz et al., 2017; hereinafter *TOAR-Surface Ozone Database*) these ozone metrics are freely accessible for research on the global-scale impact of ozone on climate (Gaudel et al., 2018), human health (Fleming et al., 2018) and ecosystem productivity (Mills et al. 2018).

The assessment report is organized as a series of papers in a special feature of *Elementa – Science of the Anthropocene* (https://collections.elementascience.org/toar), with this paper comprising the *Tropospheric Ozone Assessment Report: Tropospheric ozone from 1877 to 2016, observed levels, trends and uncertainties*, subsequently abbreviated as *TOAR-Observations*. This paper describes the different tropospheric ozone measurement techniques used since the late 19th century to the present, and characterizes the uncertainty in the measurements and the spatial and temporal information obtained from each instrument type.

Knowledge of the uncertainties associated with tropospheric ozone measurements is important to reconciling measurements from different methods and platforms and for accurate and realistic model evaluation. It is also essential for the evaluation of trends. Historical ozone observations, those made before the widespread deployment of UV-based ozone instruments, are important to climate models. The global average radiative forcing of ozone (0.4 ± 0.2 W m^{-2}; IPCC, 2013) is approximately 1/5 of the

* Environment and Climate Change Canada, Downsview, ON, CA

† Climate Science Centre, CSIRO Oceans and Atmosphere, Aspendale, VIC, AU

‡ Centre for Atmospheric Chemistry, University of Wollongong, Wollongong, NSW, AU

§ Cooperative Institute for Research in Environmental Sciences, University of Colorado, Boulder, US

‖ NOAA Earth System Research Laboratory, Boulder, Colorado, US

¶ Jülich Supercomputing Centre, Forschungszentrum Jülich, Jülich, DE

** LATMOS/IPSL, UPMC Univ. Paris 06 Sorbonne Universités, UVSQ, CNRS, Paris, FR

†† Jet Propulsion Laboratory, California Institute of Technology, Table Mountain Facility, Wrightwood, CA, US

‡‡ Research and Advanced Engineering, Ford Motor Company, Dearborn, Michigan, US

§§ NASA Goddard Space Flight Center, Greenbelt, Maryland, US

‖‖ Harvard-Smithsonian Center for Astrophysics, Cambridge, Massachusetts, US

¶¶ Empa, Swiss Federal Laboratories for Materials Science and Technology, Duebendorf, CH

*** Department of Environmental Systems Science, Zürich, CH

††† Royal Belgian Institute for Space Aeronomy (BIRA-IASB), Brussels, BE

‡‡‡ National Center for Atmospheric Research, Boulder, CO, US

§§§ Agencia Estatal de Meteorología, Izana Atmospheric Research Centre, Santa Cruz de Tenerife, ES

‖‖‖ Laboratoire Inter-universitaire des Systèmes Atmosphériques (LISA), UMR7583, Universités Paris-Est Créteil et Paris, Diderot, CNRS, Créteil, FR

¶¶¶ Department of Meteorology and Climatology, School of Geology, Aristotle University of Thessaloniki, Thessaloniki, GR

**** Cooperative Institute for Mesoscale Meteorological Studies, The University of Oklahoma, US

†††† NOAA/National Severe Storms Laboratory, Norman, OK, US

‡‡‡‡ Enable Midstream Partners, Headquarters, Oklahoma City, US

§§§§ Department of Geography and Planning, University of Toronto, CA

‖‖‖‖ School of Atmospheric Sciences, Nanjing University, Nanjing, CN

¶¶¶¶ Atmospheric and Oceanic Sciences, Princeton University, US

***** NOAA Geophysical Fluid Dynamics Lab, Princeton, New Jersey, US

††††† Remote Sensing Laboratory (RSLAB), Department of Signal Theory and Communications, Universitat Politècnica de Catalunya (UPC), Barcelona, ES

‡‡‡‡‡ Global Monitoring Division, Earth System Research Laboratory, National Oceanic and Atmospheric Administration, Boulder, Colorado, US

§§§§§ Laboratoire d'aérologie, CNRS UMR 5560, Observatoire Midi-Pyrénée, Université de Toulouse III, Toulouse, FR

‖‖‖‖‖ Institute of Atmospheric Physics, Earth System Modelling, Oberpfaffenhofen-Wessling, DE

¶¶¶¶¶ Karlsruher Institut für Technologie, Garmisch-Partenkirchen, DE

****** Jet Propulsion Laboratory, California Institute of Technology, Pasadena, California, US

Corresponding authors: David Tarasick (david.tarasick@canada.ca); Ian E. Galbally (ian.galbally@csiro.au)

radiative forcing due to CO_2, and slightly less than the radiative forcing due to methane (NOAA, 2018). This estimate has large uncertainty due to limited knowledge of pre-industrial concentrations of tropospheric ozone and its present-day spatial distribution (*IPCC*, 2013). Additional uncertainty arises from the detrimental impact of ozone on plant productivity, which due to feedbacks on CO_2 uptake, produces an indirect forcing (*Sitch et al.*, 2007). Past efforts to evaluate 19th century ozone measurements have concluded that ozone in pre-industrial times was as low as 1/5 of its present concentration (e.g. Marenco et al., 1994; Volz and Kley 1988; Bojkov, 1986; Staehelin et al., 1994), based primarily on observations at Montsouris, Paris, France in the late 19th century. However, the validity of the early Montsouris measurements as representative of the regional atmosphere has been challenged (Calvert et al., 2015; Staehelin et al., 2017), and global atmospheric chemistry models have difficulty reproducing such a large historical increase from pre-industrial times (e.g. Wang and Jacob, 1998; Mickley et al., 2001; Lamarque et al., 2005; Young et al., 2013; Parrish et al., 2014; Young et al., 2018). It is therefore important to quantify uncertainties for these older measurement methods, to establish confidence limits for reproducibility and bias, and to answer the question: how well do we know historic levels of tropospheric ozone?

Section 2 of this paper describes the many methods that have been used to measure tropospheric ozone. Section 3 is an in-depth re-evaluation of the record of ozone in surface air away from cities and other interferences. Section 4 addresses the measurement of ozone in the free troposphere, beginning with the relatively few historical measurements. Section 5 discusses several aspects of representativeness, and uncertainties associated with sampling of ozone in the troposphere. The paper concludes with a discussion of knowledge gaps and recommendations for future measurements.

2. Standards for the measurement of ozone in the atmosphere

Ozone is a highly reactive gas, with strong absorption bands in the IR and the UV. Three broad sets of techniques based on chemical reaction, UV absorption and IR absorption and emission have been used to measure ozone in the atmosphere. The methods derived from these techniques and their first use to measure ozone in the atmosphere are presented in **Table 1**. These methods have different measurement uncertainties and the results obtained from paired measurements using either the same or different techniques may differ from each other both systematically and randomly.

As a reactive gas ozone cannot currently be kept in containers nor does it persist in snow without ongoing loss. Hence no current measurements of past concentrations are possible (although they may be inferred from isotopic measurements of oxygen trapped in ice (Yeung et al., 2019)). It is also not possible to transport a sample of gas containing a known concentration of ozone from one location to another without ozone loss occurring within the container. Therefore, some other form of standard for ozone calibration to ensure world-wide traceability of measurement results is required. The current standard for tropospheric ozone measurement is based on its ultraviolet absorption cross-section at 253.65 nm of 1.148×10^{23} cm^2 molecule^{-1}. This standard originates from Hearn (1961), and has been adopted by the International Ozone Commission in 1984, the International Standards Organisation (ISO, 2017), the World Meteorological Organisation in its Guidelines for Continuous Measurement of Ozone in the Troposphere (Galbally et al. 2013) and is used by the International Bureau of Weights and Measures (BIPM) for ozone calibrations (BIPM, 2019). To propagate this standard for surface ozone and aircraft ozone measurements, specially designed ozone photometers incorporating an ozone generator, and utilizing the measurement of the absorption of UV radiation of 253.65 nm wavelength within short cells (1 m or less in length) by sample air containing ozone, have been used as ozone transfer standards (ISO, 2017; Paur et al., 2003; Viallon et al., 2006a). By referencing ambient measurements to these standards, well-understood and traceable observations of tropospheric ozone are made (Galbally et al., 2013; Tanimoto et al., 2007; Viallon, 2006a, b).

The numerical value of the ozone absorption cross-section is currently under review (Hodges et al., 2019; Orphal et al. 2016), with a recommendation that the value should be decreased by approximately 1.23% (Hodges et al., 2019). If accepted by the appropriate agencies (BIPM, WMO, ISO), this change will require all tropospheric ozone measurements on the current UV standard scale to be increased by 1.23%. This will not affect trends, but it will have a small effect on estimates that depend on the absolute ozone amount, such as calculations of ozone radiative forcing. This change will also improve agreement of the UV scale with gas phase titration (GPT) and the potassium iodide (KI) ECC ozonesondes.

A second ozone standard is gas phase titration of ozone against nitric oxide gas standards. Differences between GPT and standard UV photometry have been investigated by Tanimoto et al. (2006) and Viallon et al. (2006b, 2016) and found to be very small (~0.3%) when the newer values of the ozone absorption cross-sections (see Section 2.2.1) are used (Viallon et al. 2016). Thus GPT supports the proposed decrease in the ozone absorption cross-section at 253.65 nm. Because GPT is utilized as a standard and has not been used for ambient ozone measurements in either the historical record or the TOAR database, it is not listed in **Table 1**. Further information on GPT is included in the Supplemental Material (Text S-1).

These standards are propagated, via international co-ordination of the adoption of ozone absorption coefficients for UV and visible light (Orphal et al., 2016), to the communities using remote sensing methods for ozone measurement in the free troposphere. There is a recommendation to extend this co-ordination to infrared methods (Orphal et al., 2016).

The available record of surface ozone measurements divides into two periods: the modern period covers approximately 1975 to the present and is defined by the widespread availability of sensitive UV photometers for

Table 1: The introduction of various techniques for measurement of ozone in the troposphere. (KI = Potassium Iodide).
DOI: https://doi.org/10.1525/elementa.376.t1

Date	Method	Reference
1845	KI-Starch papers	Schönbein (1845)
1876	KI manual volumetric	Albert-Lévy (1877)
1929	UV – Umkehr Inverse method	Götz et al. (1934)
1931	Long path UV	Götz and Ladenberg (1931), Fabry and Buisson (1931)
1934	Balloon borne UV	Regener and Regener (1934)
1938	Cryotrapping and subsequent analysis	Edgar and Paneth (1941a)
1941	Automatic KI	Paneth and Glückauf et al. (1941)
1943	Aircraft KI observations	Ehmert (1949)
1955	UV ozonesondes	Paetzold (1955)
1956	IR tropospheric ozone	Walshaw and Goody (1956)
1958	KI ozonesondes	Brewer and Milford (1960)
1960	Chemiluminescent ozonesondes	Regener (1960)
1970	Chemiluminescent surface ozone analysers	Warren and Babcock (1970), Fontijn et al. (1970)
1972	UV surface ozone analysers	Bowman and Horak (1972)
1980	Tropospheric ozone lidar	Pelon and Megie (1982)
1990	Satellite tropospheric ozone residual	Fishman et al. (1990)
1996	DOAS	Stutz and Platt (1996)
1997	Satellite UV/VIS backscatter	Chance et al. (1997); Liu et al. (2005)
1998	Satellite Convective Cloud Differential	Ziemke et al. (1998)
2001	Satellite IR atmospheric emission	Beer et al. (2001); Worden et al. (2007a)
2007	Satellite Multispectral	Worden et al. (2007b); Landgraf and Hasekamp (2007)

surface ozone measurements; the historical period covers 1877–1975 and is defined by the use of other techniques and the absence of these UV photometers. There are a few years of overlap between the periods during the uptake of the modern technology.

A set of four criteria were developed and applied to select data for the historical reconstruction: (1) the measurement methods used should be related, through intercomparisions, to the current standard UV absorption photometer method; (2) the likelihood for significant contamination of the ozone measurements due to interfering pollutants in the sampled atmosphere should be low; (3) for surface ozone, the air sampled should be representative of the well-mixed boundary layer, and (4) recognizing the uncertainties associated with all of the historical data sets, the measurements should be free from major artifacts or inconsistencies. The datasets that pass these four criteria are explicitly documented.

To commence the reconstruction of a historical tropospheric ozone record, the first of the four criteria must be addressed for each of the ozone data sets examined. As many historical measurement methods pre-date the current UV method, traceability may be derived through published side-by-side intercomparisons with an intermediate method.

The surface ozone method/instrument intercomparisons found in the literature are presented in **Table 2**. The ratio of each pair of methods corresponds to either the ratio of the mean values from each method or the slope of a regression whose intercept is assumed to be zero. Often only this number is recorded. In some cases an uncertainty is cited. Where not explicitly stated, we have assumed that this corresponds to one standard deviation. **Table 2** is divided into 5 sections, the first four sections commencing with the comparison of a method with the UV method and then proceeding to other comparisons of that or closely related methods. The methods separated are Levy, Ehmert, Electrochemical Concentration Cell (ECC), and Colorimetric. The fifth section is for other relevant method comparisons not included in the first four sections. Two conclusions can be drawn from **Table 2**: (a) in the absence of other information, the relative bias of a historical set of ozone observations with the current UV standard lies in the range 0.7 to 1.2 at approximately 90% confidence limit; and (b) the uncertainty in the bias from one to another study of apparently identical instruments can be as large as 50%. Consequently, except in special

Table 2: Comparisons of (a) various surface ozone measurement methods against in-situ UV ozone measurements and other key methods and (b) ozonesonde responses in the lower troposphere. Comparisons were undertaken either sampling ambient air, (A), or via laboratory studies, (L). NBKI = neutral-buffered potassium iodide solution. Where required, older measured ratios have been adjusted to reflect the current standard UV absorption cross-sections (Hearn, 1961). DOI: https://doi.org/10.1525/elementa.376.t2

Method Comparison	Ratio	Uncertainty	Reference
KI-arsenite/UV (A)	0.78	n/a	Dauvillier (1935)
KI-arsenite/UV (L)	1	±0.02	Volz and Kley (1988)
Ehmert/UV (A)	0.98	±0.09	Galbally (1979)
Ehmert/UV (A)	0.947	±0.009	Grasso (2011)
KI/UV (A)	0.93	±0.04	Vassy (1958)
ECC/Ehmert (A)	1.02	±0.12	WMO (1972), Galbally (1979)
MPI-Pruch/Ehmert (A)	1	±0.05	Pruchniewicz (1973)
NBKI Colorimetric/Ehmert (L)	1.1	n/a	Renzetti (1959)
NBKI colorimetric/Ehmert (A)	1.22	±0.15	Galbally (1979)
Mast Brewer ozonesonde/Ehmert (A)	0.88	±0.10	Galbally (1979)
Cauer/Ehmert (A)	0.66	n/a	Warmbt (1964)
Cauer/Ehmert (corrected) (A)	0.9	n/a	Warmbt (1964)
Cryotrapping O_3/KI-thiosulfate	1	±0.05	Edgar and Paneth (1941a)
ECC/UV (A)	1.1	±0.14	Attmannspacher and Hartmannsgruber (1982)
ECC/UV (A)	1.01	±0.05	This study, Section 4.3
ECC/UV (A)	1.05	±0.04	IAGOS, this study, Section 4.8
HP-KI/UV (A)	0.94	±0.16	Attmannspacher and Hartmannsgruber (1982)
MPI-Pruch/HP-KI (A)	0.5	±0.04	This study, Section 2.1.3
NBKI colorimetric/UV (L)	0.97	n/a	Cherniack and Bryan (1965)
NBKI colorimetric/UV (A)	1.02	n/a	Cherniack and Bryan (1965)
1% NBKI/UV (L)	1.09	±0.02	Schnadt Poberaj et al (2007)
2% NBKI colorimetric/UV (L and A)	1.23	±0.06	Pitts et al. (1976a, b)
2% unbuffered KI titration/UV (L and A)	0.9	n/a	Pitts et al. (1976b)
Pressure/Volume/UV (L)	1.03	n/a	Watanabe and Stephens (1979)
Regener chemiluminescent/UV (L)	1	n/a	Regener (1964)
Ethylene-Chemiluminescent/UV (A)	0.94	±0.16	Attmannspacher and Hartmannsgruber (1982)
Ozonograph-KI/UV (A)	1.09	±0.20	Attmannspacher and Hartmannsgruber (1982)
Mast Ozone Meter/Pressure/Volume (L)	1.04	n/a	Watanabe and Stephens (1979)
Mast Ozone Meter/NBKI colorimetric (L and A)	0.86	n/a	Cherniack and Bryan (1965)
Mast Ozone Meter/NBKI colorimetric (L)	0.71	n/a	Gudiksen et al. (1966)
Regener chemiluminescent/Mast Ozone Meter (A)	1.2–1.8	n/a	Oltmans and Komhyr (1976)

cases of traceability, each past set of observations should be seen as having a substantial unknown bias and the historical record at a particular location will not necessarily sensibly relate to current measurements at the same location. Due to such inconsistenices between historical and modern ozone observations, *TOAR-Observations* estimates historical ozone levels on regional or zonal scales using all available data sets. The rationale for this new approach relies on the concept that the normalised biases of multiple sets of observations, if random, will tend to cancel out when averaged across multiple stations. A formal description of this approach is given in the Supplemental Material (Text S-2). The average of multiple sets of these past observations for multiple years and a particular geographic region is more appropriate for comparison with current observations. Therefore, we recommend that the

evaluation of models be based on the regional or zonal means of multiple sets of observations rather than individual time series. For the discussion of individual historical time series uncertainties the reader is referred to the Supplemental Material (Text S-3).

Observations cited in this paper are quoted as reported, for ease of comparison with previous work, but expressed in their equivalent SI units. Concentrations are then converted to mole fractions (Text S-4) for purposes of comparison.

Each of the techniques used in ozone data sets either selected or rejected in this study will be discussed in turn.

2.1. Potassium Iodide measurement techniques

While ozone was originally identified and investigated by its odour (Schönbein, 1840; Rubin, 2001), the first quantitative measurements were based on the reaction of ozone with potassium iodide:

$$O_3 + 2KI + H_2O \rightarrow O_2 + I_2 + 2KOH \quad (1)$$

The basis of this measurement is the assumption that for each ozone molecule reacted, a molecule of iodine is produced; this ratio is the stoichiometry of the reaction. The amount of iodine produced is (in most methods) measured, and this in mole units, equals the amount of ozone in the air volume sampled. A number of techniques based on the KI reaction have been developed during the last two centuries, and the ozone-KI reaction is still in use in balloon borne ozonesondes (**Table 1**).

The stoichiometry of the reaction is crucial, and has been studied extensively. Many studies, however, were made at ozone concentrations much higher than those in the troposphere, because of the difficulty of working with low concentrations of ozone at the time (Saltzman and Gilbert 1959a; Boyd et al., 1970; Hodgeson et al., 1971; Kopczynski and Bufalini, 1971; Dietz et al., 1973). Byers and Saltzman (1959) found using GPT a reaction stoichiometry of 1.00 (with unquantified uncertainty) at pH 7, and that the reaction stoichiometry varied with pH, being lower by 50% at pH 14. This implies that the chemistry of the KI reaction with ozone is complex, involving reactions other than (1) that produce additional iodine, as well as reactions that cause loss of iodine (Byers and Saltzman, 1959; Staehelin and Hoigné, 1985).

Without buffering, the reaction will drive the solution alkaline, so the KI solution is in most methods buffered (NBKI, for neutral-buffered KI). Dietz et al. (1973) found a NBKI/UV ratio of 1.00 ± 0.03 at pH 7 for two measurements at 100 and 400 nmol mol^{-1}. Pitts et al. (1976a) found that the 2% NBKI method gave NBKI/IR = NBKI/UV = 1.23 ± 0.06 at 50% relative humidity for 0.1 to 1 ppm ozone and NBKI/IR = NBKI/UV = 1.14 ± 0.04 at 3% relative humidity. They had no explanation of the apparent water vapour dependence. However, it was reduced when potassium bromide was added (Lanting, 1979; Bergshoeff et al., 1980), as is the case in ozonesondes. Slow side reactions involving the phosphate buffer may also change the stoichiometry from 1.0 (Saltzman and Gilbert, 1959a; Flamm, 1977; Johnson et al., 2002).

Other compounds present in air can interfere with the KI-ozone reaction. NO_2 and H_2O_2 give positive interferences (Volz and Kley, 1988), NO_2 at a level of 5–10% (Pitts et al., 1976), although this appears to be quite variable (Cherniak and Bryan, 1965; Tarasick et al., 2000). SO_2 causes a negative interference of 1:1, i.e. a quantitative reduction in the ozone detected (Pitts et al., 1976; Schenkel and Broder, 1982; Volz and Kley, 1988). NH_3 is also a negative interferent (Anfossi et al., 1991), which increases the pH of the solution as well as reacting directly with iodine although the stoichiometry is not quantified (Downs and Adams, 1973).

Losses can occur in the inlet to the sampler, but even early experimenters appear to have been aware of this, and strove to avoid it. Inlet tubes (where described) were usually of glass (e.g. Dauvillier, 1934; Glückauf et al., 1944) and the type of glass was found to be important (Carbenay and Vassy, 1953). Other materials such as polyvinyl chloride became available later (e.g. Vassy, 1958), and may have caused negative biases in some cases (Altshuller et al., 1961; Potter and Duckworth, 1965) before Teflon was introduced (Gudiksen et al., 1966). In one case a cotton wool filter was used in the inlet (Edgar and Paneth, 1941b). No information is available with which to estimate inlet losses, but they could have negatively biased some of the KI measurements.

Loss due to evaporation of the iodine produced can also occur (Brewer and Milford 1960; Kley et al., 1988). There are a number of methods based on the KI reaction (**Table 1**), and while all are similarly subject to interfering gases, they differ in terms of potential for iodine and/or ozone loss, and side reactions. In the Cauer method, the evaporation of the iodine is part of the analytical technique (Warmbt, 1964). The efficiency of the sampler needs to be considered for each case.

The contributions of each of these interfering or modifying factors cannot always be separately quantified. The best available summary of how a technique performs is obtained from comparisons in unpolluted ambient air with the UV method or with a method traceable to the UV method, as presented in **Table 2**.

2.1.1. Schönbein papers

The Schönbein paper method uses a KI and starch impregnated paper. Ozone diffusing to the paper surface reacts with the iodide, and the iodine produced forms a strongly blue-colored complex with the starch. Alternately, a pH indicator is present and the colour change is due to the alkalinity resulting from reaction (1), see Hartley (1881). Following exposure, the paper strips can be compared to a standard color scale to give a semi-quantitative ozone measurement (Fox, 1873). There are several variations on this technique, named after their inventors/developers: Schönbein, Sallon, de James, Therry and Houzeau. These methods are described in limited detail (Houzeau, 1857; Fox 1873; Hartley 1881; Linvill et al. 1980; Bokjov 1980; Kley et al. 1988; Anfossi et al. 1991).

Interest in ozone was very high in the late 19th Century, in part because of its role as an "air purifier" and the erroneous belief that it could eliminate pathogens, particularly

cholera (Fox, 1873). Measurements were therefore made with Schönbein or related papers at hundreds of sites in Europe, the Americas, Australia, Asia, Africa, and Antarctica (Smyth, 1858; Fox, 1873; Royal Society, 1908; Bojkov, 1986; Galbally and Paltridge, 1989; Sandroni et al., 1992; Sandroni and Anfossi, 1994; Pavelin et al., 1999; Nolle et al., 2005).

There are two laboratory test chamber studies of the color development response to time and ozone concentration, that either directly or indirectly relate the filter paper method to the current UV-absorption standard. Linvill et al., (1980) found a filter paper response relationship to ozone exposure where color development was very strongly dependent on the relative humidity (RH) present in the chamber. A change from 3 to 4 (of 10) color units corresponds to a 10 nmol mol^{-1} ozone change at 80% RH and a 30 nmol mol^{-1} ozone change at 60% RH. Kley et al. (1988) found the papers gave, on exposure to a constant ozone level, an initial linear color increase continuing for 3 hours or more, followed by a plateau and then a color decrease. Further exposure to ozone increased this color loss. Because of this complex behaviour, there is a region between 6 and 10 hours exposure where ozone values between 10 and 50 nmol mol^{-1} correspond to less than 1 unit difference on the Schönbein scale. For longer exposures the responses overlap and reverse order, i.e. longer exposures at high concentrations for selected conditions give lower color responses than some shorter exposures at lower concentrations. Consequently, it is impossible to uniquely relate a color development on these filter papers to an ozone concentration on the UV scale.

The filter paper method of measuring ozone concentrations is a passive measurement method that lacks a controlled diffusion barrier, the absence of which creates a wind speed dependence. There does not appear to be any information on the repeatability and reproducibility of these techniques in the field. It appears that the colour development (the signal) is dependent on ozone concentration, time of exposure, relative humidity, wind speed and light. The colour development has negative responses to ammonia and sulphur dioxide (Fox 1873; Linvill et al. 1980; Bokjov 1980; Kley et al. 1988). There may also be differences in response dependent on type of paper and method of preparation.

In 1876–1877, 289 parallel ozone measurements at the Montsouris Observatory in Paris were undertaken using KI papers and the more quantitative KI-arsenite method (Albert-Lévy, 1877). This study was repeated in the two following years (Marenco et al. 1994). The individual data are not available, but a frequency table is available from which a linear regression relationship can be determined. Several authors have used such a relationship in attempts to calibrate the KI paper measurements (Bojkov, 1986; Anfossi et al., 1991; Lisac and Grubišić, 1991; Sandroni et al., 1992; Marenco et al., 1994; Anfossi and Sandroni, 1997; Pavelin et al., 1999; Weidinger et al., 2011). These either use the Montsouris comparison directly, or use it to scale the chamber results of Linvill et al. (1980). In all cases they find that ozone was much lower in the 19th century than now. Evidently, this conclusion is entirely dependent on the calibration at Montsouris, a single site on the edge of an urban centre, not necessarily representative of the regional background atmosphere (the Montsouris measurements are discussed in section 3.1 below). Moreover, the results of the scaling are not consistent with the chamber measurements (compare Figure 1 of Pavelin et al., 1999 to Figure 1 of Linvill et al., 1980 or Figure 3 of Kley et al., 1988).

The KI papers appear to have been useful as a relative measure of ozone concentration, and showed many aspects of ozone variation and distribution that are now well known (Bojkov, 1986; Anfossi et al. 1991). However, given the high sensitivity of KI papers to relative humidity (greater than to ozone concentration), exposure time, wind speed, and other factors, and the radically different results from intercomparisons, the filter paper measurements cannot be related to modern ozone measurements with any degree of confidence, and are not recommended for quantitative use. The same recommendation was made by Fox (1873), Hartley (1881) and Kley et al. (1988).

2.1.2. The Albert-Lévy and Ehmert ozone measurement methods

In the Albert-Lévy and Ehmert KI methods, ozone is measured by bubbling a known quantity of air through an aqueous solution of iodide (I^-) and either arsenite (Albert-Lévy 1877; Dauvillier, 1934; Volz and Kley 1988) or thiosulfate (Ehmert 1951, 1952, 1959; Galbally 1969).

In the Albert-Levy technique, the sampling solution contains iodide and arsenite. Ozone bubbling through the solution reacts with the iodide, producing iodine. The iodine produced reacts with the arsenite (AsO_3^{3-}), converting it to arsenate (AsO_4^{3-}). Two titrations are performed, to determine the amount of arsenite in a vessel of the solution that has had air bubbled through it, and in an identical vessel that has not been exposed to bubbling. The titrations are conducted in an alkaline medium with a volumetric standard solution of iodine. The quantity of ozone in the air is calculated from the difference between the amounts of arsenite in the two vessels. Measurements were continuous, 24-hour sampling averages. Volz and Kley (1988) replicated the apparatus and method of Albert-Levy and found agreement in the laboratory with the UV method to ±2%.

Dauvillier (1935) undertook an intercomparison of the UV and the KI-arsenite methods using atmospheric samples over a snow surface in Abisko, Sweden. Between 22 December 1934 and 7 March 1935, there were 50 simultaneous measurements and the ratio of the derived ozone amounts was 0.78. This suggests that in practice the KI-arsenite method may underestimate atmospheric ozone levels.

In the Ehmert technique (Ehmert 1951, 1952, 1959; Galbally 1969), the sampling solution is neutral buffered and contains iodide and thiosulfate ($S_2O_3^{2-}$). Ozone bubbling through a vessel of the solution reacts with iodide producing iodine which converts the thiosulfate to tetrathionate ($S_4O_6^{2-}$). With the Ehmert technique the quantity of thiosulfate in the vessel is calculated electrochemically using a coulometric (where chemical transformation is

equated to electron flow) analysis (Ehmert, 1959; Galbally, 1969). The thiosulfate loss equals the ozone amount sampled. Dividing this amount by the air volume sampled gives the ozone concentration. Measurements can be made with air sampling as short as 30 minutes.

As presented in **Table 2**, the Ehmert, ECC and UV methods had ratios indistinguishable from 1.0 with an uncertainty of approximately ±10%. Other variations of the Ehmert method involve injection of known amounts of thiosulfate into the reacting solution which allows continuous or semi-continuous measurements (Paneth and Glückauf 1941; Glückauf et al., 1944; Bowen and Regener 1951; Carbenay and Vassy, 1953; Regener 1959). An ozonesonde based on this method was developed (Kobayashi and Toyama 1966a).

The Ehmert and ECC methods are considered suitable methods for the analyses presented here and are utilized here as intermediate methods when relating other methods to the UV standard.

2.1.3. Ozone measurement methods where the iodine accumulates in solution

A number of the KI methods accumulate iodine in solution while the air is sampled. The first approach to this is the colorimetric method of measuring ozone, where the iodine produced in the neutral buffered 1% KI solution is subsequently measured spectroscopically at 352 nm and quantified by comparison against iodine standards (Byers and Saltzman 1959; Saltzman and Gilbert 1959a). Saltzman and Gilbert (1959a) demonstrated that the iodide concentration, the pH of the solution and the time delay before measuring the iodine absorbance were all critical parameters. They also demonstrated the effectiveness of SO_2 as a negative interferent in the KI method. There have been multiple comparisons of the colorimetric NBKI method against other methods, as listed in **Table 2**. It shows a high bias with respect to UV methods, with some exceptions (e.g. Cherniak and Bryan, 1965). Before the mid-1970s, benchtop UV photometers and chemiluminescent ozone analysers were calibrated to an external calibration source, typically NBKI (e.g. Clements, 1975; Pitts et al., 1976; Torres and Bandy, 1978).

The second approach involves removal of iodine produced in the solution. In the simplest case the anode and cathode are chemically separated by the steady one-way flow of the sensing solution. The iodine produced from ozone is measured via the current from a platinum cathode downstream of the air mixing zone. The reaction at the cathode is:

$$I_2 + 2e \rightarrow 2I^- \quad (3)$$

The charge flow in the external circuit is proportional to the ozone reacted. This "coulometric" method is used in the transmogrifier (Brewer and Milford 1960) and its commercial adaption as the Mast Ozone Meter (Mast and Saunders, 1962), as well as the instrument developed at the Max Planck Institute for Aeronomy (Pruchniewicz 1970, 1973) which will be subsequently described as MPI-Pruch. This "coulometric" method is also used in the Brewer-Mast and Electrochemical Concentration Cell (ECC) ozonesondes and their adaptions for use in surface air. In the case of the ECC sonde an ion bridge is used instead of relying on the one-way flow of the sensing solution.

The Mast ozone meter has undergone other testing to that in **Table 2** (e.g. Gudiksen et al., 1966; Potter and Duckworth, 1965), indicating that under field conditions it gave responses of 50–70% of the NBKI result. A correction factor of 0.8 is used here, corresponding to the Mast Ozone Meter ratio to the UV method based on information in **Table 2** and references above.

There was widespread use of the surface ECC methods in the 1970s (Oltmans, 1981) and there are comparisons against the UV and Ehmert methods, see **Table 2**. The HP-KI method, used for surface ozone observations at Hohenpeissenberg Observatory between 1971 and 1986, is a variation of the ECC method as developed by Kobayashi and Toyama (1966b). The HP-KI method was compared with the Ehmert method via an ozone generator supplied by V. H. Regener and gives a ratio of 1.00 ± 0.02 (Attmannspacher and Hartmannsgruber 1982).

The MPI-Pruch analyser, (Pruchniewicz 1973) is another KI method relying on one way flow of the sensing solution. Comparisons give 1.0 ± 0.05 for ambient ozone measurements with the MPI-Pruch analyser and the Ehmert method at 4 sites and also laboratory comparisons against an ozone generator supplied by V. H. Regener (Pruchniewicz, 1973). However, new evaluations conducted for TOAR-Observations cast doubt on the reliability of this method in the field. A comparison of 15 months of overlapping observations of ambient surface ozone measurements by the MPI Pruch and HP-KI methods at the Hohenpeissenberg Observatory from January 1971 to May 1972, shows that the MPI Pruch method indicates 0.50 ± 0.04 of the ozone level given by the HP-KI method. Similar results were obtained comparing a MPI-Pruch analyser at Zugspitze with nearby ozonesonde results from the same height in the atmosphere. These comparisons are in sharp contrast with previously described comparisons of the HP-KI method and the MPI Pruch method (Pruchniewicz, 1973; Attmannspacher and Hartmannsgruber, 1982). One possible explanation is that the instruments, due to some unknown factor, were far more variable in their efficiency at measuring ozone than the initial tests indicated. Given the information available, no conclusion about the cause can be drawn. This is discussed further in the Supplemental Material (Text S-3).

2.1.4. The Cauer ozone measurement method

The Cauer technique (Cauer 1935, 1951) involves bubbling a large volume of air (100 to 300 litres) through a 10 ml solution buffered by sodium acetate and containing 50 μg iodine as KI. The ozone in the air converts the iodide to iodine and the iodine evaporates into the air stream. At the end of the sampling the remaining iodide is determined and the loss of iodide is equated to the quantity of ozone in the air sampled. When divided by the air volume sampled this gives the ozone concentration. Cauer (1951) writes "For experienced chemists, this analysis requires 20 minutes, but necessitates great care, and is difficult

for non-chemists." The Cauer method was used in multiple studies between 1935 and 1955 and in the national network of the then East Germany from 1952 until 1982 (Cauer 1951; Teichert 1955; Warmbt 1964; Feister and Warmbt 1987). It was compared with the Ehmert method by Warmbt (1964). An initial study, with the two systems presumably in their normal operating conditions, gives a Cauer/Ehmert ratio of 0.66. A more intense study, standardising various components and including blank corrections gives a Cauer/Ehmert ratio of 0.90. However, for low ozone concentrations, when the Cauer method measured less than 5 nmol mol^{-1}, the Ehmert method often measured 10–20 nmol mol^{-1} (Warmbt, 1964). These results cause considerable uncertainty concerning what corrections should be applied to Cauer data from different measurement periods. Here a correction factor is utilized that corresponds to the 0.9 ratio for Cauer/Ehmert in **Table 2** and the Ehmert agreement with the UV method.

2.1.5. Cryotrapping

An unusual technique that was used by only one group was the cryotrapping of ozone on silica gel, with subsequent distillation to remove NO_2 and analysis for ozone by KI and UV methods (Edgar and Paneth, 1941a). This provided a sound measurement method and atmospheric ozone concentrations were obtained over the UK for multiple days (Edgar and Paneth, 1941b).

2.2. Other methods of measuring tropospheric ozone

2.2.1. Early ultraviolet absorption methods (1929–1960)

The ultraviolet absorption method for measuring ozone is based on the strong optical absorption of ozone in the Hartley (200–300 nm) and Huggins (320–360 nm) bands. Measurements involve an artificial light source (a mercury or hydrogen lamp) and a prism-based spectrograph with a detector, typically a photographic plate, that records the intensity of light at multiple wavelengths. In early measurements, the source and detector were separated by a long atmospheric path, of hundreds of metres to several km. The long distances were required to obtain adequate attenuation of the UV radiation, owing to sensitivity issues with the detectors. The ozone concentration was calculated from the ratio of intensities measured, at night, at long and short distances from the light source (Fabry, 1950). This measurement of ozone was difficult and the uncertainties involved (e.g. Kay 1953) do not appear to be quantified.

Some 15 sets of measurements of ozone at the Earth's surface and in the free troposphere were made with the UV absorption technique between 1929 and 1960 (Fabry and Buisson, 1931; Götz and Ladenberg, 1931; Götz and Maier-Leibnitz, 1933; Chalonge et al., 1934; Chalonge and Vassy, 1934; Regener and Regener, 1934; Dauvillier, 1935; Götz et al., 1935; O'Brien et al., 1936; reported in Craig, 1950; Regener, 1938a; Coblentz and Stair, 1939, 1941; Götz and Penndorf, 1941; Vassy, 1941, data reported in Fabry, 1950; Rasool et al. 1956; Paetzold, 1959). The wavelengths used span the Hartley and Huggins bands.

Because the early UV methods are in principle the same as current methods, the main issue for comparisons of ozone data is identifying the wavelengths and absorption cross-sections used. The values used for ozone absorption cross-sections in the Hartley and Huggins bands have changed with time, particularly up to the time of the determination of Hearn (1961).

To illustrate these variations, **Table 3** extends in time and expands in wavelengths the information presented in the final table of Hearn (1961). Ozone absorption cross-sections are presented in units of cm^2 $molecule^{-1}$, with earlier units converted. Between 1913 and 2015 there is a 20% range in absorption cross-sections at 253.7 nm and a range that varies from <1% to nearly 30% at wavelengths up to 334.2 nm. These wavelengths cover the range used to measure tropospheric ozone by the UV method between 1929 and 1960.

Early UV ozone measurements discussed in the following sections are corrected for UV cross-sections to the current standard (Hearn, 1961), following **Table 3**.

2.2.2. Recent ultraviolet absorption method (1970–present)

In the early 1970s there was a revolution in tropospheric ozone measurements. A newly developed UV absorption photometer (Bowman and Horak 1972) provided a stable, low-maintenance continuous ozone analyser based on an absolute method of measuring ozone with an incremental sensitivity of 1 nmol mol^{-1}. UV photometers measure the UV light absorption in the Hartley band (220–310 nm) where ozone is a strong absorber. Usually, a mercury lamp emitting light at 253.7 nm is used as the light source.

UV absorption photometers are currently the most commonly used method for in-situ ozone observations. The method fulfils well the requirements of analyser performance such as signal-to-noise ratio, detection limit, stability of sensitivity, and negligible interferences when measuring in clean air (Galbally et al., 2013). Moreover, it requires little maintenance during operation. Consequently, it is also the recommended technique for continuous ozone observations in ambient air, e.g. in the WMO Global Atmosphere Watch Programme (Galbally et al., 2013), in the United States (US EPA, 2013), Europe (European Union, 2012), and India (Central Pollution Control Board, 2009). Data quality and consistency of records within and across networks have improved over time, as seen by comparison of time series (Logan et al., 2012; Parrish et al., 2012), and station audits by the World Calibration Centre for Surface Ozone, Carbon Monoxide, Methane and Carbon Dioxide (WCC-Empa) (Buchmann et al., 2009). The great majority of in-situ records from more than 9000 sites in the TOAR database that have operated for 3 years or more between approximately 1975 and 2015 were recorded with UV absorption photometers.

A comprehensive uncertainty evaluation was undertaken by the WMO in the *Guidelines for Continuous Measurement of Ozone in the Troposphere* (Galbally et al., 2013). There, the total expanded (95% confidence) measurement uncertainty for UV absorption photometers was estimated to be

$$u(O_3) = 2 \cdot \sqrt{(0.81)^2 + (0.0089\ O_3)^2}\ \text{nmol mol}^{-1} \quad (4)$$

Table 3: (a) Absorption cross-sections of ozone [$\times 10^{20}$ cm^2 molecule^{-1}] at selected Hg line wavelengths (in air). (b) Ratios relative to Gorshelev et al. (2014). DOI: https://doi.org/10.1525/elementa.376.t3

Wavelength (nm)	**253.65**	**263.30**	**265.20**	**269.90**	**275.20**	**280.40**	**289.36**	**292.50**	**296.73**	**302.15**	**302.50**	**312.50**	**334.15**
Fabry and Buisson (1931)	1046	917.0	–	779.9	582.8	361.7	175.7	116.6	66.85	–	30.85	8.056	0.514
Läuchli (1928)	1277	–	1054	–	–	390.8	–	–	59.13	–	–	8.227	0.600
Ny and Choong (1933)	1222	–	–	–	–	–	185.1	–	70.19	31.88	–	–	0.574
Vigroux (1953)	1065	–	–	–	–	–	156.0	–	58.53	28.20	–	–	0.497
Inn & Tanaka (1953)	1141	990.7	955.6	784.2	570.8	366.8	146.5	101.1	57.59	28.45	27.00	7.584	0.523
Hearn (1961)	1148	–	–	–	–	–	147.4	–	59.72	28.62	–	–	0.476
Mauersberger et al. (1986)	1137	–	–	–	–	–	–	–	–	–	–	–	–
Malicet et al. (1995)	1131	–	–	–	–	–	151.3	–	61.46	29.85	–	–	0.466
Gorshelev et al. (2014)	1122	988.9	939.1	806.2	582.5	386.8	153.8	106.0	61.59	30.36	28.58	7.279	0.493
Viallon et al. (2015)	1127	–	–	–	–	–	–	–	–	–	–	–	–
Hodges et al. (2019)	1133												

Wavelength (nm)	**253.65**	**263.30**	**265.20**	**269.90**	**275.20**	**280.40**	**289.36**	**292.50**	**296.73**	**302.15**	**302.50**	**312.50**	**334.15**
Fabry and Buisson (1931)	0.93	0.93	0.97	1.00	0.94	1.14	1.10	1.09	–	1.08	1.11	1.04	0.97
Läuchli (1928)	1.14	–	1.12	–	–	1.01	–	–	0.96	–	–	1.13	1.22
Ny and Choong (1933)	1.09	–	–	–	–	–	1.20	–	1.14	1.05	–	–	1.16
Vigroux (1953)	0.95	–	–	–	–	–	1.01	–	0.95	0.93	–	–	1.01
Inn & Tanaka (1953)	1.02	1.00	1.02	0.97	0.98	0.95	0.95	0.95	0.94	0.94	0.94	1.04	1.06
Hearn (1961)	1.02	–	–	–	–	–	0.96	–	0.97	0.94	–	–	0.97
Mauersberger et al. (1986)	1.01	–	–	–	–	–	–	–	–	–	–	–	–
Malicet et al. (1995)	1.01	–	–	–	–	–	0.98	–	1.00	0.98	–	–	0.95
Gorshelev et al. (2014)	1	1	1	1	1	1	1	1	1	1	1	1	1
Viallon et al. (2015)	1.00	–	–	–	–	–	–	–	–	–	–	–	–
Hodges et al. (2019)	1.01												

with the ozone reading of the analyser given in nmol mol^{-1}. Thus, at a mean level of 30 nmol mol^{-1} the total expanded uncertainty (95% confidence) is ±1.7 nmol mol^{-1}.

A comparison of this bottom-up uncertainty analysis with field results is shown in **Figure 1** with the results of 559 calibrations of UV absorption photometers in the Swiss National Air Pollution Monitoring Network. If the assumptions for the uncertainty estimation are correct, 95% of the calibration results shown in **Figure 1** should be found within the central part surrounded by the grey shaded area. In fact, in **Figure 1** less than 1.5% of the observed calibration results lie outside the estimated uncertainty range, so for this extensive dataset of UV absorption photometer field calibrations, the results fall well within the uncertainty estimate (4). This reflects the robust nature of properly undertaken ozone measurements with the UV photometric method.

The foregoing analysis does not cover all sources of uncertainty, omitting those associated with such causes as inlet losses and potential interferences. The uncertainty of the absorption cross-section is not included, as the calibrations are performed with primary standard analysers based on the same UV absorption cross-section. For the purposes of the subsequent analyses, at a mean level of 30 nmol mol^{-1}, the total expanded uncertainty (95% confidence) in modern ozone measurements is <2 nmol mol^{-1}.

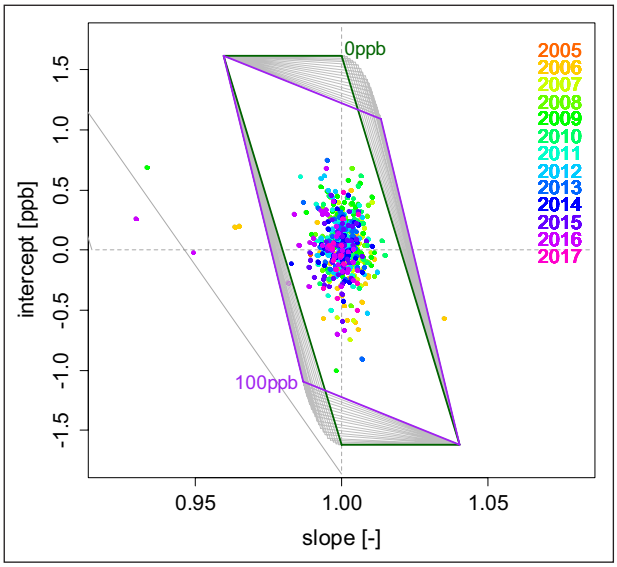

Figure 1: Intercept vs. slope plot for 559 calibrations of various ozone analysers with transfer standards within the Swiss National Air Pollution Monitoring Network between November 2005 and April 2017 for two different types of UV absorption photometers. Green and purple lines illustrate the slopes for 0 and 100 nmol mol^{-1}; the grey lines denote maximum uncertainties for ozone mole fractions from 0 to 100 nmol mol^{-1}, i.e. slope-intercept combinations within the grey lines correspond to deviations smaller than the maximum uncertainty. The maximum uncertainties for 0 and 100 nmol mol^{-1} are highlighted in green and purple. DOI: https://doi.org/10.1525/elementa.376.f1

2.2.3. Chemiluminescent methods of measuring tropospheric ozone

There are multiple chemiluminescent methods for measuring tropospheric ozone, of which the methods involving ozone reaction with either ethylene, rhodamine B or nitric oxide are relevant to this paper.

The ethylene chemiluminescent ozone analyser (Warren and Babcock, 1970) is based on the reaction of ozone and ethylene, which produces electronically excited formaldehyde. As this formaldehyde returns to the ground state, light is emitted in a band centred at 430 nm, which is detected by a photomultiplier. The count rate varies linearly with ozone concentration, provided the cell pressure and temperature, the gain of the detector (the photomultiplier tube), the ethylene and sample flows and the composition of other components of the air sample are unchanged. The ethylene chemiluminescent ozone analyser is a sensitive (~1 nmol mol^{-1}) and stable instrument with a fast response (~1 s) and importantly, is not subject to SO_2 or NO_2 interference. The analyser requires regular calibration with a standard ozone analyser, which in the 1970s was either a KI or UV instrument. When calibrated, the ethylene chemiluminescent analyser gives results that closely match those of the ultraviolet method as seen in the intercomparisons at Hohenpeissenberg, Germany (Attmannspacher and Hartmannsgruber 1982) and Cape Grim, Australia (Elsworth and Galbally 1984). These analysers were used widely in North America in the 1970s (Heidorn and Yap, 1986), following the discovery that tropospheric ozone was damaging to tobacco crops (Macdowall et al., 1964; Mukammal, 1965). Although not in common use currently, in the TOAR surface ozone database chemiluminescence is listed as the method of ozone measurement at 627 of more than 9000 sites.

The rhodamine-B solid chemiluminescent ozone analyser was developed as an ozonesonde (Regener 1960) which was calibrated both with a surface based analyser, traceable to a UV measurement, prior to launch and against the total column ozone measured by a UV (Dobson) instrument at the same location and near the time of the ozonesonde flight. This system was also developed into an aircraft and surface based analyser (Regener, 1964). The analyser was regularly calibrated with an internal ozone generator that in turn had been calibrated against UV based ozone measurements (Regener, 1964). This chemiluminescent ozone analyser was used in the 1960s in the USA and Antarctica. The Regener ozonesonde was subject to large changes in sensitivity due to the effects of ozone, humidity and temperature (Regener 1964; Chatfield and Harrison, 1977; Hering and Dütsch, 1965) and the surface-based analyser may have had similar deficiencies.

In the nitric oxide chemiluminescent ozone analyser (Fontijn et al. 1970; Stedman et al. 1972) the reaction of ozone and nitric oxide produces electronically excited nitrogen dioxide. As the nitrogen dioxide returns to the ground state, it emits light with an intensity maximum at 1200 nm and a range between 600 and 3000 nm. This light is detected by a photomultiplier. The count rate varies linearly with ozone concentration, provided the cell pressure and temperature, the gain of the detector (the

photomultiplier tube), the nitric oxide and sample flows and the composition of other components of the air sample are unchanged. The nitric oxide chemiluminescent ozone analyser is a stable instrument with a sensitive (~0.1 nmol mol^{-1}) and fast response (~1 s) and not subject to SO_2 or NO_2 interference. A current description of the instrument is available (Campos et al., 2006). The analyser requires regular calibration with a standard ozone analyser. There are no records in the TOAR surface ozone database that have employed nitric oxide-based chemiluminescence as the method of measurement, but these analysers have been used extensively in aircraft measurements of tropospheric ozone (Lenschow et al. 1980) for more than 20 years (Section 4.7).

2.2.4 Differential Optical Absorption Spectrometry (DOAS)

The DOAS technique measures the spectrally-resolved absorption features in a beam of light that is returned by a retro-reflector located at some distance from the instrument (Platt et al. 1979). A telescope is used to send and receive a beam of white light, typically from a Xenon arc lamp. A photodiode array detector is used for simultaneous detection of the UV spectrum. The absorption features measured in the returning light beam are a convolution of all the absorption bands of molecules present in the beam path. The concentrations of ozone and other absorbing species are extracted based on well-characterized absorption cross-section data. The precision of a DOAS system for O_3 is estimated at 3% due to uncertainties of the absorption cross section (~1%), and stray light in the spectrometer (~2–3%), while noise and unexplained spectral structures determine biases and detection limits (2–4 nmol mol^{-1}), which scale inversely with the path length (Stutz and Platt, 1996). A field study comparison of DOAS with UV photometric analysers found differences of ±7%, attributed to spatial and temporal atmospheric inhomogeneities, including the fact that the DOAS beam scanned over a path higher in altitude than the sampling point of the UV instrument (Williams et al., 2006). In the TOAR database DOAS is listed as the method of ozone measurement at 39 sites.

3. Ozone measurements in surface air 1870s–1970s

For the purpose of reconstructing the historical surface ozone record an extensive literature search was conducted, which unearthed several data sets that have not before been coherently analysed in a single study. As discussed in Section 2, the approach used in *TOAR-Observations* is to reconstruct regional or zonal average ozone values based on all available historical data sets rather than relying on individual data sets as in previous studies. Following is a description of the application of the four data selection critieria for the historical reconstruction.

Criterion 1: all measurements via the Schönbein and related filter paper methods are rejected; the early UV measurements (1929–1960) are corrected to the currently accepted values of absorption cross-sections (Hearn, 1961); the observations made by the Mast Ozone Meter and related transmogrifier, and the Cauer method have been adjusted following **Table 2**.

Criterion 2: It is known that SO_2 causes quantitative negative interference with the KI measurement methods (Albert-Lévy, 1907; Glückauf, 1941, 1944; Saltzman and Gilbert 1959a), with a stoichiometry reported as 1.0 (Schenkel and Broder, 1982; Volz and Kley, 1988). SO_2 is known to be present in very low concentrations in the background atmosphere of <<1 nmol mol^{-1} (Seinfeld and Pandis 2000), thus not a significant interferent there. However in urban areas in Europe following the industrial revolution coal burning was widespread (Mylona, 1996; Smith et al., 2011) and the resulting sulfur-based acid pollution is widely documented (Smith, 1872; Ladureau, 1883, Witz, 1885). This criterion can lead to some ambiguity, as "clean" sites such as Arkona, on the Baltic coast, and the hilltop site of Hohenpeissenberg in southern Germany are subject to modest levels of SO_2 interference (Feister and Warmbt, 1987; Low et al., 1990, 1991). Thus KI-based ozone measurements need to be scrutinised for possible SO_2 interference before being accepted. The interference should be quantified and small compared with the ozone signal, and the uncertainty introduced into the ozone reading due to correction should be ideally ≤5%.

Criterion 3: The ozone sampled in the air in the surface layer should be representative of the unpolluted planetary boundary layer. At times of good turbulent mixing in the lower atmosphere, due to either convection driven by solar radiation or mechanical turbulence from wind shear, vertical gradients of ozone mole fraction diminish and ozone levels in near surface air are representative of the planetary boundary layer (Auer 1939; Glückauf 1944; Teichert 1955; Galbally 1968, 1972; Garland and Derwent 1979; Fabian and Pruchniewicz, 1977; Galbally et al. 1986). At rural sites with plant and soil surfaces in flat plains away from fresh anthropogenic sources of NO, when turbulence diminishes at night, so that the rate of ozone supply from above is less than that lost due to ozone destruction, i.e. dry deposition, at the underlying surface, a night-time decrease of ozone occurs (Auer 1939; Glückauf 1944; Teichert 1955; Galbally 1968, 1971, 1972; Garland and Derwent 1979; Fabian and Pruchniewicz, 1977; Galbally et al. 1986). Consequently, nighttime measurements or 24-h average measurements of surface ozone at such continental sites are not representative of the well mixed boundary layer. Over ice, snow and water surfaces, this ozone decrease with weak mixing does not occur because the rate of ozone loss at the underlying surface is much smaller. The diurnal cycle is different at mountain top sites in steep terrain. At night the slopes cool and typically a downslope wind develops that entrains air from above, as described for Mauna Loa (Price and Pales, 1963). During the day the slopes warm and, away from urban pollution, an upslope wind brings air from below that has been depleted in ozone. Data selected in this study take into account topography and surface characteristics to ensure that only data from well mixed conditions, or conditions reasonably assumed to be well mixed, are selected.

Criterion 4: Published data may be suspect for a variety of reasons, including inconsistency with other observations, or artifacts or outliers that suggest instrument problems. The outstanding example is Pring (1914) where

the measurements appear to be of excellent quality and well documented, except that they differ by a factor of 100 from current measurements. As Fabry (1950) said, the results are absurd. Serious artifacts and inconsistencies associated with individual datasets are discussed in the Supplemental Material (Text S-3).

For every site, the method used, the possible pollution sources, the topography, surface cover and prevailing meteorology and credibility of the results have been examined to assess the suitability of the observations for inclusion in the historical record. One excluded site is explicitly included in the following discussion. This is Montsouris, Paris, which is discussed here because it has been used as a central set of data for a number of previous historical reconstructions of tropospheric ozone. For the other historical data discussed below, in all cases the method is valid and with one exception, the sites are presumed free of interfering pollutants and representative of the well-mixed boundary layer. In a few cases some of the data are excluded on credibility grounds, and some are accepted with caution; the reasons for these decisions are discussed. Before discussing the available historical data which passed the selection criteria, it is worth repeating the cautionary note from Section 2: for comparison with current observations these data should be treated as a group, because there are substantial unknown uncertainties associated with the bias corrections of each individual set of observations.

There are some other features of the data that are important to note. Some studies involve measurements at multiple sites; other studies have long records at one site that have been broken into distinct periods. Thus the number of published studies and the number of data sets do not correspond. The 60 data sets accepted into the record, their site names, locations, data references etc. are presented in **Tables 4, 5** and **6**. During the period 1870s –1950, most of the available measurements were made using KI techniques with a small number of spectroscopic measurements by UV absorption. The studies were occasional scientific experiments, usually of limited duration and initially in central and northern Europe. From 1950 to the 1970s the coverage became global and measurements at a given location moved to yearly or greater duration.

The standard deviations presented here differ for the periods 1890–1950 and 1950–1970 because of the paucity of data in the earlier period. In the period 1890–1950 the standard deviation is calculated from daily ozone values when there are 7 or more days of data. In the period 1950–1970 the standard deviation is calculated from the monthly mean ozone values for an annual cycle or longer when there is at least one year of data. For more information see the Supplemental Material (Text S-5).

The observations are grouped into the tropical (0°–30°), temperate (30°–60°) and polar (60°–90°) regions of each hemisphere. They are presented in **Tables 4–6** and discussed in the following text for different periods. Ozone is summarized for each region using a weighted mean, with the weighting proportional to the number of days with observations at each site.

3.1. The Montsouris Observatory ozone measurements 1876–1910

The ozone measurements at the Municipal Observatory at the Parc de Montsouris at the southern edge of Paris (Albert-Lévy, 1877) from 1876–1910, are the oldest active sampling ozone measurements known. As noted in Section 2.1.1, they are pivotal to conclusions in previous work that ozone in pre-industrial times was much less than its present concentration (e.g. Marenco et al., 1994). Hence the Montsouris observations are examined in detail here.

The technique used was the KI-arsenite system and is related to the UV method as described in Section 2.1.2, and is a valid method.

Volz and Kley (1988) examined daily measurements of ozone at Montsouris in 1876–86 and 1905 and correlated the results with the wind direction. The area to the southwest of Montsouris had no significant urban centers in 1876–1905 and Volz and Kley concluded that air from the southwest would be free of urban air pollutants which might interfere with the analysis. It was found that with wind from the southwest the average ozone levels measured in 1876–86 and 1905 were approximately 8 and 10 nmol mol^{-1}, and with wind from directions other than southwest the ozone levels were lower by 2 and 5 nmol mol^{-1}, respectively. The lower ozone levels observed when the wind direction was from Paris were attributed to the presence of SO_2 in the Paris urban plume. The corrected ozone data gave an average ozone level of 11 nmol mol^{-1} over the period 1876–1910 (Volz and Kley 1988). This is much lower than that found at clean mid-latitude sites today.

Observers in the 19th century were aware of the potential for interference of reducing gases with the KI reaction, and, as noted by Volz and Kley (1988), an attempt was made to quantify these interferences. Average values for 1905–07 of "gaz réducteurs" correspond to ~3 nmol mol^{-1}, with weekly values as high as 16 nmol mol^{-1} (Albert-Lévy, 1907, 1908). However, exactly how to interpret these measurements remains uncertain, as SO_2 does not react strongly with KI in the absence of ozone.

The period 1870s to 1900s was one of rapid change in Paris. During the period 1870–1880, Paris was a city of 2 million people and coal supplied 58% and wood 42% of the city's total energy needs (Kim and Barles, 2012). Coal burning releases SO_2, and two approaches are taken to estimate SO_2 in Paris at this time. Firstly, measurements of ambient SO_2 in Paris began in the 1950s, and records of coal use in the city are available from 1875. These concentration and emission data are combined to estimate SO_2 levels of 55 nmol mol^{-1} in Paris in the early 20th century (Ionescu et al., 2012). However, this approach neglects activities outside the city boundary where both building construction and the presence of gasworks that provided gas to Paris were located (Kim and Barles, 2012; Kesztembaum and Rosenthal 2014). Secondly, at Montsouris measurements were made of sulphate in rainwater with an average of 13.9 mg l^{-1} (range 3.5–37.0 mg l^{-1}) as SO_3^{-1}: (Albert-Lévy, 1907, 1908). Sulphate in rainwater is closely associated with atmospheric sulphur dioxide, and such sulphate values are typical of highly polluted

areas and correspond to a SO_2 level of ~25–75 nmol mol^{-1} (e.g. Sequeira, 1975; Davies, 1979; Aas et al., 2007; Gonçalves et al., 2007). Both approaches indicate that SO_2 interference would have biased the Montsouris measurements low. The inferred SO_2 levels suggest a large degree of interference (Section 2.1), but in the absence of actual measurements there is inadequate knowledge to quantify the problem.

Other measurements at the Observatory (Albert-Lévy, 1877; Hartley, 1881) include on average 12 nmol mol^{-1} of oxides of nitrogen (measured as nitric acid) during this period. This measured value is lower than the 28 nmol mol^{-1} estimate based on coal and other fuel use in the early 20th century (Ionescu et al., 2012). However, it compares well with values of ~8 nmol mol^{-1} found in London by Reynolds (1930) and Edgar and Paneth (1941b). As nitrogen oxides are emitted as both NO and NO_2, they can interact with O_3 in the gas phase through NO titration removing ozone and NO_2 photolysis producing O_3 particularly if reactive organic compounds are present. Also the NO_2 can act as a positive interferent in the KI ozone method. Therefore, it is not immediately apparent whether the influence of these nitrogen oxides increased or decreased the measured ozone values.

Paris at the end of the 19th century was home to large numbers of horses and dairy cattle (Barles, 2012). Measurements of NH_3 were also made at the Observatory (Hartley 1881; Albert-Lévy, 1903); an average of 28 nmol mol^{-1} is reported for the period 1883–1901. As already discussed, NH_3 is a negative interferent in the KI ozone measurement method, although the stoichiometry of the interference with the arsenite method is not known.

Overall the Montsouris observations fail Criterion 2 that the likelihood for significant contamination of the ozone measurements due to interfering pollutants in the sampled atmosphere should be low. Correction for SO_2 and other interferences is not feasible, due to their estimated magnitude, lack of a full understanding of the interference, and the absence of reliable atmospheric observations of the interfering compounds at Montsouris at that time.

Criterion 3 asks: are the measurements representative of the well-mixed boundary layer? The low sensitivity of the KI-arsenite method required 24-hour averages. The sampling was from a balcony of the Observatory building 5 m above the ground. The 24-hour averages at a clean air site would be biased low, being 0.8 of daytime average and 0.7 of daytime maximum measurements, given a typical diurnal cycle (Galbally and Roy, 1980) due to ozone dry deposition as discussed earlier. Furthermore wind speed and direction observations in Paris show an average diurnal pattern with northeasterly winds at night between 2000 and 0400 h, and southwesterly winds during the afternoon during 1100 to 1600 h between March and October 1890–1896 (Angot, late 1890s). These overnight winds would bring SO_2 enriched air to the Observatory causing chemical interference with the measurements, while cleaner air in the afternoon would have reduced the cumulative SO_2 effect.

At that time W.M. Hartley, user of the KI-arsenite method in his laboratory studies and a scientist familiar with the Montsouris work expressed concern over the possibility of ozone loss in the sampling system and wrote: "*It is impossible, therefore, to accept the figures given in the Annuaire de L'Observatoire de Montsouris as indicating anything like the true proportion of ozone usually present in country air …*" (Hartley, 1881). Indeed, the Montsouris measurements are consistent with other historical measurements in urban areas (Text S-6, Table S-1 and Figure S-1).

In summary, the measurements of ozone concentration at Montsouris were made with a valid measurement technique, however it is very likely that there is a large negative bias in the measurements, of comparable magnitude to the observed ozone concentration, due to the presence of SO_2 and ammonia and a further uncertain bias due to nitrogen oxides. Also the 24-hour sampling includes low night-time ozone values due to the occurrence of nocturnal inversions and ozone dry deposition as well as chemical interference due to the recirculation of air over Paris. Consequently, the measured ozone concentrations for Montsouris for 1876–1910 are biased low, are not representative of the regional atmosphere and are not used in this assessment of historical ozone concentrations.

3.2. Other surface measurements: 1896–1901

During 1896–1901 other surface ozone measurements, in clean air, were made with the KI-arsenite method (Albert-Lévy, 1877) and are listed in **Table 4**. De Thierry (1896) made measurements at Chamonix (~1 km asl) and Grands-Mulets (~3km asl) on Mont Blanc in southeastern France on 3 days in August and September 1896. Lespieau, (1906) made 13 measurements over 4 days in 1900 and 6 days in 1901 on glaciers at three levels (~1.25 km, ~3 km and ~4.8 km) on Mont Blanc. The mean of these observations, weighted by the number of measurement days, (hereinafter referred to as the "weighted mean"), in the temperate zone over Europe is 25 nmol mol^{-1} with a range of 20–63 nmol mol^{-1} for the period 1896–1901.

3.3. 1929–1934

The first measurements of surface ozone with the UV method were made in 1929 (Fabry and Buisson 1931; Götz and Ladenberg 1931). In Europe there were multiple measurements with long path UV (Götz and Maier-Leibnitz, 1933; Chalonge and Vassy, 1934; Götz and Penndorf 1941). The study of Chalonge et al. (1934) involved two groups making simultaneous UV measurements at two alpine sites, swapping sites mid-way during the experiment. No significant differences were observed in this early instrument intercomparison. The ozone mixing ratio, corrected for the Fabry and Buisson (1931) UV absorption coefficients, was 31 nmol mol^{-1} at Jungfraujoch, Switzerland (3450 m) and 18 nmol mol^{-1} at nearby Lauterbrunnen (800 m), showing an increase with altitude.

The weighted mean of these observations in the temperate zone over Europe is 25 nmol mol^{-1} with a range from 18–32 nmol mol^{-1} for the period 1929–1934.

Table 4: Surface ozone in northern temperate latitudes (primarily Europe), 1986–1975. Mean and standard deviations in nmol mol^{-1}. See Supplemental Material (Text S-7) for Notes. DOI: https://doi.org/10.1525/elementa.376.t4

Location	Period	Method	Reference	Value(s)	Days	Mean (nmol mol^{-1})	SD (nmol mol^{-1})	Notes
1896–1901 Northern Temperate – Europe								
1 Chamonix 45.9N, 6.9E, 1050 m	August 1896	KI-arsenite	De Thierry (1897)	35–39 μg m^{-3}	2	20.4	n/a	
2 Grands-Mulets 45.9N, 6.9E, 3020 m	September 1896	KI-arsenite	De Thierry (1897)	94 μg m^{-3}	1	63.0	n/a	
3 Glacier des Bossons 45.9N, 6.9E, 1250 m	August 1900, 1901	KI-arsenite	Lespieau, 1906	41 μg m^{-3}	5	22.9	n/a	
4 Grands-Mulets	August 1900, 1901	KI-arsenite	Lespieau, 1906	33 μg m^{-3}	2	22.3	n/a	
5 Sommet, Mont Blanc 45.9N, 6.9E, 4810 m	Sept 1900, Aug 1901	KI-arsenite	Lespieau, 1906	26 μg m^{-3}	3	21.5	n/a	
				Weighted mean		**25.2**		
1929–1934 Northern Temperate – Europe								
6 Provence 44.2N, 5.2E, 300 m	Oct. 1929–Mar. 1930	UV	Fabry and Buisson, 1931	22 nmol mol^{-1}	1	22.4	n/a	1
7 Arosa 46.8N, 9.7E, 1860 m	April 30, 1930	UV	Götz and Ladenburg (1931)	29 nmol mol^{-1}	1	32.2	n/a	2
8 Arosa	Sept. 1932–Apr. 1933	UV	Götz and Maier-Leibnitz (1933)	8–31 nmol mol^{-1} (L1929); 9–36 nmol mol^{-1} (FB1931)	5	24.9	10.5	3
9 Arosa	March–May 1934	UV	Götz & Penndorf (1941)	22–32 nmol mol^{-1}	11	28.2	2.8	4
10 Chur 46.9N, 9.5E, 600 m	Sept. 1932–April 1933	UV	Götz and Maier-Leibnitz (1933)	18–19 nmol mol^{-1} (L1929); 21 nmol mol^{-1} (FB1931)	2	20.4	n/a	3
11 Lauterbrunnen 46.6N, 7.9E, 800 m	18–31 August 1933	UV	Chalonge, Gotz & Vassy (1934)	11–26 nmol mol^{-1}	10	17.5	4.5	5,1
12 Jungfraujoch 46.6N, 8.0E, 3450 m	18–31 August 1933	UV	Chalonge, Gotz & Vassy (1934)	24–35 nmol mol^{-1}	7	30.9	5.6	5,1
				Weighted mean		**24.9**		

(Contd.)

Location	Period	Method	Reference	Value(s)	Days	Mean (nmol mol^{-1})	SD (nmol mol^{-1})	Notes
1938–1941 Northern Temperate – Europe								
13 Mt Ventoux 44.2N, 5.3E, 1912 m	October, 1938	UV	Vassy, 1941	25 nmol mol^{-1}	1	25.5	n/a	6,1
14 Friedrichshafen 47.7N, 9.5E, 400 m	8–12 Sept. 1938	KI	Regener (1938b)	15–24 nmol mol^{-1}	4	21.0	n/a	
15 Jungfraujoch	August 1938	KI	Regener (1938b)	24–43 nmol mol^{-1}	5	30.0	n/a	
16 Pfänder Mountain 47.5N, 9.7E, 1060 m	September, 1940	Ehmert	Ehmert and Ehmert (1949); Volz et al. (1988)	22 nmol mol^{-1}	7	22.0	n/a	7
17 Durham, UK. 54.8N, 1.6W, 100 m	1940–1941	KI coulometric	Paneth and Glückauf 1941; Glückauf 1944	27 nmol mol^{-1}	20	27.0	n/a	8
18 Kew 51.5N, 0.3W, 6 m	May–July 1938 & 1939	Cryogenic, KI and UV analysis	Edgar and Paneth 1941b	22–28 nmol mol^{-1}	3	24.3	n/a	
19 Southport 53.6N, 3.0W, 6 m	May–July 1938 & 1939	Cryogenic, KI and UV analysis	Edgar and Paneth 1941b	17–29 nmol mol^{-1}	3	22.7	n/a	
				Weighted mean		**25.5**		
1950s to 1970s Northern Temperate – Europe, North Africa, North America, Japan								
20 Mt. Capillo, NM 34.7N, 106.4W,3100 m	Nov–Dec 1950	KI coulometric	Bowen and Regener (1951)		30	26.0	4	9
21 Arosa	Apr.1950–Jul.1951	Ehmert	Götz and Volz (1951)	44.6 ± 10.4 μg m^{-3}	400	26.4	6.2	10
22 Arosa	Apr.1954–Oct.1958	Ehmert	Perl 1965	39.3 ± 10.8 μg m^{-3}	1500	23.2	6.4	10
23 Lindenberg 52.2N, 14.1E, 98 m	Aug–53; June–July 1954; Sept. 54	Cauer	Tiechert (1955)	31 μg m^{-3}	31	20.2	n/a	11
24 Arkona 54.7N, 13.4E, 42 m	1956–1971	Cauer	Feister & Warmbt (1987)	36.1 μg m^{-3}	5500	22.7	4.7	12
25 Arkona	1972–1984	Cauer	Feister & Warmbt (1987)	44.5 μg m^{-3}	4300	25.8	5.3	13
26 Hohenpeissenberg 48N, 11E, 975 m	1971–1975	Wet chemical iodometric	Attmannspacher et al. (1977)		1800	32.3	11.3	

(Contd.)

Location	Period	Method	Reference	Value(s)	Days	Mean (nmol mol^{-1})	SD (nmol mol^{-1})	Notes
27 Hohenpeissenberg 48N, 11E, 975 m	1969–1972	MPI-Pruch	Fabian & Pruchniewicz (1977)	64.8 μg m^{-3}	960	30.3	14.3	14
28 Norderney 53.7N, 7.2E, 16 m	1969–1975	MPI-Pruch	Fabian & Pruchniewicz (1977)	41.9 μg m^{-3}	2000	19.6	9.0	14
29 Zugspitze 47.4N, 11.0E, 2964 m	1969–1975	MPI-Pruch	Fabian & Pruchniewicz (1977)	45.1 μg m^{-3}	1920	21.1	5.9	14
30 Cagliari 39.2N, 9.1E, 18 m	1970–1975	MPI-Pruch	Fabian & Pruchniewicz (1977)	41 μg m^{-3}	1480	19.2	7.2	14
31 Westerland 54.9N, 8.3E, 8 m	1971–1975	MPI-Pruch	Fabian & Pruchniewicz (1977)	47.1 μg m^{-3}	1240	22.0	5.8	14
32 Kairouan 35.7N, 10.1E, 60 m	1970–1975	MPI-Pruch	Fabian & Pruchniewicz (1977)	56.1 μg m^{-3}	1336	26.2	9.0	14
33 Mt Norikura 36.1N 137.5E, 2770 m	Sept 1959; Aug, Sept 1960	Ehmert	Miyake et al. (1962)	48.7 μg m^{-3}	18	22.8	9.7	22
34 Mt Norikura 36.1N 137.5E, 1450 m	Sept 1959; Aug, Sept 1960	Ehmert	Miyake et al. (1962)	35.7 μg m^{-3}	18	16.7	9.1	22
35 Tomisaki 34.9N 139.8E, 12 m	Aug, Sept 1963, Feb 1965	Ehmert	Kawamura and Sakurai (1966)	44.4 μg m^{-3}	23	20.7	6.7	22
				Weighted mean		**24.0**		

Dauvillier (1934) used the KI-arsenite method at Scorsby Sund on the east coast of Greenland, from November 1932 to August 1933 (**Table 5**). His daily data (reported as 24-hour means) can be notionally divided into two sets: 225 days of data show a background value of about 50 μg m^{-3}, with less than 5% over 100 μg m^{-3} (approximately 47 nmol mol^{-1}), and 45 days of data that show major events where ozone went as high as 570 μg m^{-3}. The latter maximum is approximately 270 nmol mol^{-1}. Ozone during December 1932 was particularly high, averaging approximately 100 nmol mol^{-1}. This monthly mean is more than twice the highest December monthly mean at Arctic sites in the TOAR Surface Ozone Database. These high events were recorded by Dauvillier (1934) as interesting and remarkable. He associated them with aurora and suggested enhanced transport from the stratosphere or ionosphere to the surface air. Dauvillier (1934) also states that during the winter the inlet was close to or at the snow surface. There are two possible explanations of these high ozone levels, either (a) the KI-arsenite method is subject to large positive interference in the recorded calm conditions in the polar night or (b) there was enhanced stratospheric-tropospheric exchange or tropospheric ozone production that led to high ozone levels in surface air, that has not recurred in the Arctic during the period of UV surface ozone measurements, approximately 1980 to the present. Two points are worth noting: Dauvillier (1935) subsequently validated his method in the Arctic in winter against UV surface ozone observations; also, the ozonesonde record from Resolute Bay, in the Canadian Arctic, shows occasional very high values at the surface, only in winter, including a value of 164 nmol mol^{-1} in 1966, and Chung and Dann (1985) record surface ozone levels measured with an ethylene chemiluminescent analyser in December in Saskatchewan, Canada of up to 228 nmol mol^{-1}. With the evidence available it is impossible to resolve which explanation is correct. The considered judgement is that the 45 days of observations during the major events are not credible and omitted from the subsequent analysis, while the 225 days of background values are retained as credible. Dauvillier (1935) presents measurements from Abisko, Sweden between December 1934 and March 1935, giving average ozone concentrations of 41 μg m^{-3} from 68 UV measurements and 33 μg m^{-3} from 56 measurements with the KI-arsenite method.

Considering the qualifications above, the methods used are valid, the sites are presumed free of interfering pollutants and representative of the well-mixed boundary layer. The weighted mean of these observations in the Northern Polar region is 22 nmol mol^{-1} with a range of 15–24 nmol mol^{-1} for the period 1932–1935.

3.4. 1938–1941

The only UV measurements of surface ozone found during this period were at Mt. Ventoux (1912 m, southern France) by A. Vassy in October 1938, as reported by Fabry (1950). After correction for the Fabry and Buisson (1931) UV absorption coefficients these observations average 26 nmol mol^{-1}.

The KI method became more widely used during this period. At Jungfraujoch (3450 m) on 5 days in August 1938, Regener (1938b) observed 30 (range 24–43) nmol mol^{-1} ozone, and in September at Friedrichshafen (at 400 m near the shore of Lake Constance, southern Germany), 21 nmol mol^{-1} (range 15–24). Ehmert and Ehmert (1949) made measurements using the Ehmert method on Pfänder Mountain (1060 m in western Austria) in September, 1940. The data have been reinterpreted by Volz et al. (1988), where the original ozone measurements gave 15 nmol mol^{-1} and the revised value is 22 nmol mol^{-1}.

Edgar and Paneth (1941b) present measurements of ozone in the air in a street of South Kensington, London, UK, from the rooftop of the Royal College of Science building in South Kensington, at the Kew Observatory outside London and at Southport on the northwest coast of England, made from February 1938 to July 1939. They used a cryogenic trapping and purification method followed by both UV and KI analysis (Edgar and Paneth, 1941a; 1941b). Considering only the non-urban observations at Kew and Southport, the mean and range are 24 (17–29) nmol mol^{-1}.

Glückauf (1944), using an automated KI-thiosulfate method, presents occasional ozone data in a meteorological analysis of observations near Durham, UK. The following results are extracted from his paper. On 21 March 1941 in wind from a clean sector, the ozone mixing ratio was 31 ± 2 nmol mol^{-1}. The level in November 1940 is reported as half this. Daily maximum values varied from 24 nmol mol^{-1} in November to 68 nmol mol^{-1} in May. On 28 and 29 August 1941, in prolonged strong steady winds, ozone reached daily maxima of 25 and 27 nmol mol^{-1} with a 37-hour average of 21.5 nmol mol^{-1}. Analyses of five warm fronts indicated ozone mole fractions of 25 to 34 nmol mol^{-1}. Analyses of four cold fronts indicated ozone mole fractions of 27 to 68 nmol mol^{-1}. The high values, likely from subsidence behind the front, may have been partly of stratospheric origin. If the maximum values are treated as 95th percentiles and an annual cycle is fit to the monthly observations then the mean mole fraction of ozone in clean, well-mixed conditions is 27 nmol mol^{-1}.

Accepting the specific analysis above of Glückauf (1944), for this period the methods used are valid, the sites, or air masses sampled, are presumed free of interfering pollutants and representative of the well mixed boundary layer. The weighted mean of these observations in the temperate zone over Europe is 26 nmol mol^{-1} with a range from 21–30 nmol mol^{-1} for the period 1938–1941. These results are indistinguishable from those both 5 years and 4 decades earlier.

3.5. 1951–1970s

The period 1950s to 1970s is the first period in which there were globally distributed measurements of ozone in surface air. Series of measurements lasting a year or more became common and short-term campaigns fewer. The surface ozone records during this period include: the upsurge in observations during the International Geophysical Year of 1957–1958; measurements made initially at Dresden-Wahnsdorf in 1954 and then expanded in

Table 5: Surface measurements in polar regions. Mean values and standard deviations in nmol mol^{-1}. See Text S-7 for Notes. DOI: https://doi.org/10.1525/elementa.376.t5

Location	Period	Method	Reference	Range	Days	Mean (nmol mol^{-1})	SD (nmol mol^{-1})	Notes
1932–1935 Northern High Latitude								
36 Scoresby Sund 70.5N, 22.9, 70 m	Nov. 1932 to Aug. 1933	KI-arsenite	Dauvillier (1934)	50 μg m^{-3}	251	23.5	8	15,9
37 Abisko, Sweden 68.3N, 18.8, 400 m	22 Dec 1934–7 Mar 1935	KI-arsenite	Dauvillier (1935)	33 μg m^{-3}	56	15.2	6	16
38 Abisko, Sweden	Dec.1934–Mar.1935	UV	Dauvillier (1935)	41 μg m^{-3}	68	19.5	6	16,1
				Weighted mean		**21.5**		
1950s to 1970s Northern High Latitude								
39 Tromso 69.6N, 19.0E, 14 m	1970–1975	MPI-Pruch	Fabian & Pruchniewicz (1977)	40.4 μg m^{-3}	1480	18.9	2.6	14
40 Bredkalen 63.2N, 14.5E, 360 m	December 1968–January 1970	MPI-Pruch	Fabian & Pruchniewicz (1977)	45.7 μg m^{-3}	292	21.4	7.1	14
41 Kise 59.3N, 9.5E, 40 m	August 1970–November 1972	MPI-Pruch	Fabian & Pruchniewicz (1977)	44.8 μg m^{-3}	680	20.9	4.4	14
42 College, Alaska 64.9N, 147.8W, 137 m	August–December 1950	KI-arsenite	Wilson et al. (1952)	68 ± 27 μg m^{-3}	149	31.4	12.7	17
43 Barrow, Alaska 71.3N, 156W, 15 m	January 1965–September 1967	Mast ozone meter	Kelley (1970)	34.2 ± 15.4 nmol mol^{-1}	1003	34.2	15.4	17a
				Weighted mean		**24.2**		
1950s to 1970s Southern High Latitude								
44 Little America 78.2S, 162.2W, 10 m	March 1957–October 1958	Bowen and Regener (1951)	Wexler et al. (1960)	43.3 μg m^{-3}	443	19.2	7.1	18,19
45 Halley Bay 75.6S, 26.6E, 30 m	January–December 1958	transmogrifier	MacDowall (1962); also Roscoe and Roscoe (2006)	13.1 nmol mol^{-1}	275	15.8	3.7	20
46 Amundsen-Scott 90S, 2835 m	March 1961– July 1963	Bowen and Regener (1951)	Oltmans & Komhyr (1976)	30.3 ± 4.8 nmol mol^{-1}	780	30.3	4.8	19
47 Mirny 66.6S, 93.0E, 40 m	Feb 1960–Jan 1962	Cauer	Kolbig and Warmbt (1978)	19.4 hPa	730	21.9	5.2	9,21
48 Hallett, Antarctica 72.3S, 170.3E, 5 m	January 1962–February 1963	Regener chemi-luminescent	Aldaz (1965)	19.1 ± 5.1 nmol mol^{-1}	365	19.1	5.1	19
49 Base Roi Baudouin 70.4S, 24.3E, 30 m	April 1965–December 1966	Mast ozone meter	Wisse and Meerburg (1969)	21.9 ± 5.6 nmol mol^{-1}	600	26.3	6.7	19,20
				Weighted mean		**23.5**		

1956 to a network of 7 surface stations across Germany (Warmbt, 1964; Feister and Warmbt, 1987); and from 1969–1975 the Troposphärisches Ozon (TROZ) network of 16 surface ozone stations on a meridional zone from Norway to South Africa, run by the Max Planck Institute for Aeronomy (Fabian and Pruchniewicz, 1977). Several other sites utilized here were run on an individual or national network basis.

For the TROZ network, the largest network for this period, a coulometric KI method (Section 2.1.3) was used (Pruchniewicz 1970, 1973). Detailed consideration of the TROZ data reveals issues with (a) its traceability to the modern UV standard, (b) interferences or pollution at the sites, and (c) special features in selection of representative surface ozone data (reported ozone values are representative of daytime maximum values rather than daytime means). These issues are discussed in the Supplemental Material (Text S-3). Because this data set has data from 15 stations (one station was omitted for reasons described below), located between 90°N and 30°S, it potentially dominates the 1950s–1970s historical record. To understand the sensitivity of the historic analysis to the TROZ data and to provide robust conclusions, the quantification of the change in ozone from the historical to the modern period is performed both with and without the TROZ data (see Section 3.6).

Five surface ozone observing sites operating in Northern Polar region in the 1950s to 1970s are presented in **Table 5**. Three sites are from the TROZ network and two from Alaska: College (137 m, located in a suburb of Fairbanks in the center of the state) and Barrow (15 m, near the shore of the Beaufort Sea and now called Utqiaġvik) (Wilson et al. 1952; Kelley 1973). The College data, taken with the KI-arsenite method, show spikes of very high values like the Dauvillier (1934) record; these are truncated on credibility grounds (see Text S-3 for detailed discussion). The Barrow data are well-documented, but they show odd seasonal behaviour and some surprisingly high values, and so have questionable credibility, but are accepted (Text S-3). Considering the qualifications above, the methods used are valid, the sites are presumed free of interfering pollutants and representative of the well mixed boundary layer. The weighted mean of the accepted observations in the Northern Polar region (1950s–1970s) is 24 nmol mol^{-1} with a range of 19–34 nmol mol^{-1}. If the College and Barrow data are entirely omitted this average becomes 19 nmol mol^{-1}, but this value relies entirely upon the TROZ network.

In the Northern Temperate region there are multiple data sets. Bowen and Regener (1951) present ozone data from Capillo Peak Observatory in New Mexico (approximately 2800 m asl). Four years of ozone data were obtained at the Arosa Light Observatory (located on the northern edge of the town of Arosa in a Swiss valley, 1810 m (Staehelin et al., 2018)) using the Ehmert technique (Perl, 1965). In August 1953 and June/July and September 1954 ozone observations were made utilizing an 80 m tower using the Cauer method (Section 2.1.4) at Lindenberg (98 m) in northeastern Germany (Teichert 1955). Measurements were made at Hohenpeissenberg (975 m) from 1971 to 1975 using the HP-KI method. Six other sites, all from the TROZ network, are listed in **Table 4**. The TROZ station Lindau is omitted due to the influence of high levels of local pollution (Fabian and Pruchniewicz, 1976). The long-term site at Arkona on the north coast of Germany using the Cauer method commenced in 1956 (Warmbt 1964; Feister and Warmbt 1987). With the exception of Arkona, the methods used are valid, the sites are presumed free of interfering pollutants and representative of the well mixed boundary layer. With a correction for SO_2 interference (Warmbt 1964; Feister and Warmbt 1987), the Arkona data are accepted (see note #12 in Text S-7). Measurements from three sites in Japan made with the Ehmert method are included (Miyake et al. 1962; Kawamura and Sakurai 1966). The methods used are valid, and after the correction of the Arkona data, all sites are presumed free of the influence of interfering pollutants and representative of the well mixed boundary layer. The weighted mean of these observations in the Northern Temperate region is 22 nmol mol^{-1} with a range of 19–32 nmol mol^{-1}.

In the Northern Tropics in the 1950's to 1970's surface ozone observing sites are Fort Lamy in Chad, Africa (12°N), from the TROZ network (Fabian and Pruchniewicz, 1977), Pune (Poona) 19°N and Ahmedabad, 24°N in India (Tiwari and Sreedharan 1973; Naja and Lal 1996) and Mauna Loa, Hawaii 20°N (Price and Pales, 1963) (**Table 6**). The weighted mean of these observations in the Northern Tropics is 23 nmol mol^{-1} with a range from 16–31 nmol mol^{-1} for the period 1950–1975.

In the Southern Tropics in the 1950's to 1970's surface ozone sites of Luanda, 9°S, Sa da Bandeira 15°S, Alexander Bay 28°S and Windhoek 23°S are from the TROZ network and all are located in Africa (Fabian and Pruchniewicz, 1977). The weighted mean of these observations in the Southern Tropics is 18 nmol mol^{-1} with a range from 14–24 nmol mol^{-1} for the period 1970–1975.

In the Southern Temperate region in the 1950's to 1970's surface ozone sites are Hermanus, South Africa 34°S (Fabian and Pruchniewicz, 1977), 20 days measurements during campaigns at locations in south east Australia, ~34°S (Galbally, 1968, 1970, 1971, 1972) and two years of measurements at Macquarie Island 54°S, south of New Zealand (Galbally and Roy, 1981). The weighted mean of these observations in the Southern Temperate region is 22 nmol mol^{-1} with a range from 21–25 nmol mol^{-1} for the period 1967–1975.

Six surface ozone observing sites in the Southern Polar region operated in this period, all in Antarctica. These are Little America (Wexler et al., 1960), Halley Bay (MacDowall, 1962), Hallett and Amundsen-Scott South Pole Station (Aldaz, 1965; Oltmans & Komhyr, 1976), Base Rio Baudouin (Wisse and Meerburg, 1969), and Mirny (Kolbig and Warmbt, 1978) (**Table 5**). The 1958 data from Halley Bay have questionable credibility (Roscoe and Roscoe 2006; see Text S-3). The Amundsen-Scott South Pole Station is at 2835 m altitude, and therefore it is expected, as observed, that the ozone levels there are higher than those at the lower altitude stations. There are several other sites at southern high latitudes that

Table 6: Surface measurements in the tropics and in southern temperate latitudes. Mean values and standard deviations in nmol mol^{-1}. See Text S-7 for Notes. DOI: https://doi.org/10.1525/elementa.376.t6

Location	Period	Method	Reference	Range	Days	Mean (nmol mol^{-1})	SD	Notes
1950s to 1970s Northern Tropics								
50 Ahmedaabad, India 23N, 72.6E, 55 m	June 1954–May 1955	Ehmert	Naja and Lal (1996)	20 ± 6 nmol mol^{-1}	360	20.0	6	22
51 Mauna Loa, Hawaii 19.5N, 156W, 3400 m	August 1957–July 1959	Bowen and Regener (1951)	Price and Pales (1963)	~30 nmol mol^{-1}; winter low 20, spring high 50	670	29.9	7.4	10
52 Pune (Poona), India 18.5N, 73.5E, 560 m	September 1969–August 1970	Brewer bubbler	Tiwari and Sreedharan (1973)	45.8 μg m^{-3}	360	30.9	4.6	9,22,20
53 Fort Lamy 12.1N, 15.0E, 300 m	1970–1974	MPI-Pruch	Fabian & Pruchniewicz (1977)	33.4 μg m^{-3}	1264	15.6	3.7	14
				Weighted mean		**21.9**		
1950s to 1970s Southern Tropics								
54 Alexander Bay 28.6S, 16.5E, 21 m	1970–1974	MPI-Pruch	Fabian & Pruchniewicz (1977)	36.7 μg m^{-3}	1360	17.1	6.5	14
55 Luanda 8.9S, 13.2E, 74 m	1970–1975	MPI-Pruch	Fabian & Pruchniewicz (1977)	28.8 μg m^{-3}	1360	13.5	4.5	14
56 Sa da Bandeira 14.9S, 13.6E, 1760 m	1970–1975	MPI-Pruch	Fabian & Pruchniewicz (1977)	34.1 μg m^{-3}	1144	15.9	8.5	14
57 Windhoek 22.6S, 17.1E, 1725 m	1970–1975	MPI-Pruch	Fabian & Pruchniewicz (1977)	50.6 μg m^{-3}	1408	23.6	7.9	14
				Weighted mean		**17.7**		
1950s to 1970s Southern Temperate								
58 Hermanus 34.4S, 19.3E, 13 m	1970–1975	MPI-Pruch	Fabian & Pruchniewicz (1977)	44.3 μg m^{-3}	1464	20.7	5.8	14
59 SE Australia Hay, Mt. Buller, Edithvale	1968–1972	Ehmert plus Mast Brewer	Galbally (1968, 1971, 1972)		20	24.4	n/a	
60 Macquarie Island 54S, 159E, 0 m	1970–1971	Ehmert	Galbally and Roy (1981)	51.2 ± 14.4 μg m^{-3}	730	24.8	6.9	19
				Weighted mean		**22.1**		

operated during this period (for example Oltmans and Komhyr, 1976), but data are currently not available. With the qualifications for Halley Bay, above, the methods used are valid, the sites are presumed free of interfering pollutants and representative of the well mixed boundary layer. The weighted mean of these observations, with the Halley Bay data, is 24 nmol mol^{-1}, with a range from 16–30 nmol mol^{-1} for the period 1957–1966. Without the Halley Bay data, the range is 19–30 nmol mol^{-1}, but the weighted mean remains at 24 nmol mol^{-1}.

3.6. Changes in surface ozone

The sets of observations that pass the 4 data selection criteria imposed here for historical surface ozone observations are presented in **Tables 4–6** and **Figures 2–6**, grouped by region. To quantify the changes of ozone levels from the historical (pre 1975) to the modern period (1990–2014), the historical data are compared to all available modern ozone observations in the same regions, according to the criteria described below. The modern data are extracted from the TOAR Surface Ozone Database and averaged across 5 × 5 degree grid cells at 5-year intevals (Schultz et al., 2017).

The historical observations have been selected to be representative of the well-mixed boundary layer, and the comparable metrics from the TOAR Database for rural stations are daytime average values and daily 8 hour maxima (DMA8). As the "rural" designation in the gridded average product from the TOAR database (Schultz et al., 2017) excludes sites at elevations above 2000 m (because of the typical increase of ozone with altitude) a proper comparison should exclude the measurements at higher mountain sites. In Europe (**Figure 2**) these are Grands-Mulets, Mont Blanc, Jungfraujoch, Zugspitze, Mt. Norikura in Japan and in North America, Capillo Peak. Except for the value of 63 nmol mol^{-1} in 1896 at Grands-Mulets, disregarding these eight points does not substantially change the picture in **Figure 2** (see Figure S-2).

In **Figure 2** there is no evidence of a change in rural background ozone during the historical record (1896–1975), as noted in Section 3.4. The averages for the four historical time periods in **Table 4** differ by less than 3 nmol mol^{-1}. This is in sharp contrast with previous analyses for the historical period and arises mainly due to the application of the 4 criteria to select valid historical data. The difference is due to: (a) the rejection of the Montsouris data, (b) the corrections detailed in **Table 4**, which have raised values for the early UV measurements by as much as 11%; (c) the inclusion of some early data that are not frequently cited and (d) other corrections as noted for Mast Ozone Meter, transmogrifier, and Cauer method data. Interestingly, the overall historical average found here is similar to older well-informed estimates: for example, Fabry (1950) remarks that surface ozone is typically about 20–25 nmol mol^{-1}, with only modest daily variation.

Figure 2 indicates an increase of about 12 or 16 nmol mol^{-1} between the historical record and the modern period, depending on which metric (12-hr daytime average or DMA8) is applied to the modern data. The diurnal variation of surface ozone depends on both the underlying surface and the topography. At remote sites, as are considered here, measurements over flat continental surfaces show a distinct daytime maxima, while measurements over water, snow and ice show little diurnal variation and

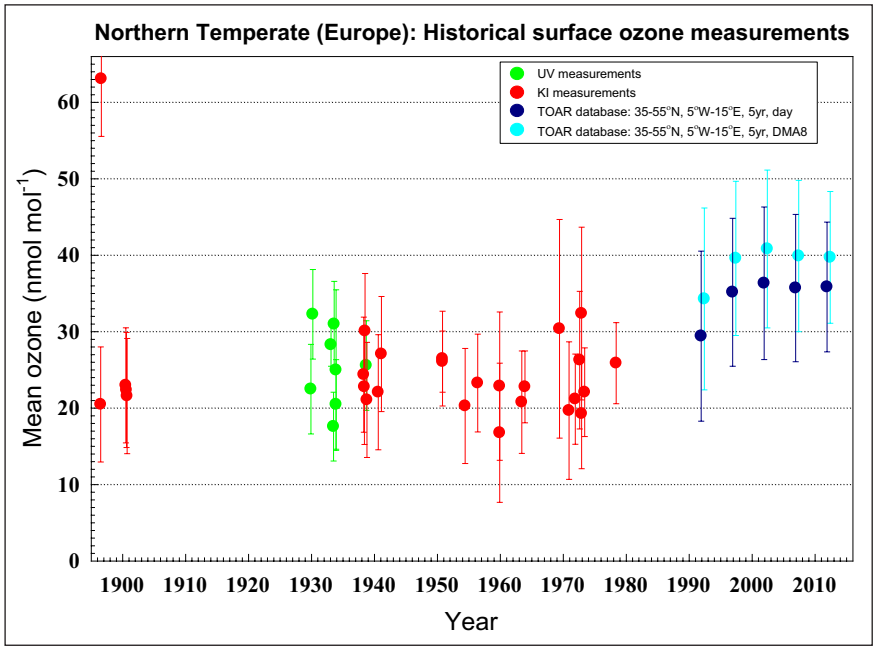

Figure 2: Historical measurements of surface ozone in the Northern Temperate region, 30°N–60°N (30 European, three Asian, one North American and one North African data sets; see Table 4 for details). Error bars represent standard deviations of the measurement averages (atmospheric variability), not uncertainty of the measurement. 5-year averages of modern UV measurements at sites below 2000 m, classified as "rural", in the 5 × 5 degree gridded product from the TOAR database are also shown, both daytime averages (day) and daily 8-hour maxima (DMA8) (Schultz et al., 2017). DOI: https://doi.org/10.1525/elementa.376.f2

measurements from hilltops or from elevated sites in valleys often show night-time maxima. Afternoon averages were chosen for the historical data where available (see **Tables 4–6** and notes above), but in a number of cases only daytime or 24-hour averages were available, and the UV measurements were all made at night, so it is difficult to ascertain whether DMA8 or the 12-hour daytime average is the best metric for comparison. However both show the same behaviour.

In the Northern Polar region (**Figure 3**), and in the Tropics (**Figure 5**), there is also some evidence of an increase, although there are fewer historical datasets with

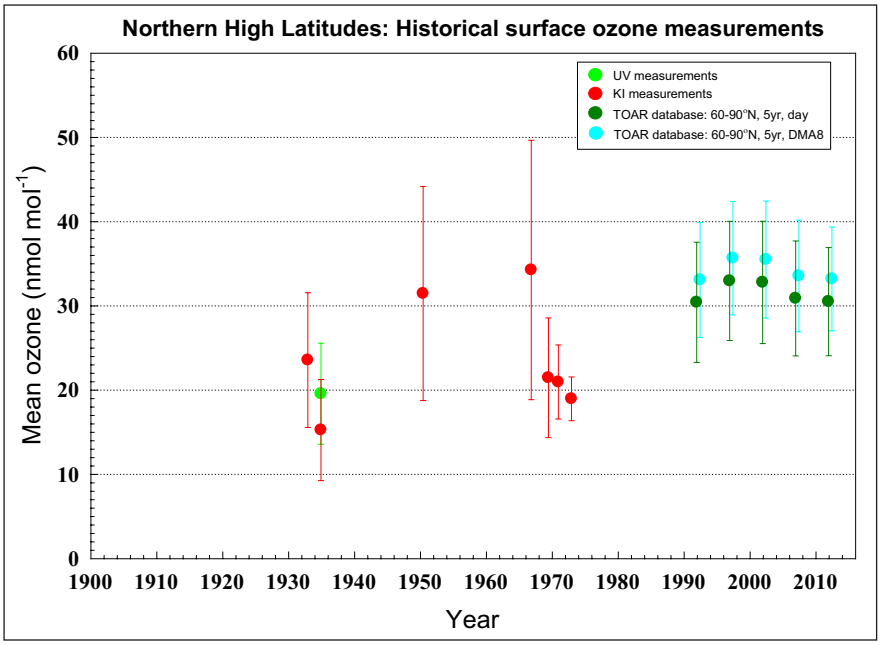

Figure 3: Historical measurements of surface ozone in the Northern Polar region (60°N–90°N; see Table 5 for details). Error bars represent standard deviations of the measurement averages (atmospheric variability), not uncertainty of the measurement. Five-year averages (daytime mean) of modern UV measurements at sites below 2000 m, classified as "rural", in the TOAR 5 × 5 degree gridded average product are also shown, for both daytime averages (day) and daily 8-hour maxima (DMA8) (Schultz et al., 2017). DOI: https://doi.org/10.1525/elementa.376.f3

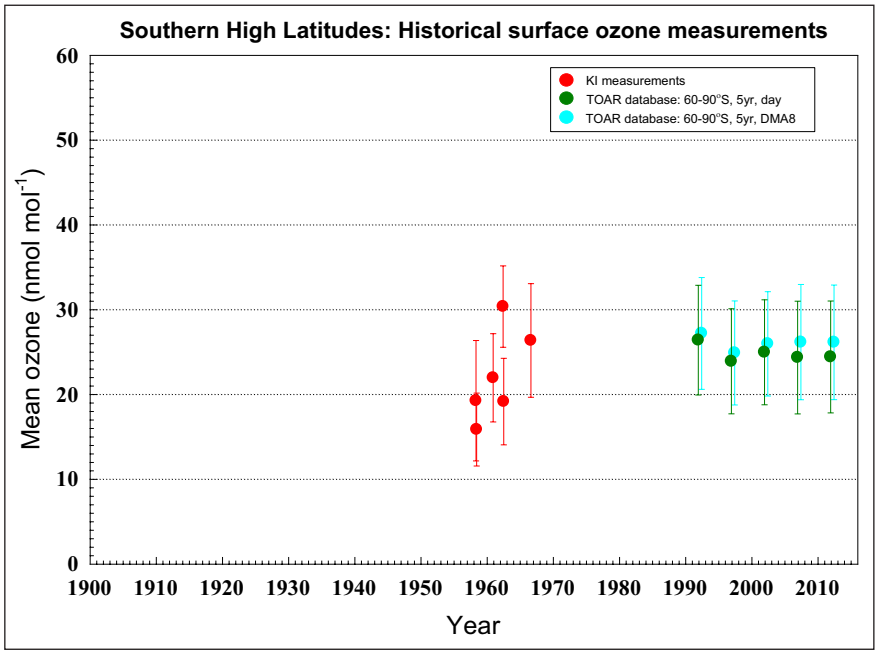

Figure 4: Historical measurements of surface ozone in the Southern Polar region (60°S–90°S; see Table 5 for details). Error bars represent standard deviations of the measurement averages (atmospheric variability), not uncertainty of the measurement. Five-year averages (daytime mean) of modern UV measurements at sites below 2000 m, classified as "rural", from the TOAR 5 × 5 degree gridded average product are also shown, for both daytime averages (day) and daily 8-hour maxima (DMA8) (Schultz et al., 2017). DOI: https://doi.org/10.1525/elementa.376.f4

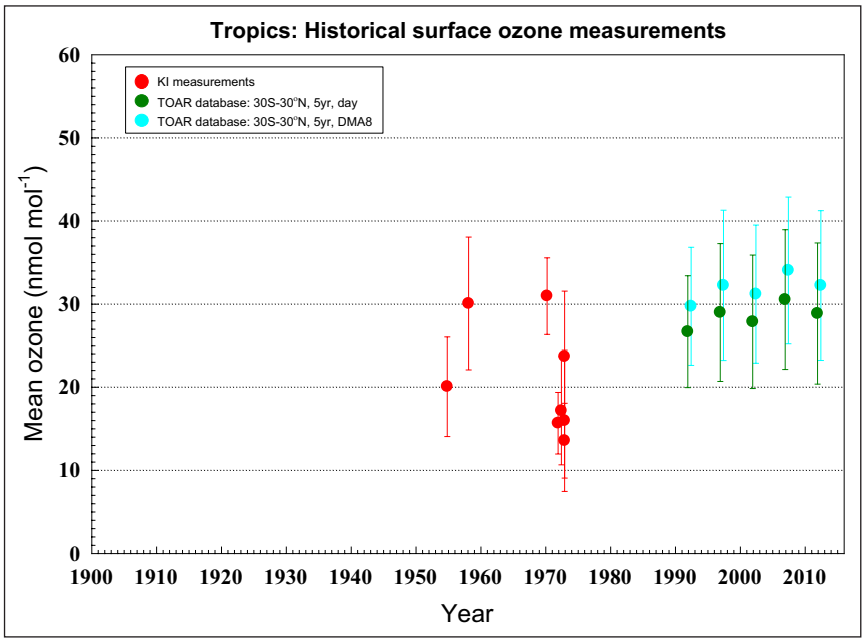

Figure 5: Historical measurements of surface ozone in the tropics (30°S–30°N; see Table 6 for details). Error bars represent standard deviations of the measurement averages (atmospheric variability), not measurement uncertainty. Five-year averages (daytime mean) of modern UV measurements at sites below 2000 m, classified as "rural", in the TOAR 5 × 5 degree gridded average product are also shown, both daytime averages (day) and daily 8-hour maxima (DMA8) (Schultz et al., 2017). DOI: https://doi.org/10.1525/elementa.376.f5

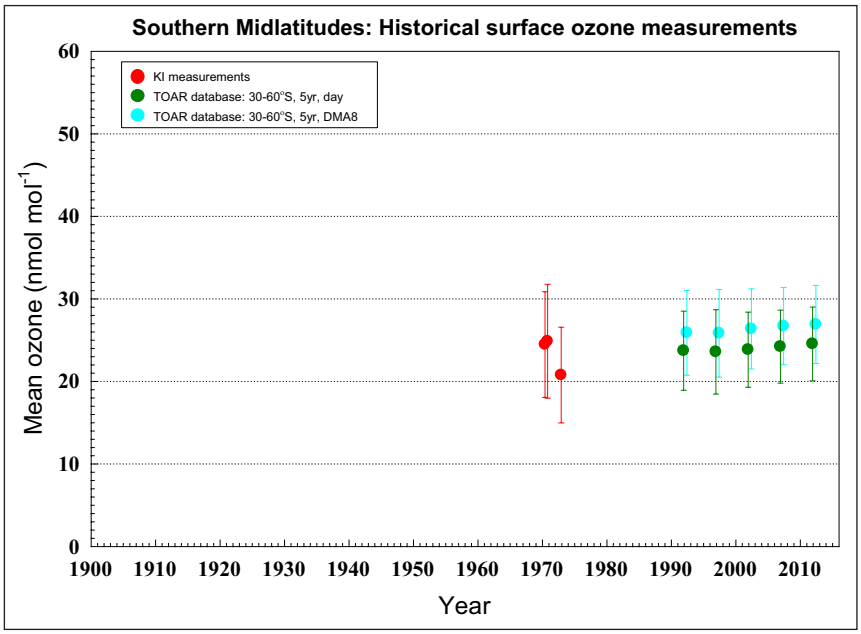

Figure 6: Historical measurements of surface ozone in the Southern Temperate region (30°S–60°S; see Table 6 for details). Error bars represent standard deviations of the measurement averages (atmospheric variability), not uncertainty of the measurement. Five-year averages (daytime mean) of modern UV measurements at sites below 2000 m, classified as "rural", in the TOAR 5 × 5 degree gridded average product are also shown, for both daytime averages (day) and daily 8-hour maxima (DMA8) (Schultz et al., 2017). DOI: https://doi.org/10.1525/elementa.376.f6

which to make the comparison. In the southern hemisphere (**Figures 4** and **6**), there is no clear evidence of a change.

A quantification of the change in ozone mole fraction from the historic to the modern measurements has been performed for each latitude band in **Tables 4**–**6** and is presented in **Table 7**. **Table 7a** presents changes of surface ozone from the historical period to the modern period using all available historical observations below 2000 m elevation. The modern period is based on rural ozone observations below 2000 m for the years 1990–2014, and the metric for the modern data is the 12-hr daytime average. The modern data were extracted from the TOAR Surface Ozone Database and reduced to monthly means

across 5° × 5° grid cells. Within all zones the changes in mean ozone mole fraction are either positive, or there is no clear indication of a change. Together they, along with the comparable data for DMA8 (see Text S-8 and Tables S-2 and S-3), indicate that surface ozone has increased by 30–70% from historical levels to the present in rural air in the temperate and polar regions of the Northern Hemisphere, and negligibly changed in the remote locations in the Southern Hemisphere. Statistical tests were performed using Welch's generalization of Student's *t*-test for unequal variances (Welch, 1947).

As described above and in the Supplemental Material (Text S-3), some of the historical data sets have questionable reliability due to a variety of documented issues. To understand the sensitivity of the results in **Table 7a** to these less reliable data sets, analyses were also performed with all questionable historical data sets omitted (see Text S-8 and Tables S-2 and S-3 for details), and also with all KI-based data omitted (this limits the historical measurements to seven long-path UV data sets in the Northern Temperate region and one in the Northern High Latitude zone). These results (**Table 7b**) are very similar, indicating that the results in **Table 7a** are robust with respect to the choice of historical data sets included in the analysis. Other tests (omitting only the observations from the Fabian and Pruchniewicz (1977) TROZ network, and using the non-parametric Wilcoxon rank sum test (Mann and Whitney, 1947) also yielded similar results (Table S-2), with smaller p-values for the non-parametric test. Comparisons were also made to the modern data using the daily 8-hour maximum (DMA8) metric; as expected these increases are about 20% larger (Table S-3).

The modern set of measurements utilized for this analysis is comprised of all rural sites with surface ozone measurements within the geographical boundaries of the region. There is considerable variability in the behaviour

Table 7: (a) Change of ozone from the historical period to the modern period based on all available historical observations below 2000 m elevation. Results in bold font are different from zero at the 95% confidence level. For the Northern Temperate zone, historical data were compared with modern data for a large region covering western Europe (16 5° × 5° grid cell averages), and also for a single 5° × 5° grid cell which encompasses most of the historical observations from western Europe. For the latter comparison monthly means from the individual rural sites were used, rather than a single average across the grid cell. **(b)** As for Table 7a, but with all questionable historical data sets omitted; in addition, results are shown for the Northern Temperate and Northern High Latitude zones with historical data sets limited to those that measured ozone via long-path UV methods. For details of the analysis and data sets used, see Tables S2 and S3. DOI: https://doi.org/10.1525/elementa.376.t7

(a) Region	Historical ozone[1]	Modern[1]	Ozone change[2]	p
Northern High Latitude	23.1 (8)	30.5 (21)	**31.8% (2.9%, 60.7%)**	**0.05**
Northern Temperate (35–55°N and 5°W–15°E)	23.6 (27)	36.1 (16)	**53.1% (29.8%, 76.4%)**	**<0.01**
Northern Temperate (45–50°N, 5–10°E, individual sites)	23.6 (27)	32.5 (23)	**37.8% (22.8%, 52.8%)**	**<0.01**
Northern Low Latitude	22.2 (3)	31.8 (12)	**43.4% (9.9%, 76.9%)**	**0.04**
Southern Low Latitude	17.5 (4)	16.3 (5)	–7.0% (–54.8%, 40.8%)	0.78
Southern Temperate	23.3 (3)	23.5 (10)	0.8% (–34.3%, 35.8%)	0.97
Southern High Latitude	20.5 (5)	24.1 (6)	17.9% (–17.2%, 52.9%)	0.34

(b) Region	Historical ozone[1]	Modern[1]	Ozone change[2]	p
Northern High Latitude	19.4 (3)	30.5 (21)	**57.1% (15.2%, 99.0%)**	**0.04**
	19.4 (1) *UV data only*	30.5 (21)	57.1%	
Northern Temperate (35–55°N and 5°W–15°E)	23.6 (22)	36.1 (16)	**52.9% (29.4%, 76.4%)**	**<0.01**
	24.4 (7) *UV data only*	36.1 (16)	**47.7% (16.9%, 78.5%)**	**0.01**
Northern Temperate (45–50°N, 5–10°E, individual sites)	23.6 (22)	32.5 (23)	**37.6% (22.4%, 52.9%)**	**<0.01**
	24.4 (7) *UV data only*	32.5 (23)	**33.0% (9.3%, 56.6%)**	**0.03**
N Low Latitude	25.5 (2)	31.8 (12)	24.8% (–10.2%, 60.0%)	0.30
Southern Low Latitude	N/A			
Southern Temperate	24.6 (2)	23.5 (10)	–4.6% (–46.5%, 37.4%)	0.86
Southern High Latitude	21.6 (4)	24.1 (6)	11.6% (–24.9%, 48.0%)	0.56

[1] Values indicate mean ozone in nmol mol^{-1}; sample size (for historical data = number of sites) in parentheses.

[2] Values indicate the percent change in mean ozone from the historical to the modern period with the confidence interval in parentheses, for the 12-hr daytime mean metric, using Welch's *t*-test.

and levels of ozone in both rural surface air and the lower atmosphere within Europe (Chevallier et al. 2007, Lyapina et al., 2016). To test the sensitivity of these calculated changes to the choice of modern data sets, two domains were selected to represent the modern ozone observations for the Northern Temperate region. The first domain covers most of Western Europe and utilizes monthly mean observations from 16 grid cells, each 5° × 5°. The second domain focuses on a single 5° × 5° grid cell that encompasses most of the historical ozone observations from Western Europe, especially those that were based on UV methods. Within this single grid cell monthly means from the individual rural sites were used.

The differences in the estimated changes for the Northern Temperate region, based on these two modern domains are notable, both in **Table 7a** and **7b**. However, for both modern domains the differences between **Table 7a** and **7b** are quite small. This suggests that the uncertainty in the estimated increases in **Table 7** depends more on the modern region chosen for comparison than on the historical data. Data representativeness thus seems to be the more important source of uncertainty.

It is therefore not surprising that the increases determined here are different from some past analyses (e.g. Parrish et al., 2012, 2014). Past analyses have used data from a few selected stations with long-term records, while this analysis has used all available historical and modern measurements. A more detailed matching of co-located historical and modern sites will provide additional insight and is being undertaken.

In the southern hemisphere, there is little evidence for an increase of ozone from the historical to the modern period.

It is worth emphasizing that these results do not depend on particular individual records, as has been noted with regard to several data sets judged to be of questionable credibility; indeed, if only the long-path UV measurements are retained, the increase in Europe is in the range 33–48%, with p-values between 0.01 and 0.03.

In summary, our best estimate for the increase of ozone at northern temperate and high latitudes is a range of 32–53%, based on all historical measurements, using the 12-hour daytime average as the modern metric, and 43–71% using the daily 8-hour maximum metric. These increases are different from zero at the 95% confidence level. Similar results are found using non-parametric statistical tests, and for calculations using (the most reliable) subsets of the historical data.

4. Free tropospheric measurements

Many of the measurement techniques described in Section 2 have been applied to measurements in the free troposphere through balloon and aircraft profiling, and more recently through ground and satellite-based remote sensing. Recent studies have examined free tropospheric ozone data quality issues by comparing time series of surface observations with commercial aircraft and ozonesonde profiles from nearby locations (Logan et al., 2012; Tanimoto et al., 2015). In some cases laboratory and field intercomparisons can provide information about instrument response changes with time (e.g. (Attmannspacher and Dütsch, 1970, 1978; Hilsenrath, 1986; Kerr et al., 1994; Smit et al., 2007). The different methods and their biases and uncertainties as established through intercomparisons are each reviewed, and related to the UV standard.

4.1. Early measurements

Historical observations of free tropospheric ozone that pass the relevant data selection criteria are presented in **Table 8** and **Figure 7**. The first direct measurement of ozone from a balloon ascent was made with three flights near Stuttgart, Germany in 1934 (Regener and Regener, 1934). A quartz UV spectrograph was used to observe the change with altitude of the total amount of ozone above the balloon. The derived profile increases very smoothly from a value equivalent to 40 nmol mol^{-1} near the ground to ~180 nmol mol^{-1} at 10 km; this integrates to about 40 Dobson units (DU) below 10 km.

A similar differential method was used on the manned flight of the high-altitude balloon Explorer II on November 11, 1935 in the western USA. This showed very little ozone below the tropopause: less than 10 DU (O'Brien et al., 1936; reported in Craig, 1950 and Fabry, 1950). This first flight also showed an unusually sharp tropopause.

Additionally, ozone measurements using wavelengths 310–330 nm were made on two unmanned balloon flights in Germany on 30 October 1937 and 11 December 1937 by Regener (1938a). These appear to have been more sensitive (reduced stray light) and found a good deal of variation in the troposphere, with maximum values that correspond to ~110 nmol mol^{-1} at 3 km. These high values are questioned by Fabry (1950), who also points out that the differencing method is subject to large errors below the tropopause, where changes are small. However, 0–10 km column amounts of 23 and 37 DU on the ascent and descent of 30 October 1937 and 15 DU on both the ascent and descent of 11 December 1937 (Regener 1938) compare well, on average, to November averages of 1–10 km columns measured over Europe by ozonesondes since 1990 (27–35 DU). These estimates of historical ozone levels include a 10% upward correction for the ultraviolet absorption coefficients used (Lauchli, 1928, 1929). The large variation between the ascent and descent of 30 October 1937 is probably an indication of the uncertainty of the differencing method, since it is unlikely that ozone changed by that much in less than a day.

Coblentz and Stair made a series of 19 balloon launches in 1938–40 from the eastern USA with a filter-based optical ozonesonde using wavelengths 290–330 nm (Coblentz and Stair, 1939, 1941); average values correspond to ~24 nmol mol^{-1} in the lower troposphere and ~96 nmol mol^{-1} near 10 km. These estimates include a 13% upward correction for the ultraviolet absorption coefficients used (Ny and Choong, 1933 and Fabry and Buisson, 1931).

In the early 1950s Paetzold (1955a, b) conducted 32 balloon flights with a UV spectrograph using wavelengths 295–318 nm, over Weissenau, Germany, of which 25 gave results in the 0–10 km region. From the cross-sections he

Table 8: Historical measurements of free tropospheric ozone (0–10 km column) in Europe and North America. Mean values and standard deviations in DU. See Text S-7 for Notes.
DOI: https://doi.org/10.1525/elementa.376.t8

Location	Period	Method	Reference	Range	Profiles	Mean (DU)	SD (DU)	Notes
1933–1955 Northern Temperate								
Stuttgart 48.8N, 9.2E	26 June, 7, 31 July 1934	Differential UV	Regener and Regener (1934)	40 DU	3	40	n/a	24
Rapid City 44.1N, 103.2W	28 July 1934; 11 November 1935	Differential UV	O'Brien et al. (1936)	10 DU	2	10	n/a	25
Friedrichshafen 47.7N, 9.5E	30 October 1937; 11 December 1937	Differential UV	Regener (1938a)	15–37 DU	4	22.5	10.4	26
Beltsville 39.0N, 76.9W	June 1938, 1939, 1940	Differential UV	Coblentz and Stair (1939, 1941)	22–40 DU	11	28	10.4	27
Darmstadt 49.9N, 8.7E	August 15–25, 1942	KI	Ehmert (1949)	11–19 DU	5	14.4	3.4	28
Weissenau 47.8N, 9.6E	February 1953–May 1954	Differential UV	Paetzold (1955a, b)	0–50 DU	31	22.3	12.8	29
Tromso 69.6N, 19.0E	May–July 1955	Ehmert	Brewer (1955)	24–44 DU	4	33.2	8.3	30

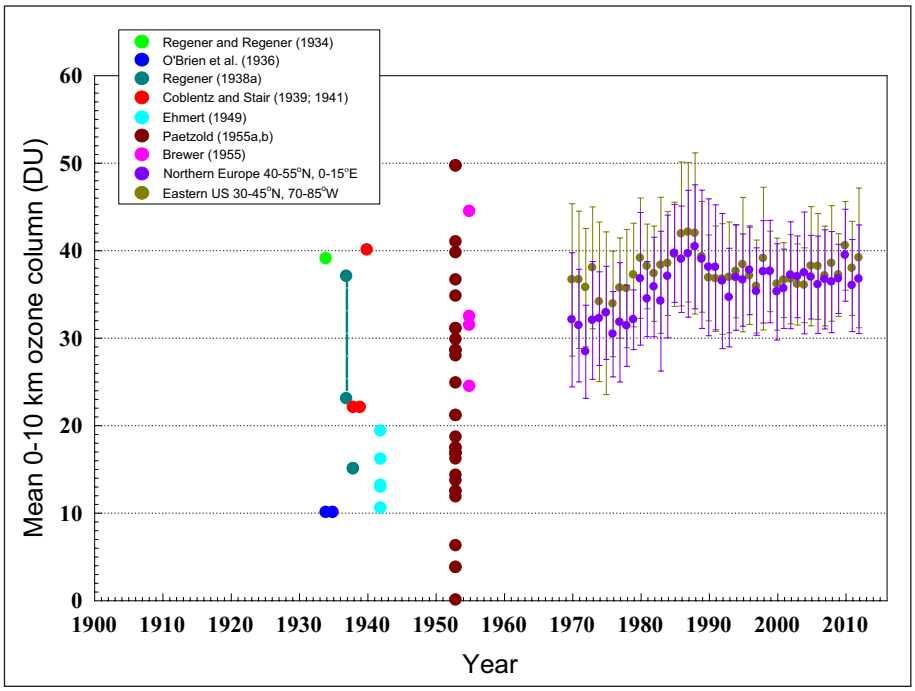

Figure 7: Historical measurements of free tropospheric ozone. Values shown are integrated 0–10 km ozone amounts. The difference between the ascent and descent of 30 October 1937 (dashed line) is probably an indication of the uncertainty of the differencing method, since it is unlikely that ozone changed by that much in less than a day. The modern values shown are annual averages for the 15° × 15° regions around the locations of most of the historical ascents (northern Europe and the eastern US), calculated from ozonesondes using the TOST product (Section 4.4). The error bars indicate standard deviations of the monthly averages (atmospheric variability), not uncertainty of the measurement. DOI: https://doi.org/10.1525/elementa.376.f7

quotes for 306 and 318 nm an estimated 24% upward correction is required, so that these flights show a seasonal maximum in April of 27 DU and a minimum in October of 15 DU, and an extreme range of 0–50 DU for the 0–10 km ozone amounts.

In 1942, ozone sampling with a wet chemical technique was conducted on 6 aircraft flights over Germany giving ozone profiles up to 9 km (Ehmert 1949). Subsequently Kay (1953) and Brewer (1955) presented data using the Ehmert method from aircraft flights over the UK and Norway. The former are quite low, and failed to detect the tropopause, possibly because of losses in the intake (Brewer, 1955). These data are excluded based on criterion 4. The latter show an average profile increasing from 30 nmol mol^{-1} at launch to ~95 nmol mol^{-1} just below the tropopause, very similar to a typical contemporary profile.

While some data sets show a large variability (e.g. Paetzold 1955a, b), the approach here is to include all of the early measurements that meet the relevant selection criteria (1, 2 and 4). The weighted mean of the observations in **Table 8** is 23 DU, with a range of 0–50 DU for the period 1934–1955.

The corresponding modern average 0–10 km tropospheric column amount of ozone is 36 DU, for both the northern Europe and the eastern US regions in **Figure 7**. When the historical datasets are treated as separate observations with equal weight (as for the surface data in Section 3.6), the estimated increase in free tropospheric ozone in the temperate Northern Hemisphere is 47.4 ± 30% (*t*-test) or 47.9 ± 28% (Wilcoxon test), where the uncertainty indicates a 95% confidence interval. The increase is consistent with the increases inferred for surface ozone at northern midlatitudes. This free tropospheric increase is significant for climate studies, since it is primarily ozone in the upper troposphere that contributes to radiative forcing (IPCC, 2001).

4.2. Umkehr

Umkehr measurements rely on the fact that the scattering intensity of solar UV (effective scattering height) changes with solar zenith angle (SZA). Since most of the ozone in the atmospheric column is in the stratosphere, the information content of the tropospheric part of the retrieval is limited, and only ~50% or less of the information in layer 1 (1000–250 hPa in the standard retrieval) comes from the troposphere (Stone et al., 2015; Text S-9), while the rest of the information comes from the adjacent stratospheric layers.

In 1932–33 a series of 46 Umkehr profiles were made at Arosa, Switzerland (Götz et al., 1934) for determining the atmospheric profile of ozone. These yielded estimates of ~30–70 nmol mol^{-1} at 2 km, ~80–100 nmol mol^{-1} at 5 km and ~180–220 nmol mol^{-1} at 10 km. These values are high compared to modern measurements, but carry a substantial uncertainty due to stratospheric influence, and are therefore excluded from the analysis of Section 4.1.

The accuracy of Umkehr profile retrievals has improved with time as a result of modifications to the retrieval algorithm and better a priori information from ozonesonde and satellite-derived climatologies. Early comparisons

(Kulkarni and Pittock, 1970) indicate a high bias of ~45% in the troposphere (likely in part due to the bias to lower response of the Brewer-Mast sondes; see Section 4.3). A 1989 field study (Komhyr et al., 1995) comprised of 6 morning and 6 afternoon co-incident Umkehr and ozonesonde measurements found tropospheric ozone in Umkehr profiles to be on average 16% low against ECC sondes launched in the morning, and 29% high in the afternoons. In a 2004–2005 comparison, 60 co-incident Umkehr and ozonesonde profiles taken at Belsk, Poland showed on average a slight (~2% ±25%) low bias of the Umkehr partial ozone column below 250 hPa, relative to the sonde column (Krzyścin and Rajewska-Więch, 2007). Umkehr profile measurements are currently made twice daily, at ~16 sites worldwide (**Figure 8**).

4.3. Ozonesondes

Ozone soundings were undertaken at a global network of 11 sites from 1962 to 1966 by the US Environmental Science Services Administration. This network operated in parallel with a North American network of 13 sites, coordinated by the US Air Force Cambridge Research Laboratories from 1963–1965. Together these networks released over 2000 Regener, Brewer-Mast and carbon-iodine sondes (Komhyr and Sticksel, 1967, 1968; Hering, 1964; Hering and Borden, 1964, 1965, 1967). Regener chemiluminescent sondes were used regularly for only a brief period in the 1960s, as they showed somewhat erratic response, with an average bias of about –40% in the troposphere (Chatfield and Harrison, 1977; Wilcox, 1978; Hering and Dütsch, 1965). Regular chemical ozone soundings at a number of sites in Europe, North America, Australia and Antarctica began in the latter half of the 1960s. Balloon-borne ozonesondes therefore provide the longest time series of the vertical ozone distribution throughout the troposphere. However, ozone soundings are limited in spatial and temporal coverage. Routine ozonesonde launches have been made at less than 100 stations worldwide; these are unevenly distributed, although this is much improved since the introduction of the Southern Hemisphere ADditional OZonesondes (SHADOZ) network in the 1990s. Launch frequency is typically weekly, and at most 2–3 times per week. Vertical resolution is high: the ozone sensor response time (e^{-1}) of about 25–40 seconds (Smit and Kley, 1998) gives the sonde a vertical resolution of about 100–200 metres for a typical balloon ascent rate of 4–5 m s^{-1} in the troposphere.

All "modern" sonde types – ECC, Brewer-Mast (BM), Brewer-GDR (GDR), Indian and the Japanese KC – use the reaction of ozone with aqueous potassium iodide (KI), which assumes that two electrons are produced for each molecule of ozone, as the method of ozone detection. As discussed in Section 2.1, there can be variations in the stoichiometry of the ozone-iodide reaction. Also, there may be losses of ozone in the pump and of ozone or iodine to the walls of the sensor chamber, as well as iodine evaporation and possibly adsorption to the platinum cathode (Tarasick et al., 2002). Both the GDR and Indian sondes are similar in design to the BM sonde (Brewer and Milford, 1960), while the KC sonde is similar to the early Komhyr carbon-iodine (CI) sonde (Komhyr, 1964; Komhyr et al., 1968). The ECC (Komhyr, 1969) is an electrochemical concentration cell with two chambers connected by an ion bridge. These different instrumental layouts cause differences in response (Smit, 2002) and ozone losses depend both on these differences and on sonde preparation. Losses can be as large as 40% in poorly prepared sondes, although such issues are much less common after about 1980. Slow side

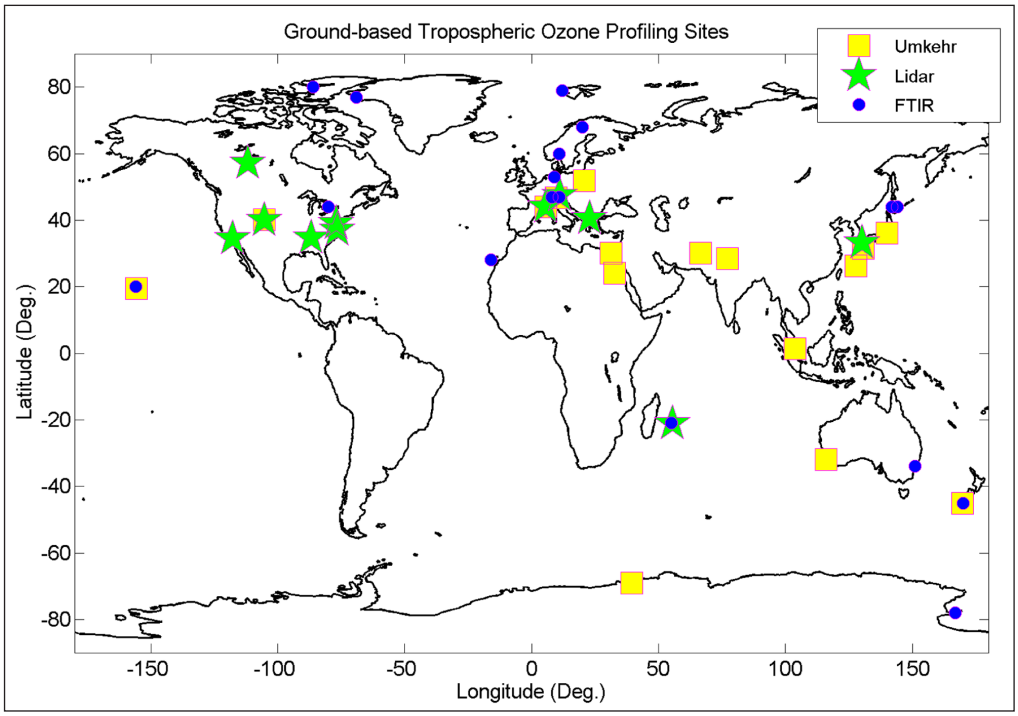

Figure 8: Umkehr, and ground-based DIfferential Absorption Lidar (DIAL) and Fourier Transform Infra-Red (FTIR) sites with measurements of tropospheric ozone. DOI: https://doi.org/10.1525/elementa.376.f8

reactions in the sensing solution can cause excess iodine to be produced (Saltzman and Gilbert, 1959a; Flamm, 1977; Johnson et al., 2002). This effect is modest except when there are sharp ozone gradients, as it causes a slow (~20 min) second-order time response. As for surface KI monitors, interference from other gases can be a problem (generally restricted to the boundary layer) in polluted areas (Schenkel and Broder, 1982; Tarasick et al., 2000). Pump rate or temperature errors, as well as radiosonde pressure biases, will also produce ozone measurement errors (positive or negative), but these are generally small (<1%) in the troposphere. Background currents cause ozone offsets that are typically as large as 5% in the upper troposphere. The use of sensing solutions other than those recommended for each type of ECC sonde can introduce additional biases of 2–8% (Smit and ASOPOS panel, 2011), although these can be corrected. Ozonesondes can, therefore, under certain conditions significantly underestimate ozone concentrations, but it is difficult to explain positive errors larger than about 10–20%.

Ozonesondes record a surface measurement at release time, but this is subject to negative errors if the sonde is not allowed to run for a few minutes after removal of the ozone filter. Also, the sonde is released at about 1 metre above the ground, and strong gradients often exist in the first few metres above the ground (Galbally, 1968). Aliasing from diurnal cycles is also an issue in the planetary boundary layer if release times are variable (Tarasick et al., 2005; Thompson et al., 2014). Ozonesonde profiles are very useful for detecting the transition from the boundary layer to the free troposphere, however.

Numerous field and laboratory intercomparisons of ozonesondes have attempted to characterize ozonesonde biases and uncertainties. These show considerable variability (Text S-10, Figure S-4, Tables S-4 to S-8 and Figures S-5 to S-8) in part due to differences in preparation, and also as in a number of studies a UV reference photometer was not available, and so the results are relative to an average profile, different for each study. A clearer picture emerges if only the comparisons with a UV reference (the modern standard) are retained. This is done for ECC sondes in **Figures 9** and **10**. Several adjustments for consistency are described in the figure caption. Despite the fact that there have been several models of

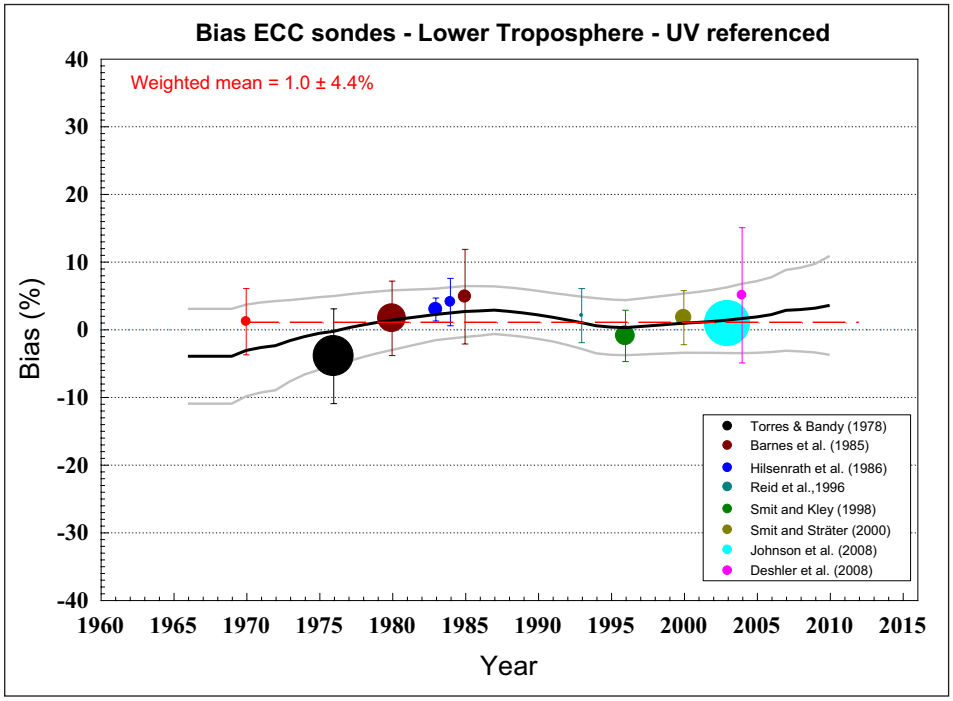

Figure 9: Published intercomparison results of Electrochemical Concentration Cell (ECC) sondes with UV photometer measurements. The symbol size is inversely proportional to the standard error of the mean difference, while the error bars show standard deviations. The curves are running means (weighted by the standard error) of the mean difference (black) and the one standard deviation uncertainty (grey). Included are unpublished data (1980) from Barnes et al. (1985). The 1985 point has been adjusted to account for a positive bias due to the use of 1.5% KI solution (6.2 ±1%, from Barnes et al. (1985) and Peterson (1978)). The 1980 point and that for Torres & Bandy (1978) were not adjusted for this bias, as it apparently was not observed before the early 1980s (as discussed by Barnes et al. (1985)). Instead, following JCGM 100:2008, an additional uncertainty of $6.2/\sqrt{3} = 3.6\%$ has been added to these points. The data from Hilsenrath (1986) are for the NOAA (1% KI) sondes. Data from Smit and Kley (1998) are averaged over all ECC results, and from Smit and Sträter (2004) are an average of results for the two types using recommended solutions (1% for SciPump and 0.5% for EnSci). Sondes were operated according to standard operating procedures for the agency participating. Data after about 1995, with some exceptions, have not been normalized to a total ozone measurement. DOI: https://doi.org/10.1525/elementa.376.f9

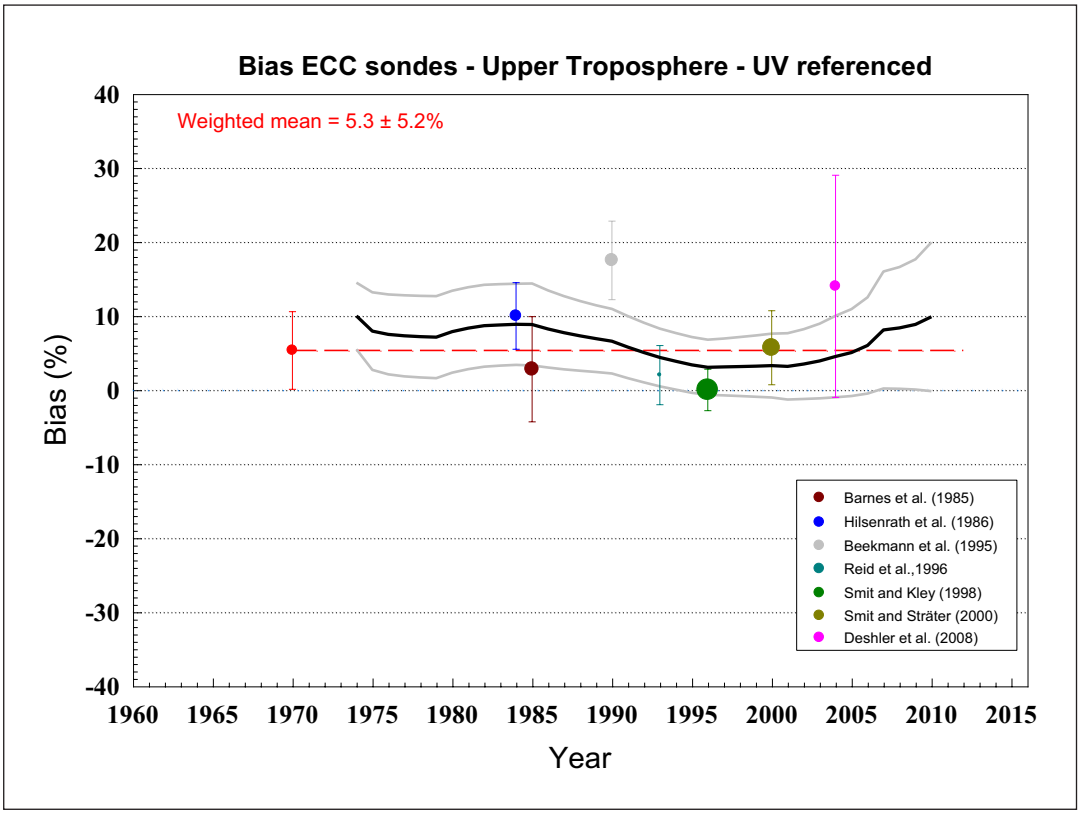

Figure 10: As Figure 9, for the upper troposphere. Beekmann et al. (1995) shows a very high bias; the normalized data, corrected for background current (3.5 ± 3.5%) have been used, as suggested. DOI: https://doi.org/10.1525/elementa.376.f10

ECC sondes, the running averages show no significant trend in bias over the 50-year period, despite the model changes. This is independent of normalization to coincident total ozone measurements, as normalization factors at most long-term sites show no trend. A mean offset, weighted by the standard error of each point is therefore found (shown as a red dashed line). Using the ECC sondes as a transfer standard, this value is then used to transfer the UV reference to the bias results for other sondes, for intercomparisons without a UV reference photometer (**Figures 11**–**14**). The calculated uncertainty of this weighted mean is also added, and we note that this may be an underestimate, as sample sizes in intercomparisons are small, and experimental conditions may not reflect the full range of conditions found in long-term field operations.

The result (**Figures 11** and **12**) indicates that the BM sonde shows an increase in tropospheric response of about 20% between the 1970s and the 1990s. Improved preparation procedures for BM sondes (Attmannspacher and Dütsch, 1978; Claude et al., 1987; DeBacker, 1999; Favaro et al., 2002; Tarasick et al., 2002) may have contributed to this, and there may have been minor changes in sonde manufacture over the long period of record (World Climate Research Programme, 1998). This is consistent with the conclusion of Schnadt Poberaj et al. (2009), who compared European BM sondes with UV-measurements from the GASP and MOZAIC flights (Sections 4.7 and 4.8, below).

Over the same period, the KC sondes also show a modest increase in tropospheric response (**Figures 13** and **14**).

In addition, although almost all current ozonesonde data are from ECC sondes, the transition to the ECC has been gradual (**Figures 15** and **16**). Since the other sonde types historically show negative biases in the troposphere relative to the ECC sonde (see also Tables S7 and S8), this transition may itself introduce an apparent trend in free tropospheric ozone derived from ozonesondes, if data are combined without adjustments. The BM sondes were used extensively in the 1970s and in Europe in the 1980s, and are currently in use at only one site (Hohenpeissenberg). Large amounts of data prior to the early 1990s exist from the Brewer-GDR, Indian, and the Japanese KC sondes.

Currently, station records are being re-evaluated for artifacts introduced by changes of sonde type, manufacturer, strength of sensing solution, or preparation procedure, under the Ozonesonde Data Quality Assessment activity (Smit et al., 2017). This has resulted in changes to the Canadian record of 2–5% in the 1980–2015 period, and as much as 20% to the pre-1980 BM data (Tarasick et al., 2016). Tropical stations in the SHADOZ network show changes of up to 8% (Witte et al., 2017). A large part of this is due to the fact that after about 1995, stations using the new EnSci sonde with 1% KI solution show a 4–8% positive bias in the lower troposphere and 2–6% in the upper troposphere (Table S-5). Sites in Europe and the US show changes of 1–2% (van Malderen et al., 2016; Witte et al., 2019).

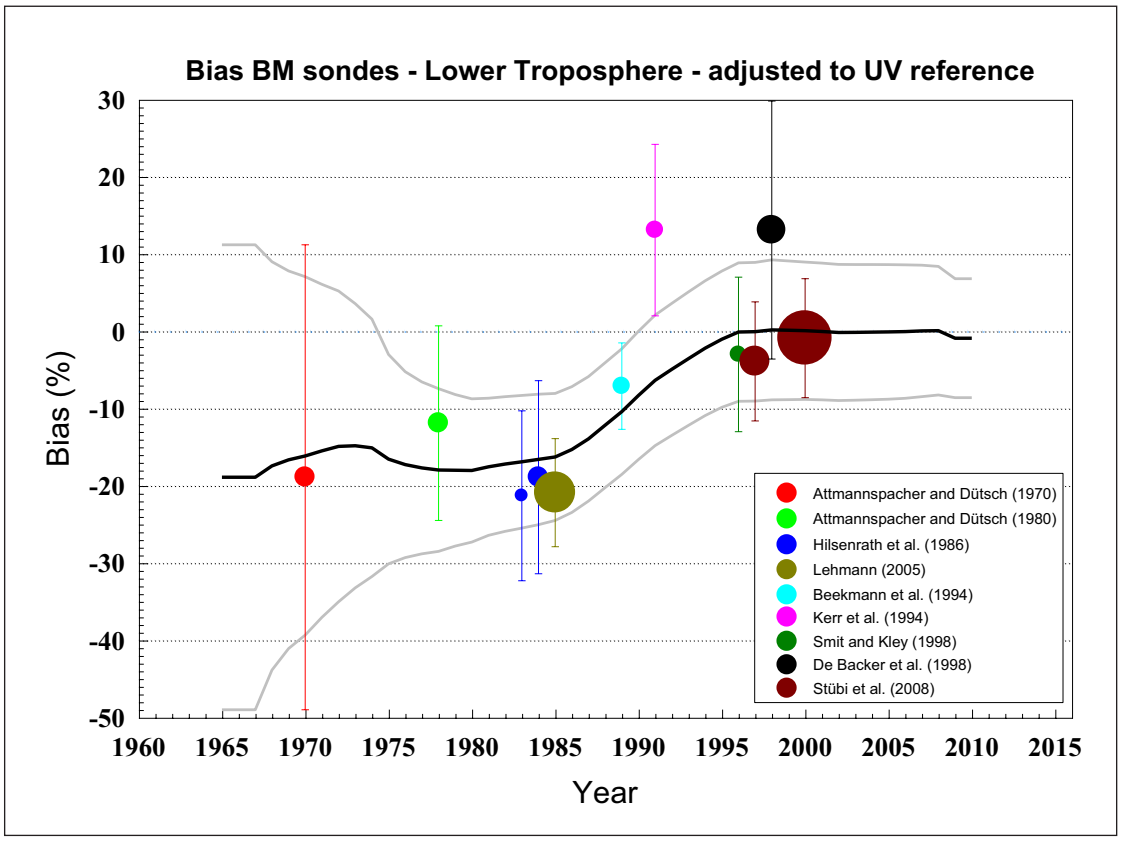

Figure 11: Intercomparison results of Brewer-Mast (BM) sondes. Those without a UV photometer reference have been adjusted to the UV standard using the ECC average bias. Adjusted uncertainties include the quoted ECC uncertainty from the intercomparison, and the bias uncertainty from Figure 9. Lehmann (2005) uses SAGE and Dobson data as a UV reference. Sondes were operated according to standard operating procedures for the agency participating. Profile data were normalized to a total ozone measurement. DOI: https://doi.org/10.1525/elementa.376.f11

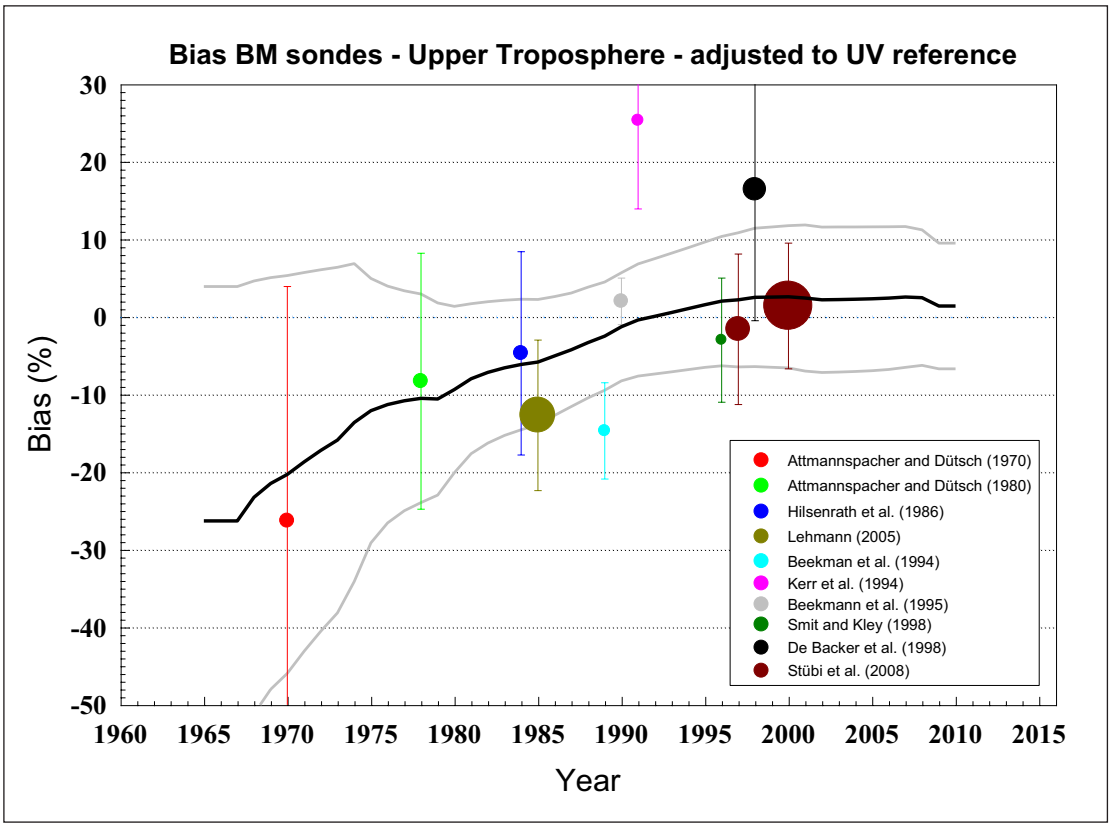

Figure 12: As Figure 11, for the upper troposphere. DOI: https://doi.org/10.1525/elementa.376.f12

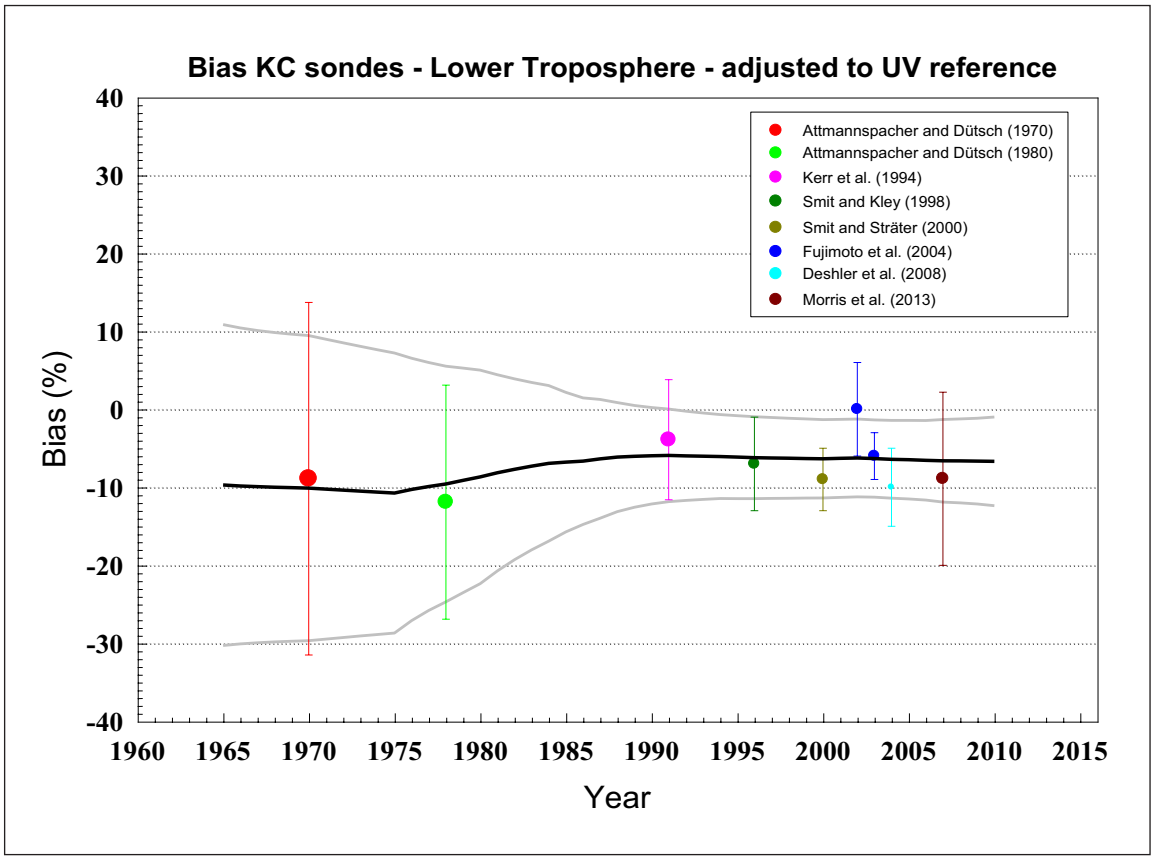

Figure 13: As Figure 11, for Japanese KC sondes. Sondes were operated according to standard operating procedures for the agency participating. Profile data were normalized to a total ozone measurement. DOI: https://doi.org/10.1525/elementa.376.f13

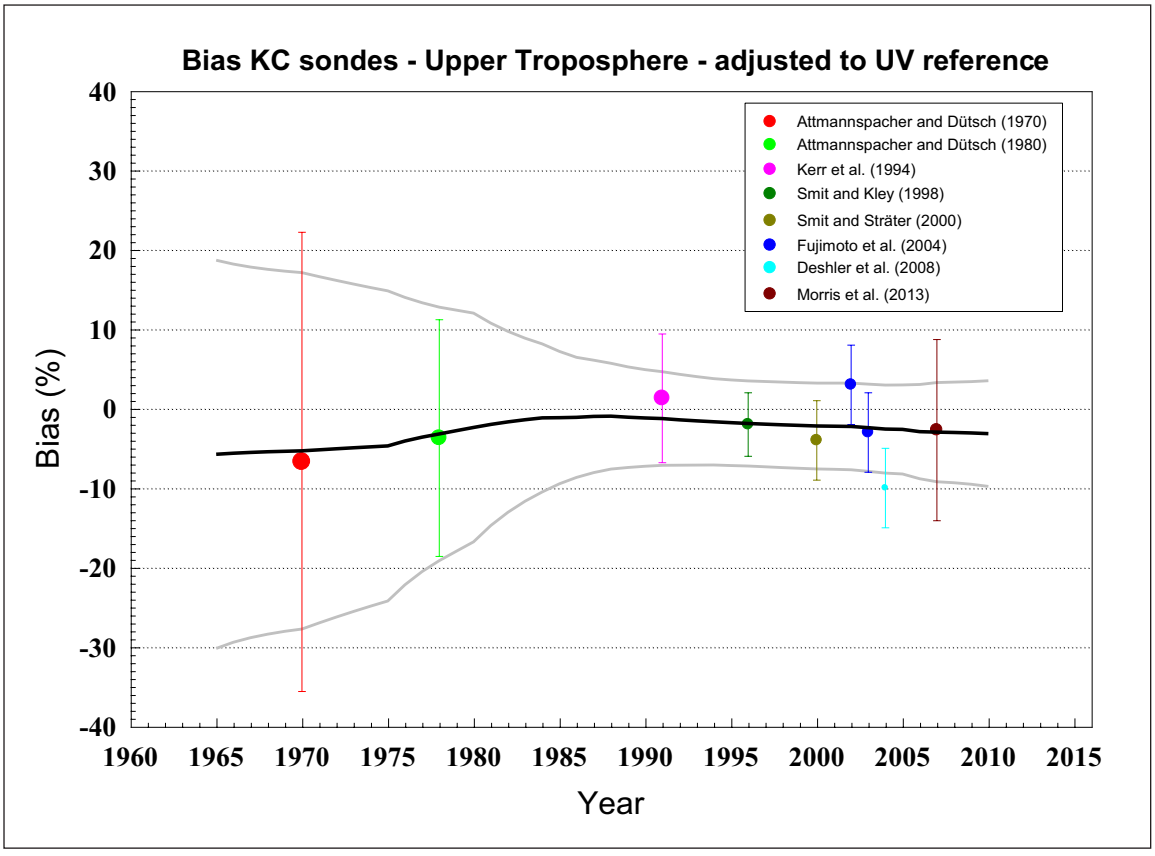

Figure 14: As Figure 13, for the upper troposphere. DOI: https://doi.org/10.1525/elementa.376.f14

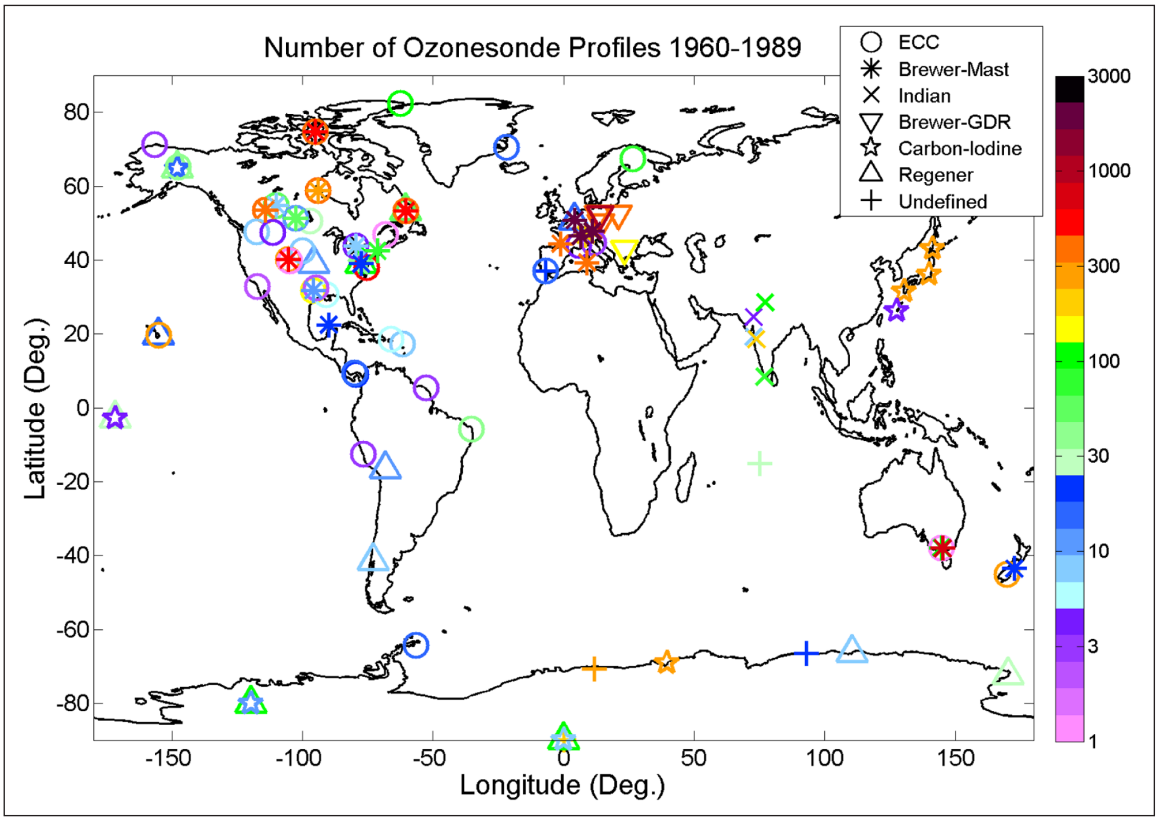

Figure 15: Ozonesonde profiles 1960–1989. The color bar indicates the number of profiles of each type available from each station. Data from the World Ozone and UV Data Centre (WOUDC). Most stations launch weekly; at three sites in Europe launches are three times weekly. DOI: https://doi.org/10.1525/elementa.376.f15

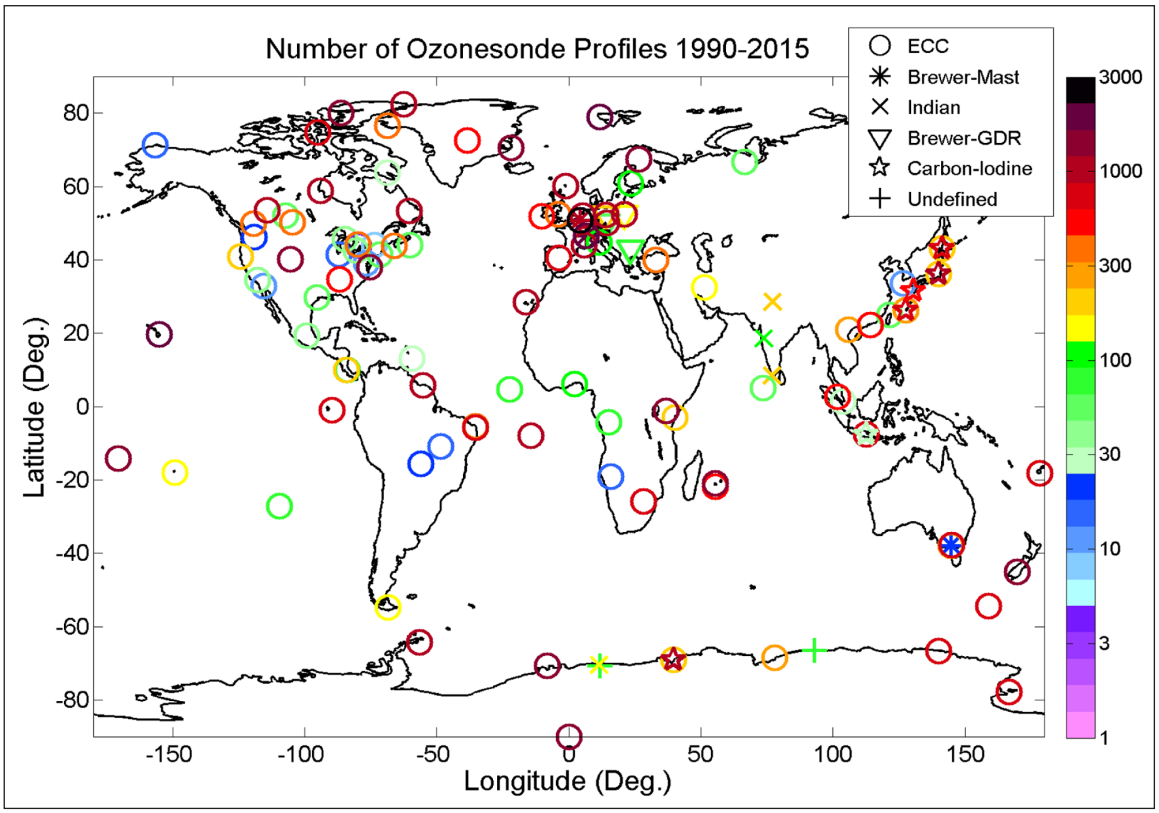

Figure 16: Ozonesonde profiles 1990–2015. The color bar indicates the number of profiles of each type available from each station. Data from the WOUDC and the Network for Detection of Atmospheric Composition Change (NDACC). DOI: https://doi.org/10.1525/elementa.376.f16

4.4. Ozonesonde derived data products

Ozonesonde data are global and long-term, but sparse in space and time. Several products attempt to remedy this deficiency by combining ozonesonde data with satellite ozone data or meteorological information. The ML climatology (McPeters and Labow, 2012; McPeters et al., 2007) uses Microwave Limb Sounder (MLS) data to produce a zonally-averaged climatology in 10° latitude bands from 0 to 65 km. BSVertOzone (Hassler et al., 2018; Bodeker et al., 2013) uses several satellite data sources and a sophisticated regression-interpolation scheme to produce a zonally-averaged climatology in 5° latitude bands from 0 to 70 km.

The Trajectory-mapped Ozonesonde dataset for the Stratosphere and Troposphere (TOST), used elsewhere in this paper and in *TOAR-Climate* (Gaudel et al., 2018), uses the Hybrid Single-Particle Lagrangian Integrated Trajectory (HYSPLIT) model (Draxler and Hess, 1998) and meteorological fields from National Centers for Environmental Prediction (NCEP) reanalyses to fill the gaps between ozonesonde stations, by extending each ozone record along its trajectory path forward and backward for 4 days. Over this 4-day period ozone production and loss is assumed to be negligible. Ozone values along these trajectory paths are binned into a 3-dimensional grid of 5° × 5° × 1 km (latitude, longitude, and altitude), from sea level or ground level up to 26 km (**Figure 17**). Tropospheric column ozone (TCO) is calculated from ozone mole fractions below the tropopause, found using the WMO 2 K/km lapse-rate definition applied to the NCEP reanalysis data.

TOST has been evaluated using individual ozonesondes, excluded from the mapping, by backward and forward trajectory comparisons, and by comparisons with aircraft profiles and surface monitoring data (Tarasick et al., 2010; Liu, G. et al., 2013; Liu, J. et al., 2013). Differences are typically about 10% or less, but there are larger biases in the UTLS, the boundary layer, and in areas where ozonesonde measurements are sparse. The accuracy of the TOST product depends largely on the accuracy of HYSPLIT and the meteorological data on which it is based. Data products are available at http://woudc.org/data/products/#related-ozone-products.

4.5. Tropospheric ozone lidar

UV DIAL (DIfferential Absorption Lidar) technique is a well-established technique for tropospheric ozone monitoring, from as low as 100 m to the tropopause, from ground-based sites (**Figure 8**; Table S-9) or aircraft (Browell et al. 1983, Ancellet and Ravetta, 2003). Differences between existing lidar instruments are in the wavelength choice and number of wavelength pairs used for the ozone retrieval, the size of the telescope or the laser power. Vertical resolution is variable, depending on wavelength choice, signal strength and integration time, but can be as fine as 50–100 m in the lower troposphere. Temporal resolution can be very high (1 min). Temporal coverage is generally limited by the need for human operators. The recent deployment of an autonomous system (Strawbridge et al., 2018), however, removes this handicap.

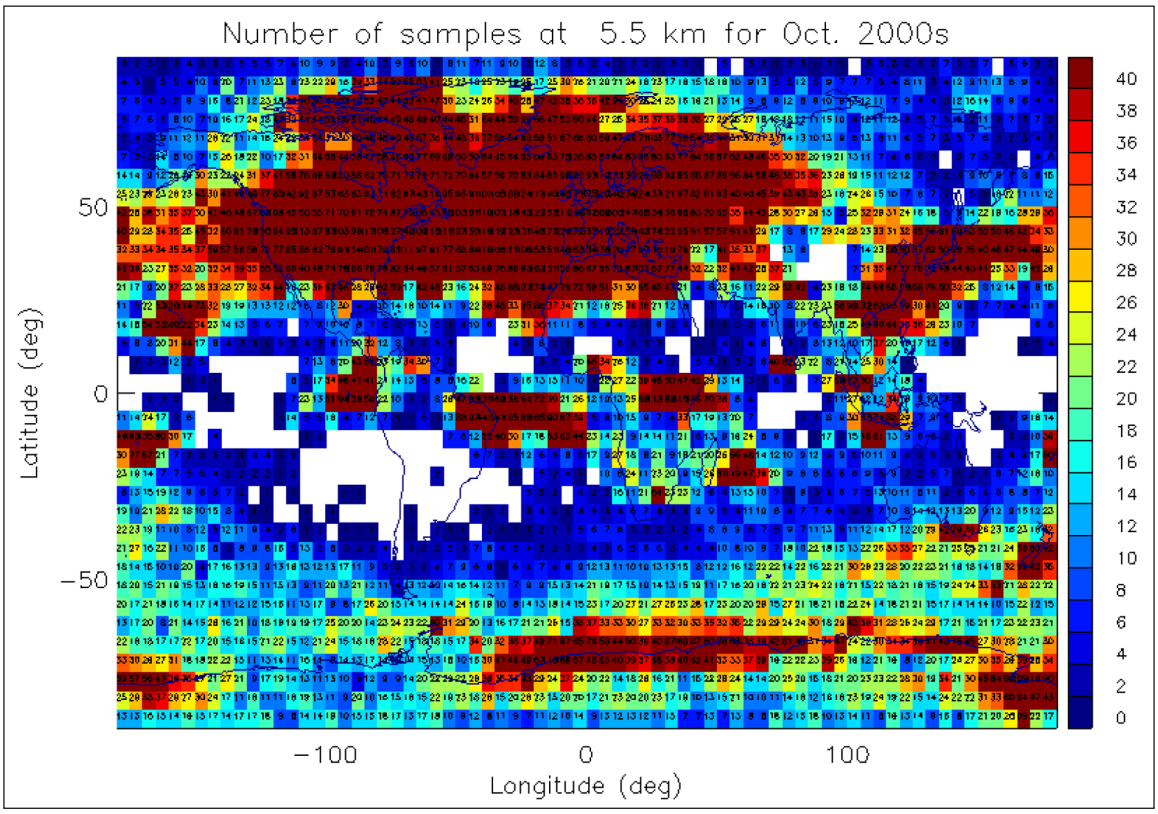

Figure 17: Number of data values resulting from the trajectory mapping averaged in each 5° × 5° × 1 km bin at 5–6 km in the TOST decadal average ozone field for October 2000–2009. The standard errors are generally of the order of a few nmol mol^{-1}, although where data density is low they can be higher. DOI: https://doi.org/10.1525/elementa.376.f17

DIAL errors may arise from electronic interference in the detected signals, unaccounted effects of particulate backscatter and extinction, errors in ozone absorption cross sections, insufficient knowledge of the near-range geometrical overlap function, and errors in the cross-sections or a priori concentrations of interfering atmospheric molecules (Eisele and Trickl, 2005; Leblanc et al., 2016b). Beam misalignment can be avoided by comparing the ozone profiles obtained for different wavelength pairs. Relative uncertainties can be as low as 2–5% in the lower and middle troposphere, for averaging times of ~1 min, if the "on" (i.e. more strongly-absorbed) wavelength selected is below 280 nm (Trickl, 2019). For longer "on" wavelengths, used for higher altitudes, the uncertainties grow, and significantly longer signal averaging or a reduction of the vertical resolution must be applied.

The accuracy of tropospheric ozone measurements using lidar systems has been analysed using three different approaches: 1) a system uncertainty analysis based on estimated uncertainties from component sources, 2) simultaneous differences with other techniques (ozonesonde, UV instruments on aircraft and mountain stations) during intercomparison campaigns, 3) differences between seasonal averages from two instruments over a long time period.

The system uncertainty analysis considers random uncertainty (altitude, resolution and ozone-dependent signal to noise ratio), as well as the sources of systematic uncertainty noted above. Details may be found in Leblanc et al. (2016a, b).

Table 9 summarizes results of the small number of published intercomparison campaigns. The weighted mean of the quoted lidar bias in **Table 9** is approximately 0% ±2% in the lower troposphere, and –3% ±3% in the upper troposphere. The bias is also small below 3 km, but uncertain as lidar systematic errors increase at low altitude (high aerosol load, lidar misalignment).

Several sites (Boulder, Observatoire de Haute Provence, La Reunion (France), Garmisch-Partenkirchen, Huntsville) currently have DIAL running in parallel with other techniques (**Figures 8** and **16**), and so further comparisons are possible.

One example of lidar-ECC comparison results is shown in **Figure 18** for a set of 13 co-located and simultaneous measurements with the Table Mountain Facility (TMF) lidar during the SCOOP campaign (Leblanc et al. 2018). Average agreement is excellent; throughout the profile it is within the theoretical total uncertainty. For the lidar, this includes detection noise, and systematic errors as described above, while for the ozonesonde profiles it is assumed to be 5%.

Gaudel et al. (2015) examined differences between 5-year ozone seasonal averages, using regular, not necessarily simultaneous, lidar and ECC profiles. Over a 20 year period, the ECC sondes averaged about 1 nmol mol^{-1} higher in the free troposphere above 4 km. Seasonal differences fluctuated generally between ±5 nmol mol^{-1}, with a maximum of 11 nmol mol^{-1}, at 6–8 km. This was shown to be due to significant transport differences, correlated with the requirement for clear sky conditions for lidar measurements, inducing a meteorological bias in lidar sampling.

The three different analyses yield results consistent with a precision better than 10% and a slight negative bias of 0–3% with ECC sondes. When adjusted for the mean ECC biases found in Section 4.3, this corresponds to a mean bias of +1% ±8% in both lower and upper troposphere. These results depend on good aerosol and cloud screening, based on the backscatter lidar signal analysis; under these conditions the lidar accuracy (as from these published intercomparison campaigns) is better than that calculated from the system uncertainty analysis.

4.6. Ground-based Fourier Transform Infra-Red (FTIR)

Global FTIR observations are coordinated by the Infrared Working Group of NDACC (Network for the Detection of Atmospheric Composition Change, https://www2.acom.ucar.edu/irwg, www.ndacc.org). Calibration and retrievals for ozone are standardized across the network (Vigouroux et al., 2015). The retrieval follows Optimal Estimation (OE) theory (Rodgers, 2000) and requires a priori data for the atmospheric state and other forward model parameters. A priori atmospheric composition profiles are constant for all retrievals in the time series for a given site. They are derived from climatological runs of the WACCM V4 (Whole Atmosphere Community Climate Model) model. Daily a priori temperature and pressure profiles are from NCEP. The instruments are solar viewing and so observations are biased to clear sky daytime, with seasonal limitations at high latitudes. Typically, several observations are taken per day if there is a clear line of sight to the sun.

Typical degrees of freedom for signal (DOFS) are 4–5 (see Text S-11). Averaging kernels are shown in Figure S-11a (and see Figure 1 of Vigouroux et al. (2015)). They represent the contribution to the retrieval from the measurement. Table S-10 lists stations that obtain at least 0.8 DOFS for the ground – 8 km layer. The remainder of the information is from the a priori best estimate. Those stations with sufficiently long and dense time series are used in *TOAR-Climate* (Gaudel et al., 2018) where most have DOFS (to 8km) >0.9. Only a small portion of this first summed partial kernel is sensitive to the lower stratosphere (Figure S-11b). Further details about the information content of ozone retrievals can be found in Schneider et al. (2008), Vigouroux et al. (2015), and in Wespes et al. (2012) focusing on tropospheric ozone.

Figure 19 shows time series of the partial columns of ozone measured by the FTIR at the Izaña Atmospheric Observatory (IZO), together with columns derived from the coincident ozonesonde profiles. The sondes were launched weekly at Santa Cruz de Tenerife (35 km northeast of IZO) from 1999 to 2006 and at Guimar station (15 km east of IZO) since October 2006. The FTIR data are averaged in a temporal window of 6 hours around the ECC launch time (12 UTC).

Table 10 gives the ozone uncertainty budgets estimated by the OE approach and from ECC sonde intercomparisons at the Izaña Atmospheric Observatory. Uncertainties in the tropospheric columns (from station altitude = 2.37 km for IZO) are shown. Total theoretical random uncertainty

Table 9: Lidar bias and precision derived from intercomparison campaigns between lidar, ozonesonde, aircraft and mountain site simultaneous measurements. Bias and Precision represent means and standard deviations of differences from the ECC sonde profiles. Theoretical accuracy is the expected lidar accuracy from the system uncertainty analysis. (OHP: Observatoire de Haute Provence; GAP: Garmisch-Partenkirchen). DOI: https://doi.org/10.1525/elementa.376.t9

Campaign	Reference	Altitude (km)	Bias	Precision	Theoretical accuracy	Altitude (km)	Bias	Precision	Theoretical accuracy
OHP, 1989: 8 ECC+BM sondes	Beekmann et al., 1994					5–9	−6% ± 3.5%	9%	10%
OHP, 1991: 8 ECC+BM, 8 aircraft profiles	Beekmann et al., 1995	3–8	−4% ± 2%	5%	10%				
Huntsville, 2008: 12 ECC sondes	Kuang et al., 2011	1–6	2.8% ± 0.8%	3%	<10%	6–8	−10% ± 3%	10%	<20%
Saga 2013, 2 ECC sondes	Uchino et al., 2014	2–7	3% ± 2.8%	4%	10%				
OHP, 5-year seasonal mean, ~240 sondes	Gaudel et al., 2015	4–6	−1% ± 1.5%	9%	10%	6–8	−1% ± 2%	9%	10%
TMF, 2016: 15 ECC	Leblanc et al., 2018	3–10	−1.5% ± 10%	4%	10%				
GAP, >20 BM sondes; mountain sites	Trickl, 2019	2–5	0% ± 1.5%	2–5%	2–5%	5–12	0% ± 1.5%	5–20%	5–20%

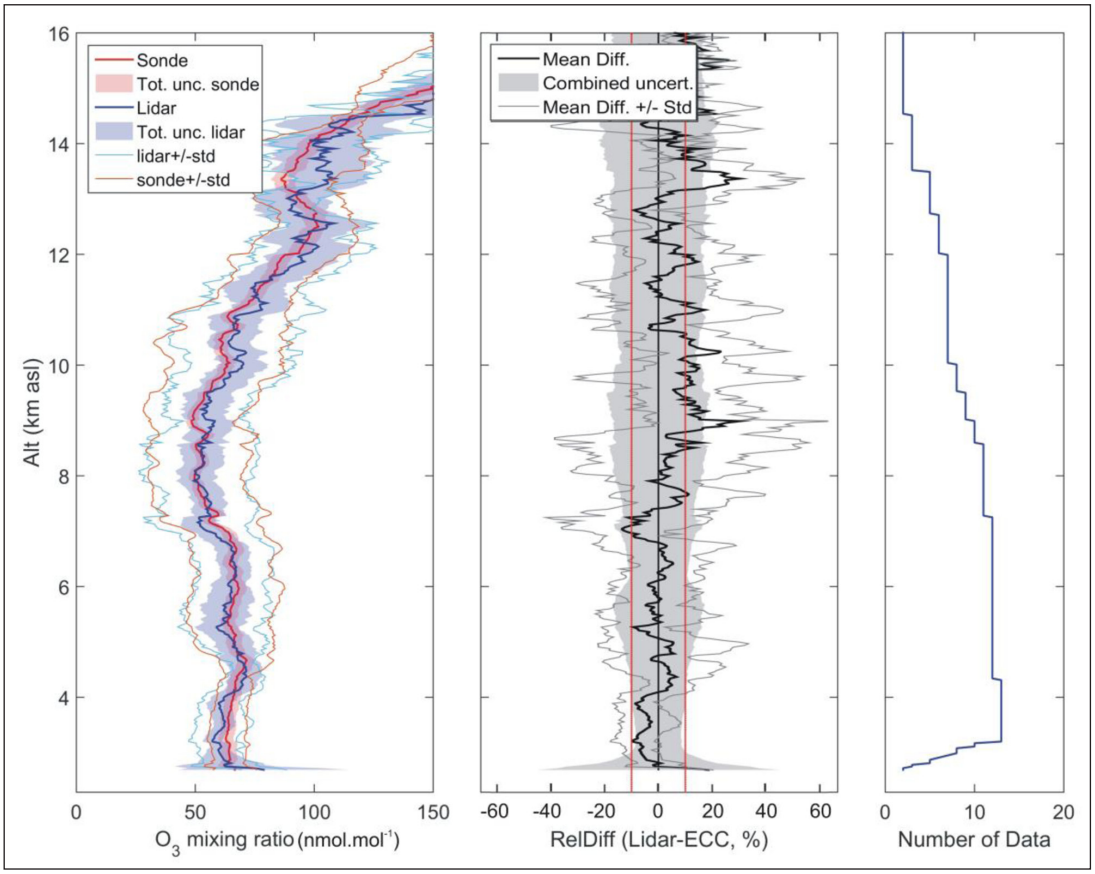

Figure 18: Blind comparison between the Table Mountain Facility (TMF) tropospheric ozone lidar profiles and ozonesonde profiles, from co-located and simultaneous measurements during the SCOOP campaign in August 2016. DOI: https://doi.org/10.1525/elementa.376.f18

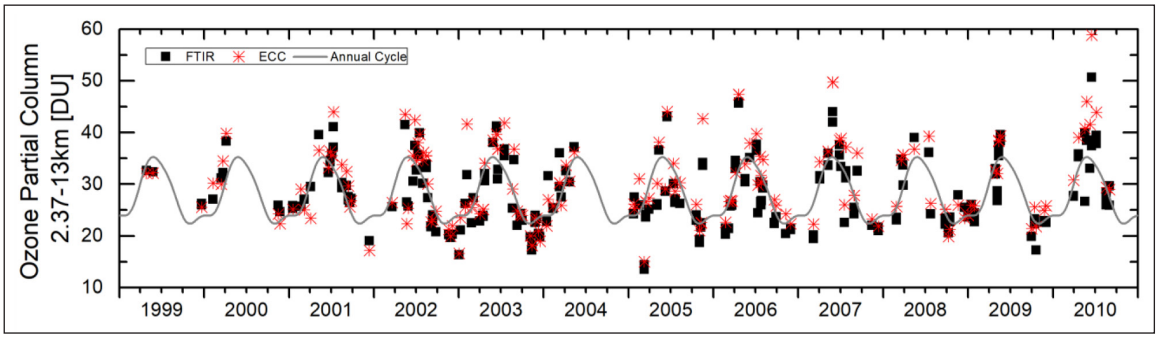

Figure 19: Partial columns (2.4–13 km) measured at Izaña Atmospheric Observatory, with integrated ozone partial columns from ECC sondes at a nearby site. DOI: https://doi.org/10.1525/elementa.376.f19

is estimated as the sum of the random parameter uncertainty and the smoothing uncertainty (associated with the limited vertical sensitivity of the FTIR technique). Significant contributors to the the random parameter uncertainty are uncertainties in the temperature vertical profiles, the instrumental line shape, and the measurement noise, while the systematic uncertainty is dominated by spectroscopic uncertainties (Schneider and Hase, 2008; Schneider et al., 2008; García et al., 2012). The overall theoretical uncertainty of ~11% in tropospheric ozone partial columns is dominated by the smoothing uncertainty.

Smoothing uncertainty is also important in sonde-FTIR comparisons: the scatter (one standard deviation) of the relative differences is reduced from ~9% to ~7% when comparing ECC sonde profiles smoothed with the FTIR averaging kernels.

The mean bias between ozone partial columns from FTIR and ECC sondes of 4%, which can be up to ~6% with alternate retrieval strategies (García et al., 2012), is in excellent agreement with the positive bias of 1–5% (±5%) for ECC sondes found from UV-referenced sonde intercomparison studies (Section 4.3), and with the positive bias of 5–8% found from MOZAIC/IAGOS comparisons (Section 4.8).

Recent laboratory work recommends simultaneous measurements of ozone absorption coefficients in the IR and the UV (Orphal et al., 2016), which will lend further confidence in FTIR methods by tying them directly to the UV standard.

Table 10: Estimated random and systematic uncertainties relative to the FTIR retrieved tropospheric ozone partial column (2.37–13 km) for the Izaña Bruker 120/5HR, obtained by comparing to 515 coincident ECC sondes (García et al., 2012). DOI: https://doi.org/10.1525/elementa.376.t10

	Uncertainty (%)
Theoretical random parameter uncertainty	3
Smoothing uncertainty	10
Total theoretical random uncertainty	~11
Theoretical systematic uncertainty	4
Experimental random uncertainty – ECC sondes	9
Experimental systematic uncertainty: FTIR–ECC sondes	–4

4.7. Ozone measurements from aircraft

In addition to the early measurements described in Section 4.1, observations were made using a KI method by Fabian and Pruchniewicz (1977) on 34 regular airline flights. The first major program of ozone measurements from regular passenger aircraft began after the observation of high ozone inside the cabin of planes flying over the US (V. Mohnen, personal communication). Ozone levels over 350 nmol mol^{-1} were observed on some flights over the US in 1973, and as high as 600 nmol mol^{-1} on polar flights (Bischof, 1973). The problem was exacerbated in 1975 when the long-range Boeing 747 SP was introduced, as this flew higher and further north, and so frequently well into the lower stratosphere. Ozone levels over 600 nmol mol^{-1} were observed frequently and passengers and crew complained of severe headaches and nosebleeds. This became a crisis for airlines, which was initially dealt with by pilot advisories (FAA, 1977) and flight planning to avoid areas of expected high ozone (based on the measurements available in the 1970s). New FAA regulations, AC_120–38 (FAA, 1980) which restrict maximum cabin ozone levels to 250 nmol mol^{-1} (peak) and 100 nmol mol^{-1} (3-hour average) were developed and are still in effect. Most passenger jet aircraft now have ozone destruction filters on the cabin air intakes, but not all, as avoidance is still an option. This is not always successful, however, as even these high limits are sometimes exceeded (Bekö et al., 2015).

This urgent issue, combined with concern about adverse effects of aircraft exhaust emissions on the atmosphere, led to a collaboration between NASA and several US airlines to operate the Global Atmospheric Sampling Program (GASP). From March 1975 to June 1979, GASP provided the first representative ozone measurements from regular aircraft (Falconer and Holdeman, 1976; Nastrom, 1977). A commercially available 253.7 nm UV photometer was modified for automated operation. The air sample from the inlet for gas phase measurements was pressurized by means of a PTFE (Teflon)-coated diaphragm pump to well above cabin pressure. Losses in the inlet and pump were as large as 16% in 1975–76, reduced to <6% in 1977. Overall uncertainty is estimated at ±8.4% in 1975–76, and ±3.3% from 1977, with a known bias of +9% from the calibration via NBKI (Schnadt Poberaj et al., 2007). Four passenger B-747 aircraft made a total of 6149 flights, with measurements at altitudes between 6 and 13.7 km. The program mostly covered the North Atlantic and Pacific Oceans, as well as North America, but also to a lesser extent Europe (Schnadt Poberaj et al., 2009), with a few flights to India, Singapore, Australia, New Zealand, and Brazil.

NOXAR (Nitrogen Oxides and Ozone along Air Routes) provided measurements onboard a B-747 from Zurich (Switzerland) to Atlanta, Boston, New York and Chicago and also Beijing, Bombay and Hong Kong. The system was operated from May 5, 1995, until May 13, 1996 (540 flights), and from August 12 until November 23, 1997 (104 flights). The analyzer was a modified Environics S-300 253.7 nm UV absorption instrument. The air sampling contained an aerofoil-sectioned aluminum boom with a PTFE core, just forward of the aircraft's rearmost starboard door. The boom extended 23 cm into the slipstream from the aircraft skin. Ambient air at ~200 hPa was compressed to aircraft cabin pressure (~800 hPa) using a PTFE-coated diaphragm pump. Losses in the inlet and pump were as large as 7%, adding ±3.5% to the overall uncertainty. Precision is estimated at ±0.5 nmol mol^{-1}, and overall uncertainty at ±5 nmol mol^{-1} ±6% (Dias-Lalcaca et al., 1998; Brunner et al., 2001).

More than three decades of dedicated research aircraft measurements, mostly with UV absorption instruments and also with some O_3-NO chemiluminescence measurements, are also archived (e.g. LARC, 2019; BADC, 2019; ESRL, 2019; NCAR, 2019). Typically these flights were directed at observing particular atmospheric phenomena (e.g. biomass burning plumes), and so sampling may be biased accordingly.

4.8. MOZAIC/IAGOS

In-service Aircraft for a Global Observing System (IAGOS) and its predecessor Measurement of Ozone and water vapor by Airbus in-service airCraft (MOZAIC) have been making automatic and regular measurements of O_3, water vapour and standard meteorological parameters onboard long-range commercial Airbus A330/A340 aircraft since August 1994 (Marenco et al., 1998, Petzold et al., 2015).

Ozone measurements are made by dual-beam UV absorption monitors with a response time of 4 s, a detection limit of 2 nmol mol^{-1}, and an uncertainty of ±2 nmol mol^{-1} ±2%, including a 1% uncertainty in the reference instrument (Thouret et al., 1998; Nédélec et al., 2015). As in GASP and NOXAR, the sampled air is compressed by a Teflon-coated diaphragm pump before entering the UV-photometer, but losses in the inlet and pump are estimated at less than 1%, based on laboratory and ground tests (Thouret et al., 1998). Quality assurance procedures have not changed since the beginning of the record in 1994. No calibration drift has been observed, nor inconsistency between MOZAIC and IAGOS instruments (Blot et al., in preparation). Ozone monitors are calibrated annually to a reference analyser at the Bureau Internationale

des Poids et Mesures (BIPM), and also compared every 2 hours to an in-flight ozone calibration source. MOZAIC can be considered a reference dataset (e.g. Thouret et al., 1998, 2006; Schnadt Poberaj et al., 2009; Logan et al., 2012), due to its known calibration history.

Previous comparisons of MOZAIC/IAGOS data with ozonesondes show negative biases of a few per cent (sonde values higher), with larger differences in the earlier part of the MOZAIC record (Thouret et al., 1998; Staufer et al., 2013, 2014). Recent results also show small (6% or less) negative biases against ECC sondes (Zbinden et al., 2013; Tanimoto et al., 2015). Despite the large number of profiles in either case, coincidences between aircraft and sonde launches are few. However, a comparison (**Figure 20**) of trajectory-mapped averages of ozonesonde and MOZAIC/IAGOS profile data (see description of TOST, above) indicates that over 1994–2012 sonde measurements are about 5 ± 1% higher in the lower troposphere, and 8 ± 1% higher in the upper troposphere, consistent with the 1 ± 5% and 5 ± 5% average biases found for ECC sondes in Section 4.3, from UV-referenced sonde intercomparison studies. In addition, some of the routine soundings during this period will be from EnSci sondes used with 1% KI solution, which may account for the additional bias (Section 4.3).

Unlike ozonesonde sites, airports are typically urban, but MOZAIC/IAGOS ozone data do not appear largely affected by local boundary layer chemistry (Petetin et al., 2016, 2018). This is also indicated by **Figure 20**. The IAGOS database (http://www.iagos.org) currently contains data from more than 100,000 vertical profiles of tropospheric ozone, measured during takeoff and landing from 148 airports around the world since August 1994. The data sampled from the ascents and descents at these airports are unevenly distributed both spatially and temporally because the frequency of visits to airports by aircraft that take part in MOZAIC/IAGOS varies, depending on commercial airlines' operating constraints. In particular, data are sparser in the southern hemisphere (**Figure 21**).

A year-by-year comparison (Figure S-10) shows considerable variability (almost certainly due to sampling differences) but no overall trend if the first two years, 1994–95, are excluded. The apparent high bias of the sondes is reduced to ~4% and ~7% if 1994–95 are excluded. These larger differences in the first two years of the MOZAIC/IAGOS record have been noted previously (Logan et al., 2012; Staufer et al., 2014) and may also be due to sampling differences.

4.9. Tropospheric ozone satellite and residual measurements

The measurement of tropospheric ozone from space is a challenge, because of the large stratospheric ozone burden that satellite instruments must look through. Typical variations in the stratosphere at mid-latitudes (more than 10%) are larger than the entire amount of ozone in the troposphere. A number of techniques have been developed to derive information about tropospheric ozone from nadir-pointing spectrometer data. The tropospheric ozone residual (TOR) technique (Fishman et al. 1990, 1996, 2003; Ziemke et al., 1998; Chandra et al., 2003) uses height-resolved ozone information from the Solar Backscatter Ultraviolet (SBUV/2) or the Stratosphere Aerosol and Gas Experiment (SAGE), Halogen Occultation Experiment (HALOE) or Microwave Limb Sounder (MLS) instruments to subtract stratospheric ozone from the total column ozone measured by the Total Ozone Mapping Spectrometer (TOMS), or more recently, the Ozone Monitoring Instrument (OMI) (Ziemke et al., 2006; Jing et al., 2006). An extension of this technique uses forward tra-

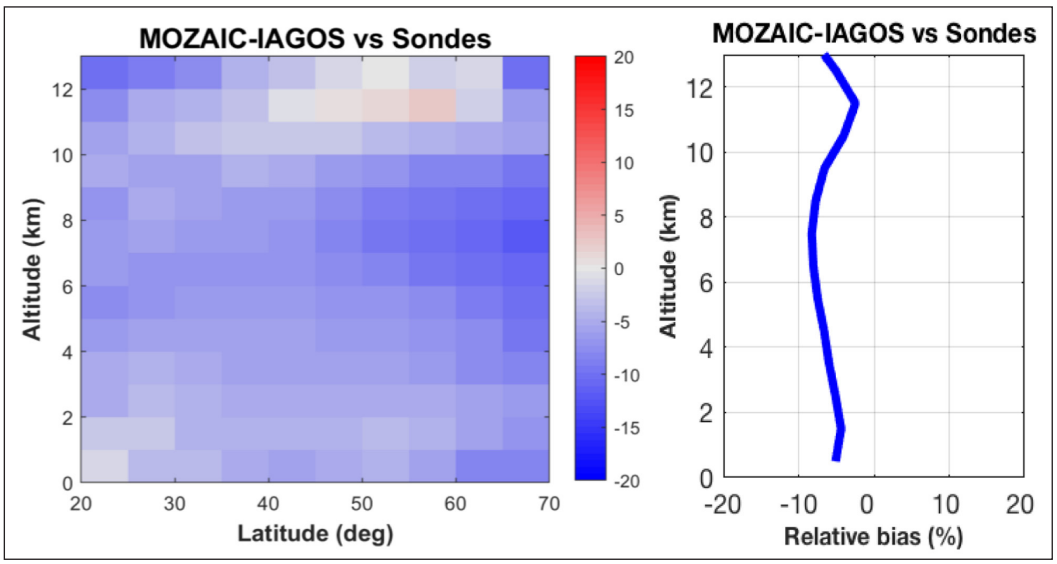

Figure 20: Average (1994–2012) relative differences (%) of trajectory-mapped MOZAIC/IAGOS profile data minus trajectory-mapped ozonesonde data (*Osman et al.,* paper in preparation). Variations with latitude in the left-hand plot are likely due to differences in sonde type and preparation, which may cause biases of several percent. When averaged over latitude, sonde measurements are about 5 ± 1% higher, in the lower troposphere, and 8 ± 1% higher in the upper troposphere, consistent with the average biases found from UV-referenced sonde intercomparison studies (Section 4.3). DOI: https://doi.org/10.1525/elementa.376.f20

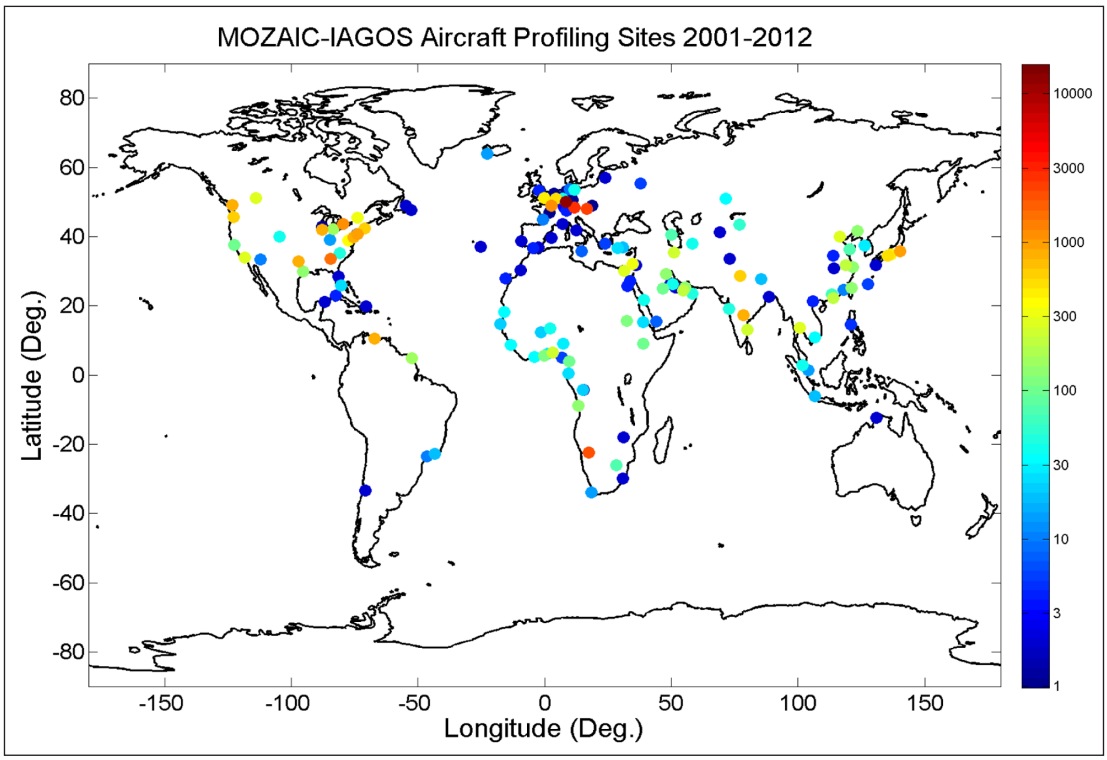

Figure 21: Airports visited by MOZAIC/IAGOS aircraft from 2001–2012. The color bar indicates the number of profiles available from each airport. Sampling frequency varies with time, as it is dependent on commercial aircraft schedules. DOI: https://doi.org/10.1525/elementa.376.f21

jectory model calculations or potential vorticity mapping with MLS data (Schoeberl et al., 2007; Yang et al., 2007), to produce stratospheric column estimates with higher horizontal resolution, suitable for producing a daily TOR product. Winds are from NASA's Modern Era Retrospective Reanalysis (MERRA). Similarly, the Global Modeling and Assimilation Office (GMAO) assimilated ozone product is produced by using OMI and MLS retrievals as input to the global data assimilation system used to produce MERRA (Wargan et al., 2015). Tropospheric ozone has also been derived from the TOMS data alone by assuming the longitudinal distribution of stratospheric ozone (Kim et al., 1996; Hudson and Thompson, 1998).

Cloud differential methods employ the fact that, particularly in the tropics, the tops of the highest clouds are essentially at the tropopause, and so the tropospheric ozone column can be found from the difference in total ozone measured in adjacent cloudy and cloud-free pixels. The Convective Cloud Differential (CCD) method (Ziemke et al., 1998) or the Cloud-Clear Pair (CCP) method (Newchurch et al., 2003) use this approach with TOMS. This method has been applied to OMI, GOME, GOME-2, and SCIAMACHY data (Ziemke et al., 2017; Valks et al., 2014; Leventidou et al., 2016). A second method, called "cloud slicing" (Ziemke et al., 2001, 2003, 2009, 2017), uses measurements of above-cloud column ozone together with cloud-top pressure data to derive ozone column amounts in the upper troposphere. Used in combination, these methods can estimate 400 to 1000 hPa lower tropospheric column ozone. Similarly, lower tropospheric ozone amounts near mountainous regions have been derived from TOMS data using a topographic contrast method (Jiang and Yung, 1996; Kim et al., 1996; Newchurch et al., 2001), and tropical tropospheric ozone has been derived from TOMS data alone, based on differences in ozone-column retrieval sensitivity as a function of scan angle (Kim et al., 2001).

More recent satellite instruments with higher spectral resolution and broader spectral coverage retrieve tropospheric ozone directly from the backscattered radiances in the Hartley (200–320 nm) and Huggins (320–350 nm) bands. Information on the ozone vertical distribution is derived from the effective scattering depth at different wavelengths, and also from the temperature dependence of the ozone absorption cross-sections in the Huggins bands, which separates ozone in the warmer troposphere from colder stratospheric ozone (Chance et al., 1997). GOME profiles have been retrieved at 20 or more layers from the surface to ~60 km using the OE technique (Munro et al., 1998; Hoogen et al., 1999; van der A et al., 2002; Liu et al., 2005), Tikhonov-Philips (TP) regularization (Hasekamp and Landgraf, 2001), and neural networks (Del Frate et al., 2002; Müller et al., 2003). Layer values are not independent, however; total degrees of freedom for signal (DFS) are about 5–6.5, with most in the stratosphere; only about 1 independent point is retrieved in the troposphere. These algorithms are reviewed and compared in Meijer et al. (2006). Similar methods have been applied to GOME-2 (Cai et al., 2012; van Peet et al., 2014; Miles et al., 2015; van Oss et al., 2015), SCIAMACHY (Sellitto et al., 2012a, b), OMI (Kroon et al., 2011; Liu et al., 2010a, b; Mielonen et al., 2015; Sellitto et al., 2011; Di Noia et al., 2013), and OMPS (Bak et al., 2017). Table S-11 compares GOME and OMI retrievals.

The Tropospheric Emission Spectrometer (TES) is an FTIR interferometer that uses the 9.6 micron ozone absorption band to retrieve ozone concentrations. Its 0.1 cm^{-1} spectral resolution is sufficiently fine to distinguish the pressure-broadening of ozone absorption lines at atmospheric pressures in the lower troposphere, giving vertical information to discriminate tropospheric and stratospheric ozone. Like ground-based FTIR, it uses OE algorithms to retrieve vertical profiles of ozone concentration (Bowman et al., 2006). It is mostly sensitive to tropospheric ozone between 700 and 300 hPa, owing to the higher thermal contrast there with respect to the surface.

The Infrared Atmospheric Sounding Interferometer (IASI) instrument is also an FTIR, similarly operating in the 3.7 to 15.5 μm spectral range, but with 0.5 cm^{-1} spectral resolution (see Table S-11 for details). Ozone profiles are retrieved with similar vertical resolution in the troposphere to that of TES. **Table 11** summarizes the characteristics of these satellite data products. More detailed descriptions are found in the Supplemental Material (Text S-12).

For enhancing sensitivity in the lower troposphere, IASI profiles may also be retrieved using a TP altitude-dependent regularization (Eremenko et al., 2008), which

Table 11: Summary of characteristics of tropospheric ozone satellite and residual measurement products. Resolution is given as nadir footprint and either tropospheric column ozone (TCO) or degrees of freedom for signal (DFS) in the troposphere. DOI: https://doi.org/10.1525/elementa.376.t11

Product	Dates	Type	Coverage	Resolution	Sampling	Reference
TOR	1979–2005	Residual TOMS +SAGE or SBUV	Global w/o polar night	1° × 1.25° TCO	Monthly	Fishman et al. (2003)
OMI/MLS	2004–2015	Residual OMI-MLS	Global w/o polar night	1° × 1.25° TCO	Monthly	Ziemke et al. (2006)
TRAJ	2005–2014	Residual OMI-MLS	Global w/o polar night	1° × 1.25° TCO	Daily	Schoeberl et al. (2007)
OMI/MLS (GMAO DA)	2005–2014	Assimilated product	Global w/o polar night	2° × 2.5° TCO	Daily	Wargan et al. (2015)
TOMS CCD	1979–2005	Cloud differential	Tropics	5° × 5° TCO	Monthly	Ziemke et al. (2005)
GOME-1,2, SCIA CCD	1996–2012	Cloud differential	Tropics	2.5° × 5° TCO	Monthly	Leventidou et al. (2016)
GOME-2 CCD	2007–2014	Cloud differential	Tropics	1.25° × 2.5° TCO	Monthly	Valks et al. (2014)
GOME	1995–2003	UV spectral fitting, neural network	Global w/o polar night	960 × 80 km ≤1.2 DFS	3-day	Munro et al. (1998); Liu et al. (2005); Müller et al. (2003)
GOME-2	2007–present	UV spectral fitting	Global w/o polar night	40 × 80/640 km ≈1 DFS	Daily	van Oss et al. (2015)
GOME-2	2007–present	UV spectral fitting	Global w/o polar night	160 × 160 km ≈1 DFS	Daily	Miles et al. (2015)
OMI profile	2004–present	UV spectral fitting	Global w/o polar night	13 × 48 km ≤1.2 DFS	Daily	Kroon et al. (2011)
OMI profile	2004–present	UV spectral fitting	Global w/o polar night	52 × 48 km ≤1.2 DFS	Daily	Liu et al. (2010a, b), Huang et al. (2017, 2018)
TES	2004–present	IR spectral fitting	50S to 70N, 16 tracks	5 × 8 km ≤1.6 DFS	2-day	Nassar et al. (2008); Boxe et al. (2010)
IASI-LISA	2007–present	IR spectral fitting	Global	12 × 25 km ≤1.6 DFS	Twice daily	Dufour et al. (2012)
IASI-FORLI	2007–present	IR spectral fitting	Global	12 × 25 km ≤1.6 DFS	Twice daily	Boynard et al. (2009, 2016, 2018)
IASI-SOFRID	2007–present	IR spectral fitting	Global	12 × 25 km^2	Twice daily	Barret et al. (2011)
OMI+TES	2004–2008	IR + UV spectral fitting	82S to 82N, 16 tracks	13 × 48 km 2.0 DFS	2-day	Fu et al. (2013)
IASI+GOME-2	2009–present	IR + UV spectral fitting	Global w/o polar night	12 × 25 km 1.7 DFS	Daily	Cuesta et al. (2013)

optimizes the retrieval constraints to maximize the DOFS in the lower troposphere (Dufour et al., 2010, 2012, 2015). These IASI (TP) retrievals are able to depict the horizontal distribution of ozone plumes within the lower troposphere (**Figure 22**) with a relative maximum of sensitivity typically between 3 to 4 km, in case of positive thermal contrasts (i.e. over land during summer) but with limited sensitivity to near surface ozone.

Multispectral measurements can also enhance retrieval sensitivity to lower tropospheric ozone. Examples include: UV radiance + polarization (Hasekamp and Landgraf, 2002), UV + IR (Worden et al., 2007b; Landgraf and Hasekamp, 2007), UV + IR + VIS (Natraj et al., 2011), and VIS + IR (Hache et al., 2014) measurements using OE or TP regularization techniques. The polarization measurements in the UV show higher sensitivity to ozone in the troposphere than to ozone in the stratosphere.

IASI+GOME2: A multispectral satellite approach that simultaneously fits IASI measurements in the thermal IR and co-located UV spectra from GOME-2, at the IASI spatial resolution (12 × 25 km) has allowed the spaceborne observation of ozone plumes below 3 km, both over land and ocean (Cuesta et al., 2013). Sensitivity in the surface-3 km layer peaks at 2 to 2.5 km asl over land (**Figure 22**), while the DOFS for this layer are 0.35, 40% more than IASI (TP). Validation with ozonesondes in 2009–10 show that ozone is retrieved in this layer with a mean bias of 4% and a precision of 17%, when smoothing by the retrieval vertical sensitivity (9% mean bias and 27% precision for direct comparisons).

TES+OMI: A similar multispectral approach combines radiances from TES and OMI (Fu et al., 2013). The joint TES/OMI retrieval provides 2 DOFs in the troposphere with approximately 0.4 DOFS for near surface ozone (surface to 700 hPa).

Figures 23 and **24** display bias and uncertainty information for satellite retrievals and data products, from published validation studies. Systematic biases, however, can vary by region (see *TOAR-Climate*, Gaudel et al., 2018). In all cases evaluations were with respect to ECC sondes; there are very few comparisons with other tropospheric data sources (e.g. Safieddine et al., 2016). The published

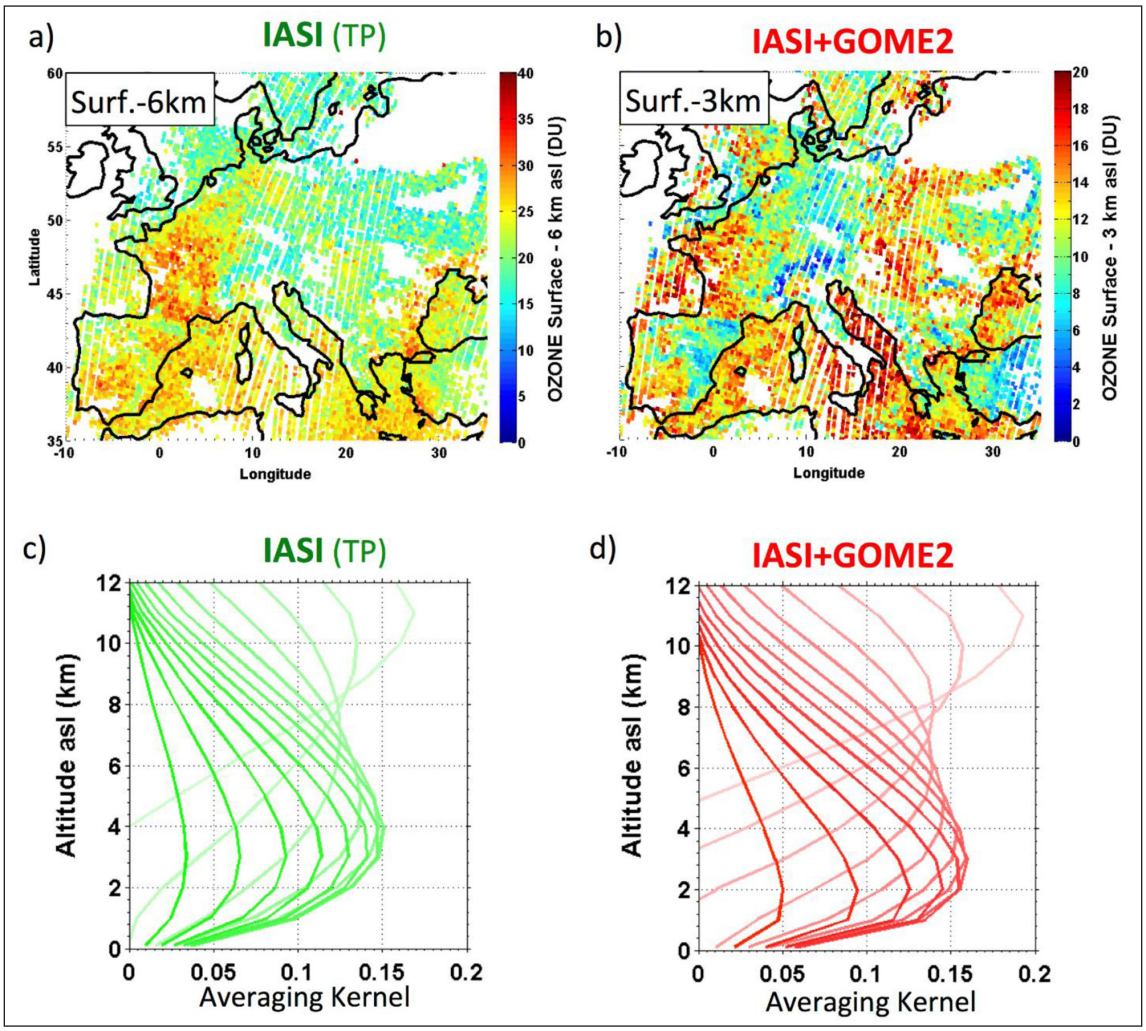

Figure 22: Satellite retrieval of ozone on 19 August 2009 over Europe **(a)** in the lower troposphere (up to 6 km asl) derived from the IASI Tikhonov-Philips approach (Eremenko et al., 2008) and **(b)** in the lowermost troposphere (up to 3 km asl) from the IASI+GOME2 multispectral synergism (Cuesta et al., 2013). Examples of averaging kernels in the troposphere for a satellite pixel over land for **(c)** IASI (TP) and **(d)** IASI+GOME2. DOI: https://doi.org/10.1525/elementa.376.f22

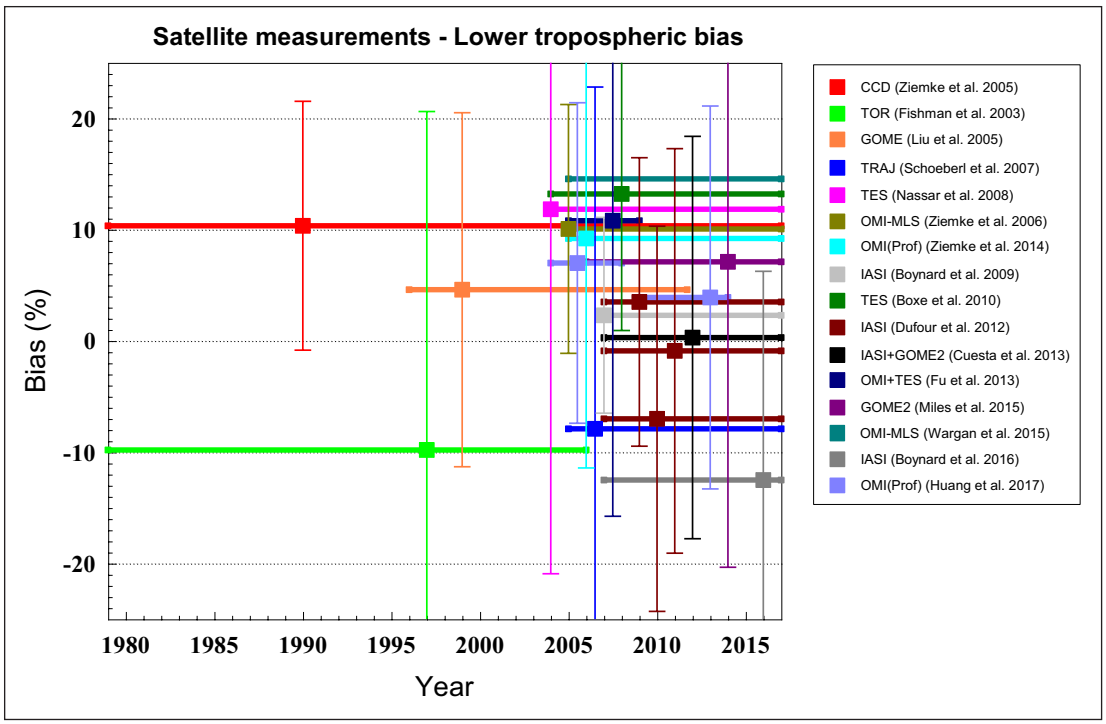

Figure 23: Bias estimates for satellite retrieval and data products. The horizontal bars indicate the individual time series length. The error bars show the standard deviation of the sonde comparison, and the square symbols indicate the approximate date of the comparison. Published evaluations are in general single averages over a short period of time. Biases are fairly modest, but standard deviations are large. DOI: https://doi.org/10.1525/elementa.376.f23

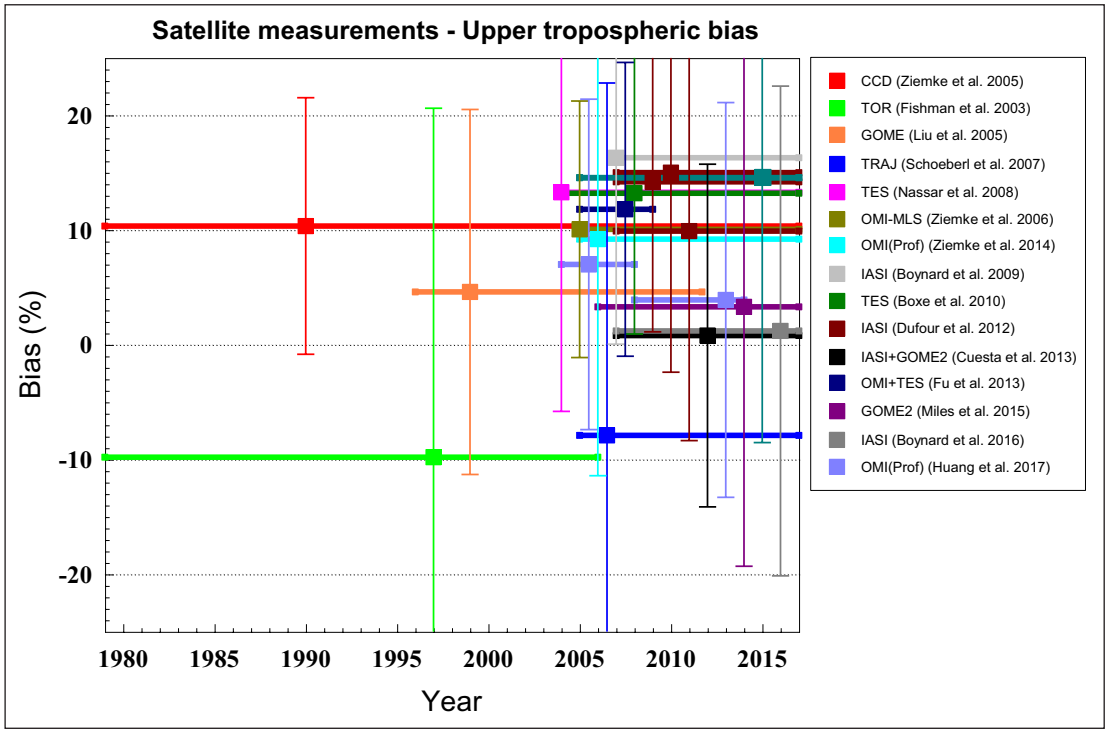

Figure 24: As Figure 23, for the upper troposphere. DOI: https://doi.org/10.1525/elementa.376.f24

biases and uncertainties have therefore been adjusted with the biases derived for ECC sondes in Section 4.3. Evaluations are in general single averages over a short period of time; there are very few published evaluations of instrument drift with respect to time (Huang et al., 2017; Boynard et al., 2018; Gaudel et al., 2018).

It is apparent from **Figures 23** and **24** that while biases are fairly modest, ranging between −10% and +20%, but often much smaller, standard deviations are large, compared to those of the other measurement systems discussed above: about 10–30%, versus 5–10% for sondes, aircraft, lidar and ground-based FTIR. Nevertheless, as

satellite data products offer global or near-global coverage with few gaps, their value is correspondingly large. Other measurement systems suffer from errors of representativeness, when point measurements are interpolated or extrapolated to infer information at points other than the place and time of the original measurement.

5. Representativeness

Ozone is a highly reactive secondary pollutant with many processes such as photochemical formation, deposition and titration playing a role in determining atmospheric mole fractions. Although several thousand ground-based stations measure ozone concentrations at high temporal frequencies world-wide (*TOAR-Surface Ozone Database*), the globe is nevertheless undersampled, since surface ozone over land surfaces may vary locally on scales of a few kilometres or less. (Here the spatial representativeness of observations down to an urban/regional scale is considered. The issue of measurements being representative of the well-mixed boundary layer addressed earlier with Criterion 3, is on a smaller scale and not addressed in this section.) Sites are unevenly distributed, with relatively few in the tropics and southern mid-latitudes (Sofen et al., 2016; *TOAR-Surface ozone database*). Spatial representativeness is therefore often the largest source of uncertainty in the use of ground-based data. For a well-calibrated analyzer, measurement uncertainty is in the 1-nmol mol^{-1} range (Section 2.2.2), while two locations with different site characteristics (e.g. urban vs rural) may show average differences an order of magnitude larger. Land use may also change with time, complicating trend analysis by inducing changes that do not reflect background ozone trends. Remote baseline sites with minimal influence of local processes are usually representative of a larger area than sites located for catching the plumes of particular sources (e.g. monitoring stations at curbsides) which reflect local conditions. The application of the data may also determine the area of representativeness, as correlation lengths are typically longer for monthly averages than for daily data (e.g. Sofen et al., 2016).

Standard attempts to assess the representativeness of in-situ air quality monitoring stations classify the sites into categories like urban, suburban, rural, or remote, in terms of their exposure to sources and sinks (e.g. European Union, 2008). These classifications are somewhat qualitative. More quantitative approaches use station metadata. Ozone concentrations at urban stations are strongly controlled by NOx titration, and so population density (which can be seen as a proxy for NOx emissions) is often used to classify sites as urban, suburban, and rural. The intensity and nature of sources (traffic, industrial or background) can be used to refine the classification. *TOAR-Surface ozone database* has developed a globally consistent classification scheme based on population density, nighttime light intensity, OMI tropospheric column NO_2, and station altitude. Due to the need to define thresholds for each of these parameters, this classification based on metadata is still partly subjective.

Beyond the use of ozone monitoring station data for trends, their broader use for model evaluation and data assimilation raises the question of objectively quantifying station spatial representativeness, i.e., how a single measurement is related to its spatial surroundings (Spangl et al., 2007). Methods have been developed to characterize station representativeness with more objective criteria. Janssen et al. (2012) show that using a classification parameter based on land use improves model validation results by ~20%. Henne et al. (2010) have proposed a classification based on an explicit estimation of emissions, deposition and transport influencing a particular station. They use population density as a proxy of emissions, land cover from the Wesely (1989) dry deposition parameterization to derive deposition fluxes, and a Lagrangian trajectory approach to evaluate transport impact. Methods based solely on the characteristics of the measurements themselves, especially the diurnal profile amplitude, have also been employed (Flemming et al., 2005; Tarasova et al., 2007; Gaubert et al., 2014). Urban stations exhibit larger diurnal amplitude (due to strong night time ozone loss and strong daily photochemical production) while remote and high elevation stations show much flatter diurnal profiles. Joly and Peuch (2012) have refined this approach by adding other parameters such as the weekend effect to describe the station characteristics. These methods are used to evaluate models with objectively classified station data (Marécal et al., 2015), and to build assimilation systems of observational data. Solazzo and Galmarini (2015) have proposed an alternative approach employing spectral analysis of the ozone time series, and correlation analysis of different spectral components. They find that the area of representativeness is generally very non-isotropic and quite heterogeneous (as also shown by the catchment areas of Henne et al. (2010)). Noting that certain spectral components of ozone variability showed discontinuities between countries (Europe) and networks (North America), they discard those as noise, and note an improvement in evaluated model performance of ~5%. Schutgens et al. (2016) have shown how high sub-grid variability, such as is prominent with ozone observations, can result in imperfect matches between individual stations and the regionally averaged values.

All these methods show grouping significantly different from the metadata approach, and also demonstrate both the value and challenge of representative station classifications. These findings also suggest that trend analyses using the large number of observations available from surface ozone sites benefit from applying objective classification methods (*TOAR-Surface ozone database*; Fleming et al., 2018, hereinafter *TOAR-Health*).

In the free troposphere local effects are less important and representativeness areas are larger. Typical correlation lengths in the free troposphere, for individual measurements, are about 500 km (Liu et al., 2009; Nastrom, 1977). However, the distances between ground-based observing sites are usually larger than this (**Figures 8, 15, 16, 21**), and as in the case of surface data, sites are unevenly distributed. Observations are also less frequent, so the ozone distribution is in general undersampled, both in space and time. Several authors have noted that this raises representativeness issues (Logan et al., 2012; Tilmes et al.,

2012), which can be serious when comparing to model fields or attempting to determine global or regional trends (Saunois et al., 2012; Lin et al., 2015b). MacDonald (2005) illustrates how infrequent temporal observations in the free troposphere can directly add uncertainty on monthly averages and can limit ability to detect trends.

To address the problem of uneven distribution of sites, they are sometimes grouped according to geographic region or ozone characteristics (Tilmes et al., 2012; Stauffer et al., 2016). Alternatively, a subset of sites is chosen (e.g. Oltmans et al, 2013). The generalized additive mixed model (GAMM) technique has also been used to derive regional trends for large regions with uneven monitoring networks (Chang et al., 2017). Linear interpolation of widely-separated sites yields unsatisfactory results (Logan, 1999), but interpolation methods that take meteorological representativeness into account can produce better regional estimates from limited sampling (Tarasick et al., 2010; Liu et al., 2013). Such methods have their limitations, however: in Figure S-10 the interannual differences in average bias, from thousands of profiles annually, are much larger than can be expected from instrumental uncertainty, and so must result from sampling differences.

Sampling differences can add additional uncertainty to regional trends. This will be independent of the metric used, as most of the metrics described in TOAR-Metrics are linear transformations of the measured data. The ozone trend found by *Cooper et al.* (2010), based on all available mid-tropospheric ozone measurements over western North America during 1984–2008 (more than 1200 data points per year on a 0.2° × 0.2° × 200 m grid), passed a number of statistical tests for robustness. However, in springtime, meteorological variability in ozone over western North America is large and heterogeneous in space and time (e.g. Lin et al. 2015a; Stauffer et al., 2016). The Cooper et al. (2010) dataset was re-examined by *Lin et al.* (2015b), using chemistry-climate model hindcast simulations driven by observed meteorology. The GFDL-AM3 model co-sampled in space and time with observations reproduces the observed ozone trend (0.65 ± 0.32 nmol mol^{-1} $year^{-1}$) over 1995–2008, while the model with continuous temporal and spatial sampling indicates a smaller trend (0.25 ± 0.32 nmol mol^{-1} $year^{-1}$). This comparison suggests that the sampling frequency and distribution of ozone profile measurements does not capture the full interannual and spatial variability of ozone across western North America. *Lin et al.* (2015b) noted that if the meteorology of the model forced with reanalysis winds is approximately correct, then the differences between the model median and the median of model points co-sampled with observations can be used as a measure of the "data representativeness uncertainty". When this "representativeness uncertainty" is added to the statistical uncertainty on the trend from observations, that trend estimate for 1995–2008 becomes 0.65 ± 0.57 nmol mol^{-1} $year^{-1}$, which overlaps with the model trend of 0.25 ± 0.32 nmol mol^{-1} $year^{-1}$.

Spatial correlation can exist on different scales. Sofen et al. (2016), using monthly averages, found much longer spatial correlation lengths than Liu et al. (2009), who examined individual ozone soundings. Similarly, Eriksson and Chen (2002) found vertical correlation lengths of 2–5 km in ozonesonde data, while Sofieva et al. (2004) found vertical correlation lengths of ~1 km for small-scale deviations from a smoothed profile.

Like spatial representativeness, temporal autocorrelation in ozone exists on a variety of timescales. Hourly averaged ozone measurements are uncorrelated if more than a few days apart (Galbally et al. 1986; Liu et al. 2009; Lehman et al, 2004), but monthly averages nevertheless show significant autocorrelation (e.g. Tarasick et al., 2005, Oltmans et al., 2006). The temporal persistence, or autocorrelation can differ by location and can be closely linked to weather patterns and variations in sources and sinks. Frequent observations can allow quantification of temporal autocorrelation at most relevant timescales.

A number of research groups have developed techniques to optimize and evaluate proposed network changes that can be applied to tropospheric ozone monitoring. Spatial coherence has been studied by McBratney (1981) and Yost (1982) who identified "areas of influence." Dantzig et al. (1963) and Cressie (1985) pioneered research efforts on optimization of networks, work that has been carried forward with more respect for the specific goals of environmental monitoring by Nychka and Salzman (1998), among others. Weatherhead et al. (2017) have addressed the challenge of designing monitoring systems when realistic constraints, including financial budget constraints, must be considered.

6. Conclusions and recommendations for design of a future global observational program

From the earliest measurements in the 19th century, both measurement methods and the portion of the globe observed have evolved and changed significantly. The historical methods have different uncertainties and biases, and the data records differ with respect to coverage (space and time), information content, and representativeness. There are significant uncertainties with the 19th and early 20th century measurements with regard to representativeness, and interfering gases. SO_2 levels in particular appear to have been quite high in urban areas, and may have negatively biased urban ozone measurements. There is therefore no unambiguous evidence of very low ozone values in the 19th century.

There are 49 and 11 sets of measurements of surface ozone, by KI and spectroscopic methods respectively, made before the mid-1970s and suitable for this historical analysis. Values of ozone absorption coefficients used before 1960 varied, however, and caused ozone to be underestimated by up to 11%. Overall, the 60 available datasets during 1896–1975 indicate an ozone mole fraction in the well-mixed unpolluted boundary layer that lies in the range 22 to 26 nmol mol^{-1}. Comparison with modern measurements from the TOAR database suggests that surface ozone has increased by 32–71%, with large uncertainty, in rural air in the temperate and polar zones of the northern hemisphere, and by much smaller amounts in the southern hemisphere. This estimate depends much more on the modern region chosen for comparison than on

Table 12: Scientific tasks, goals, and requirements for future tropospheric ozone monitoring. DOI: https://doi.org/10.1525/elementa.376.t12

Scientific task or question	Goals and Requirements	Station location	Comment
Long-term tropospheric ozone monitoring	Detection of long-term ozone distribution changes, ozone transport changes. Need decadal stability of ~1 nmol mol^{-1}. Vertical profiling important.	Multiple sites in different regions and land use classifications. Choice of sites should be guided by objectively quantified station spatial representativeness.	Current global network is unevenly distributed and covers only ~25% of the globe (*TOAR-Surface ozone database*). Sites with long-term records are very important.
Air quality model validation	Moderate accuracy and precision, preferably 3–5% level. Need vertical resolution of ~0.2 km or better. Need hourly time resolution, at least for short (campaign) periods. Flux measurements.	Multiple sites in different regions. Choice of sites should be guided by objectively quantified station spatial representativeness. Collocated profile measurements of other species desirable. Sites with multi-year data records are of value for background climatology.	Measurement campaigns at multiple sites are desirable. Measurements of surface deposition fluxes for different environments are needed (Hardacre et al., 2015; Bariteau et al., 2010; Luhar et al. 2017, 2018).
Chemical data assimilation	Moderate accuracy and precision, preferable 3–5% level. Vertically-resolved measurements desirable. Daily or better time resolution.	Many sites in different regions. Choice of sites should be guided by objectively quantified site spatial representativeness. Satellite, surface monitor, aircraft data.	Can we increase the impact of sparse measurements? Aircraft, lidar, ozonesondes have small measurement errors, relative to model error. Data impact should therefore be significant.
Satellite ozone data validation	High accuracy and high precision, preferably 2–3% level. Profile (free tropospheric) information required.	Location should represent different observational conditions (latitude, ozone profiles, etc.) and preferably have related measurements (surface O_3, total O_3, aerosol)	Data quality of prime importance; periodic re-evaluation needed.
How do ozone levels in the free troposphere affect levels in the planetary boundary layer (PBL)?	Measurement campaigns with vertical sounding at a resolution down to a few hours – lidar, satellite, sonde and other met measurements, possibly at multiple sites.	Sites in different latitude bands. Sites with multi-year measurement records are of value for background climatology. More sites at lower latitudes.	Important to interpreting satellite measurements, which are primarily sensitive to ozone above the PBL (Crawford and Pickering, 2014; Martins et al. 2015).

(Contd.)

Scientific task or question	Goals and Requirements	Station location	Comment
Model processes: Can we properly model and quantify long-range transport (e.g. Stohl and Trickl, 1999), and stratosphere-troposphere transport events and their effects on ozone levels in both the free troposphere and PBL? How well is plume mixing represented? (Osman et al., 2016; Trickl et al., 2014, 2016; Eastham and Jacob, 2017)	Measurement campaigns with lidar, global satellite observations, met sonde or ozonesonde (daily launches).	Sites in different latitude bands. Sites near tropopause breaks. Sites with multi-year measurement records are of value for background climatology.	Global flux is moderately well-estimated by models; regional flux varies (Stohl et al., 2003a, b) and is not well characterized by scattered observations. Models show great improvement in capturing tropopause folding events (e.g. Trickl et al., 2010, 2011; He at al., 2011; Langford et al., 2015; Lin et al., 2015a), in part due to better spatial resolution, but effects on surface ozone may be underestimated (Zhang et al., 2011; Lin et al., 2012a, b; Hess and Zbinden, 2013; Zanis et al., 2014; Lefohn et al., 2014; Akritidis et al., 2016).
Climate change effects: How will temperature increases affect ozone photochemistry, transport? Will more forest fires increase photochemical ozone production? Will the Brewer-Dobson circulation increase stratospheric O_3 transport to the troposphere? What is causing the observed trend in Arctic surface ozone depletion events (ODE)?	Detection of long-term ozone distribution changes, ozone transport changes. Need vertical resolution of ~0.2 km or better, to separate PBL, mid-troposphere and UTLS processes. Need global coverage, and long-term stability of ~1 nmol mol^{-1}. Long term measurements in the background atmosphere of ozone precursors	Several sites in different latitude bands. Sites with long-term measurement records are preferable.	Climate change is expected to increase planetary wave activity and so produce an increased Brewer-Dobson circulation (e.g. Butchart et al., 2006; Butchart, 2014). In the lower troposphere increases will be offset by losses due to reaction with water vapour to produce OH (Stevenson et al., 2013). At some Arctic sites a long-term increase is observed in surface ODEs (Tarasick et al., 2014), possibly related to changes in snow and sea ice cover (Simpson et al., 2007).
Oil and gas extraction: Will increased activity in oil and/or gas fracking release NO_x and VOCs, leading to high ozone formation?	Measurement campaigns with surface monitors, measurements of other species; possibly at multiple sites. Vertical profiling would be useful.	Near extraction areas. Sites with multi-year measurement records are of value for background climatology.	

the historical data, as when some of the historical datasets judged less reliable are omitted the results are quite similar. The ±20% range of the estimated increase comes primarily from the variability of present-day surface ozone. Data representativeness thus seems to be the more important source of uncertainty.

Based on a more limited, but completely independent set of data, free tropospheric ozone appears to have also changed by a similar amount, in the mid-latitudes of the Northern Hemisphere. In spite of the extensive efforts to identify and evaluate early ozone data records, other data may be available that could pass the selection criteria from this study.

Representativeness, especially for surface sites, is a potential source of significant biases, which are difficult to quantify. Recent research into objective methods of determining areas of representativeness has made valuable progress in reducing this source of uncertainty.

The great majority of validation and intercomparison studies of free tropospheric ozone measurement methods are undertaken with ECC ozonesondes. ECC sondes have been compared to UV-absorption measurements in a number of intercomparison studies. The sondes show a modest (~1–5%) high bias in the troposphere, with an uncertainty of 5%, but no evidence of an instrument change with time. Other methods – Umkehr, lidar, FTIR and UV instruments on commercial aircraft – all show modest low biases relative to the ECCs, and so, using ECC sondes as a transfer standard, all appear to agree to within 1σ with the UV-absorption standard.

Relative to the UV standard, BM sondes show a 20% increase in sensitivity to tropospheric ozone from 1970–1995. The KC sondes show a smaller increase of 5–10%. In combination with the gradual shift of the global network to ECC sondes, this will, if uncorrected, introduce an erroneous positive trend in the free troposphere, to analyses based on sonde data.

Satellite biases are often larger than those of other free tropospheric measurement systems, ranging between −10% and +20%, and standard deviations are large: about 10–30%, versus 5–10% for sondes, aircraft instruments, lidar and ground-based FTIR. Although measurement drift has been examined extensively for satellite measurements of stratospheric ozone (Harris et al., 2015; Hubert et al., 2016), there is relatively little information on temporal changes of bias for satellite measurements of tropospheric ozone. This is an evident area of concern, and one that must be addressed if satellite retrievals are used for trend studies (*TOAR-Climate*, Gaudel et al., 2018).

The importance of ECC sondes as a transfer standard for satellite validation means that more effort should be placed on understanding and reducing their uncertainties. The overall accuracy of the global ozonesonde network has improved: at many important sites the historical record has been homogenized, by correcting for known changes in station records (e.g. Tarasick et al., 2016; van Malderen et al., 2016; Witte et al., 2017, 2019; Sterling et al., 2018, Thompson et al., 2018). In addition, spatial inhomogeneity has been reduced by adopting strict standard operating procedures (Smit and ASOPOS panel, 2011). These continuing efforts should proceed in tandem with research to better quantify systematic and random uncertainty in ECC data and to understand changes therein. The global network is also unevenly distributed (**Figures 15** and **16**), and so additional sites, in southern midlatitudes, North Africa, Asia and other areas with limited coverage, are recommended, possibly as a measurement campaign (Thompson et al., 2011; Lelieveld et al., 2002).

Planning future observations of ozone will need to make careful use of known spatial and temporal coherence. Decisions concerning spatial choices and temporal frequency need to be made with consideration for measurement accuracy and co-location with other observations, including NOx, windspeed and direction, and other relevant information needed to understand both ozone and its sources. The integration or merging of data from different platforms, which has had little attention to date, can improve coverage.

Although tropospheric ozone monitoring has evolved from sporadic measurements at a few locations to extensive, well-calibrated networks with formal international collaboration (e.g. Schultz et al., 2015), as well as global satellite observations, it is not comprehensive, nor evenly distributed. It is recommended that the design of the global observational program in the future be guided by several current and emerging scientific issues (**Table 12**). Each method of observation has its inherent advantages and limitations, and so different techniques will continue to complement and support each other. For example, satellite observations are likely to be of great importance to ozone data assimilation, but ozonesonde and lidar profiles are required for satellite product evaluation. It is to be hoped that commercial aircraft monitoring will be expanded, to close monitoring gaps with reliable, well-calibrated measurements. Some modest improvements in the distribution of ground-based observing sites could yield significant benefits in global coverage. International cooperation and data sharing will be of paramount importance, as the TOAR project has demonstrated.

Data Accessibility Statement

No new measurements were made for this review article. All datasets discussed in the text were obtained from the published scientific literature. Lidar, FTIR, Umkehr and ozonesonde data used in this publication are publicly available, from the World Ozone and UV Data Centre (http://www.woudc.org) and the Network for the Detection of Atmospheric Composition Change (http://www.ndacc.org), and MOZAIC/IAGOS data at (http://www.iagos.org). Satellite data products are available at the URLs listed in Supplemental Material, Text S-12.

Supplemental files

The supplemental files for this article can be found as follows:

- **Text S-1.** Instrumental method: Gas phase titration (GPT). DOI: https://doi.org/10.1525/elementa.376.s1
- **Text S-2.** Comparison of modern surface ozone observations with historical records. DOI: https://doi.org/10.1525/elementa.376.s1

- **Text S-3.** Data selection identified as questionable under Criterion 4. DOI: https://doi.org/10.1525/elementa.376.s1
- **Text S-4.** A note on units and nomenclature. DOI: https://doi.org/10.1525/elementa.376.s1
- **Text S-5.** Standard deviations used in representing data sets. DOI: https://doi.org/10.1525/elementa.376.s1
- **Text S-6.** Historical measurements of urban and suburban ozone in northern Europe. DOI: https://doi.org/10.1525/elementa.376.s1
- **Figure S-1.** Some historical measurements of urban and suburban ozone in northern Europe. DOI: https://doi.org/10.1525/elementa.376.s1
- **Table S-1.** Some historical measurements of urban and suburban ozone in northern Europe. DOI: https://doi.org/10.1525/elementa.376.s1
- **Figure S-2.** Historical measurements of rural background surface ozone at low altitudes in northern temperature regions. DOI: https://doi.org/10.1525/elementa.376.s1
- **Text S-7.** Notes on Tables 4–6, 8, S1. DOI: https://doi.org/10.1525/elementa.376.s1
- **Table S-2.** Change of ozone from the historical period to the modern period for 3 categories of observations: 1) all available historical observations below 2000 m elevation (blue rows); 2) same as for Category 1, but with all observations from Fabian and Pruchniewicz (1977) omitted (gray rows); 3) same as for Category 2, but with three questionable high latitude data sets omitted (Barrow, College and Halley Bay) and with the Northern Temperate sites limited to just those that measured ozone with UV methods (white rows). The modern period is based on rural ozone observations below 2000 m for the years 1990–2014. *The metric for the modern data is the 12-hr daytime average*. DOI: https://doi.org/10.1525/elementa.376.s1
- **Table S-3.** Change of ozone from the historical period to the modern period for 3 categories of observations: 1) all available historical observations below 2000 m elevation (blue rows); 2) same as for Category 1, but with all observations from Fabian and Pruchniewicz (1977) omitted (gray rows); 3) same as for Category 2, but with three questionable high latitude data sets omitted (Barrow, College and Halley Bay) and with the Northern Temperate sites limited to just those that measured ozone with UV methods (white rows). The modern period is based on rural ozone observations below 2000 m for the years 1990–2014. *The metric for the modern data is the daily maximum 8-hour average (DMA8)*. DOI: https://doi.org/10.1525/elementa.376.s1
- **Text S-8.** Analysis of changes in surface ozone. DOI: https://doi.org/10.1525/elementa.376.s1
- **Text S-9.** Umkehr retrieval algorithms. DOI: https://doi.org/10.1525/elementa.376.s1
- **Figure S-3.** (left) Umkehr averaging kernels. (right) Uncertainties for standard Umkehr levels. DOI: https://doi.org/10.1525/elementa.376.s1
- **Text S-10.** Analysis of ozonesonde intercomparison results. DOI: https://doi.org/10.1525/elementa.376.s1
- **Figure S-4.** Left: Average estimated uncertainty of ECC (4A and 5A) soundings in the 1990s at a Canadian site, showing contributions from selected sources. DOI: https://doi.org/10.1525/elementa.376.s1
- **Tables S-4 to S-8.** Ozonesonde Intercomparison results 1960–2015. DOI: https://doi.org/10.1525/elementa.376.s1
- **Figure S-5.** Published intercomparison results of ECC sondes without adjustments. DOI: https://doi.org/10.1525/elementa.376.s1
- **Figure S-6.** As Figure S5, for the upper troposphere. DOI: https://doi.org/10.1525/elementa.376.s1
- **Figure S-7.** Intercomparison results of BM sondes, without adjustments. DOI: https://doi.org/10.1525/elementa.376.s1
- **Figure S-8.** As Figure S7, for the upper troposphere. DOI: https://doi.org/10.1525/elementa.376.s1
- **Table S-9.** Sites and characteristics existing of tropospheric ozone lidar systems. DOI: https://doi.org/10.1525/elementa.376.s1
- **Figure S-9.** Reproducibility test of the ozone DIAL at Garmisch-Partenkirchen (German Alps, at 740 m) at intervals of 1 min, under conditions of moderately elevated ozone. DOI: https://doi.org/10.1525/elementa.376.s1
- **Figure S-10.** Average (1994–2012) relative differences (%) between trajectory-mapped MOZAIC/IAGOS profile data and trajectory-mapped ozonesonde data. DOI: https://doi.org/10.1525/elementa.376.s1
- **Text S-11.** FTIR retrieval and information content. DOI: https://doi.org/10.1525/elementa.376.s1
- **Figure S-11.** Ozone averaging kernels at a typical NDACC site, Thule, GR, on the retrieval grid (left), and for layers containing at least one DOFS (red, green, blue, cyan). DOI: https://doi.org/10.1525/elementa.376.s1
- **Table S-10.** Sites and characteristics existing of tropospheric FTIR stations. DOI: https://doi.org/10.1525/elementa.376.s1
- **Text S-12.** Tropospheric ozone satellite and residual measurements: Instrument and method details. DOI: https://doi.org/10.1525/elementa.376.s1
- **Table S-11.** Comparison of retrieval algorithms and datasets. DOI: https://doi.org/10.1525/elementa.376.s1
- **Table S-12.** Comparison of GOME, OMI, TES and IASI specifications. DOI: https://doi.org/10.1525/elementa.376.s1

Acknowledgements

The authors thank the many observers who, over many years, obtained the ozone measurements used in this study. Their careful work has stood the test of time and is gratefully acknowledged.

Funding information

C. Vigouroux was supported financially by the EU H2020 project GAIA-Clim (No 640276). M. Steinbacher acknowledges funding from the GAW Quality Assurance/Science

Activity Centre Switzerland (QA/SAC-CH), which is supported by MeteoSwiss and Empa. OHP observations are funded by the NDACC French program. The Laboratoire Inter-universitaire des Systèmes Atmosphériques (LISA) acknowledges the support from CNES (Centre National des Etudes Spatiales)/TOSCA (Terre Océan Surface Continentale Atmosphère), PNTS (Programme National de Télédétection Spatiale) and ANR (Agence Nationale de la Recherche – project: ANR-15-CE04-0005) for the development and production of ozone observations from IASI+GOME-2 and IASI. The MLS, OMI and TES projects are supported by the National Aeronautics and Space Administration (NASA) Earth Observing System (EOS) Aura Program. Part of this research was carried out at the Jet Propulsion Laboratory, California Institute of Technology, under a contract with NASA. The National Center for Atmospheric Research is sponsored by the National Science Foundation. J.W. Hannigan is supported under contract by NASA.

Competing interests

The authors have no competing interests to declare.

Author contributions

- As co-ordinating Lead Authors, DWT and IEG were responsible for conception and design of the paper, and all aspects of the analysis, acquisition and expert evaluation of historic datasets
- ORC provided extensive insightful analysis of some historic datasets, and valuable comment and revision to all aspects of the paper
- MGS also provided insightful comment on the historic data analysis, and extensive comment and revision to all aspects of the paper
- Other authors contributed text, analysis and expert comment in their areas of particular expertise: historic datasets (IEG, TJW, SJO, JS, MS); statistical analysis (KLC); ground-based methods (IEG, MS); Umkehr (IP); ozonesondes (DWT, AMT, MO, JL, SJO, BH); lidar (GA, TL, TT, MGM); FTIR (CV, JH, OG); aircraft (JS, VT, MO); representativeness (MS, EW, ML, GF); satellite methods (JZ, XL, AG, HW, JC, GD, JLN), stratospheric intrusions (PZ), as well as comments throughout the paper
- All authors contributed to interpretation, revision of several drafts, and approved the submitted version for publication

References

Aas, W, Shao, M, Jin, L, Larssen, T, Zhao, D, Xiang, R, Zhang, J, Xiao, J and **Duan, L.** 2007. Air concentrations and wet deposition of major inorganic ions at five non-urban sites in China, 2001–2003. *Atmos. Environ.* **41**: 1706–1716. DOI: https://doi.org/10.1016/j.atmosenv.2006.10.030

Akritidis, D, Pozzer, A, Zanis, P, Tyrlis, E, Škerlak, B, Sprenger, M and **Lelieveld, J.** 2016. On the role of tropopause folds in summertime tropospheric ozone over the eastern Mediterranean and the Middle East. *Atmos. Chem. Phys.* **16**: 14025–14039. DOI: https://doi.org/10.5194/acp-16-14025-2016

Albert-Lévy. 1877. *Annuaire de l'Observatoire de Montsouris pour l'an 1877*, 398–405. Paris.

Albert-Lévy. 1903. *Annales de l'Observatoire Municipal (Observatoire de Montsouris) Tome IV – Année 1903*, 259–268.

Albert-Lévy. 1907. *Annales de l'Observatoire Municipal (Observatoire de Montsouris) Tome VIII – Année 1907*, 289–291; 8; 277.

Albert-Lévy. 1908. *Annales de l'Observatoire Municipal (Observatoire de Montsouris) Tome IX – 1908*, 62; 305.

Aldaz, L. 1965. Atmospheric ozone in Antarctica. *J. Geophys. Res.* **70**(8): 1767–1773. DOI: https://doi.org/10.1029/JZ070i008p01767

Altshuller, AP, Wartburg, AF and **Taft, RA.** 1961. The interaction of ozone with plastic and metallic materials in a dynamic flow system. *International Journal of Air and Water Pollution.* **4**: 70–78.

Ancellet, G and **Ravetta, F.** 2003. On the usefulness of an airborne lidar for O_3 layer analysis in the free troposphere and the planetary boundary layer. *J. Environ. Monit.* **5**: 47–56. DOI: https://doi.org/10.1039/b205727a

Anfossi, D and **Sandroni, S.** 1997. Ozone levels in Paris one century ago. *Atmos. Environ.* **31**(20): 3481–3482. DOI: https://doi.org/10.1016/S1352-2310(97)00124-6

Anfossi, D, Sandroni, S and **Viarengo, S.** 1991. Tropospheric ozone in the nineteenth century: the Moncalieri series. *J. Geophys. Res.* **96**: 17,349–17,352. DOI: https://doi.org/10.1029/91JD01474

Attmannspacher, A and **Dütsch, HU.** 1970. International ozone sonde intercomparison at the Observatory Hohenpeissenberg. *Ber. Dtsch. Wetterdienstes.* **120**: 1–85.

Attmannspacher, W and **Hartmannsgruber, R.** 1982. Intercomparison of Instruments measuring Ozone near the Ground at the Hohenpeissenberg Observatory 1 October 1978–30 April 1979. *Berichte des Deutschen Wetterdienstes Nr.* **161**: 14.

Auer, R. 1939. Über den täglichen gang des ozongehalts der bodennahen luft. *Beitraege Zur Geschichte Der Geophysik and Kosmischen Physik.* **54**: 137–145.

BADC. 2019. British Atmospheric Data Centre. *Natural Environment Research Council.* https://webarchive.nationalarchives.gov.uk/20090705125637/http://badc.nerc.ac.uk/data/. Accessed July 2, 2019.

Bak, J, Liu, X, Kim, J-H, Haffner, DP, Chance, K, Yang, K and **Sun, K.** 2017. Characterization and correction of OMPS nadir mapper measurements for ozone profile retrievals. *Atmos. Meas. Tech.* **10**: 4373–4388. DOI: https://doi.org/10.5194/amt-10-4373-2017

Bariteau, L, Helmig, D, Fairall, CW, Hare, JE, Hueber, J and **Lang, EK.** 2010. Determination of oceanic ozone deposition by ship-borne eddy covariance flux measurements. *Atmos. Meas. Tech.* **3**: 441–455. DOI: https://doi.org/10.5194/amt-3-441-2010

Barles, S. 2012. Undesirable nature: Animals, resources and urban nuisance in nineteenth-century Paris. In: *Animal cities: Beastly urban histories*, Atkins, P. (ed), Aldershot, UK: Ashgate Publishing Ltd.

Barnes, RA, Bandy, AR and **Torres, AL.** 1985. Electrochemical concentration cell ozonesonde accuracy and precision. *J. Geophys. Res.* **90**(D5): 7881–7887. DOI: https://doi.org/10.1029/JD090iD05p07881

Barret, B, Le Flochmoen, E, Sauvage, B, Pavelin, E, Matricardi, M and **Cammas, J-P.** 2011. The detection of post-monsoon tropospheric ozone variability over south Asia using IASI data. *Atmos. Chem. Phys.* **11**: 9533–9548. DOI: https://doi.org/10.5194/acp-11-9533-2011

Beekmann, M, Ancellet, G, Martin, D, Abonnel, C, Duverneuil, G, Eideliman, F, Bessemoulin, P, Fritz, N and **Girard, E.** 1995. Intercomparison of tropospheric ozone profiles obtained by electrochemical sondes, a ground-based lidar and an airborne UV-photometer. *Atmos. Environ.* **29**: 1027–1042. DOI: https://doi.org/10.1016/1352-2310(94)00336-J

Beekmann, M, Ancellet, G, Mégie, G, Smit, HGJ and **Kley, D.** 1994. Intercomparison campaign of vertical ozone profiles including electrochemical sondes of ECC and Brewer-Mast type and a ground-based UV-differential absorption lidar. *J. Atmos. Chem.* **19**: 259–288. DOI: https://doi.org/10.1007/BF00694614

Beer, R, Glavich, TA and **Rider, DM.** 2001. Tropospheric emission spectrometer for the Earth Observing System's Aura satellite. *Applied Optics.* **40**: 2356–2367. DOI: https://doi.org/10.1364/AO.40.002356

Bekö, G, Allen, JG, Weschler, CJ, Vallarino, J and **Spengler, JD.** 2015. Impact of Cabin Ozone Concentrations on Passenger Reported Symptoms in Commercial Aircraft. *PLoS ONE.* **10**(5): e0128454. DOI: https://doi.org/10.1371/journal.pone.0128454

Bergshoeff, G, Lanting, RW, Prop, JMG and **Reynders, HFR.** 1980. Improved neutral buffered potassium iodide method for ozone. *Anal. Chem.* **52**: 541–546. DOI: https://doi.org/10.1021/ac50053a038

BIPM. 2019. http://www.bipm.org/en/bipm/chemistry/gas-metrology/ozone.html. Accessed July 12, 2019.

Bischof, W. 1973. Ozone measurements in jet airliner cabin air. *Water Air Soil Pollut.* **2**: 3–14. DOI: https://doi.org/10.1007/BF00572385

Bodeker, GE, Hassler, B, Young, PJ and **Portmann, RW.** 2013. A vertically resolved, global, gap-free ozone database for assessing or constraining global climate model simulations. *Earth Syst. Sci. Data.* **5**: 31–43. DOI: https://doi.org/10.5194/essd-5-31-2013

Bojkov, RD. 1986. Surface ozone during the second half of the nineteenth century. *Journal of Climatic and Applied Meteorology.* **25**: 343–352. DOI: https://doi.org/10.1175/1520-0450(1986)025<0343:SODTSH>2.0.CO;2

Bowen, IG and **Regener, VH.** 1951. On the automatic chemical determination of atmospheric ozone. *J. Geophys. Res.* **56**(3): 307–324. DOI: https://doi.org/10.1029/JZ056i003p00307

Bowman, KW, Rodgers, CD, Kulawik, SS, Worden, J, Sarkissian, E, Osterman, G, Steck, T, Lou, M, Eldering, A, Shephard, M, Worden, H, Lampel, M, Clough, S, Brown, P, Rinsland, C, Gunson, M and **Beer, R.** 2006. Tropospheric Emission Spectrometer: Retrieval Method and Error Analysis. *IEEE Trans. Geosci. Remote Sensing.* **44**: 1297–1307. DOI: https://doi.org/10.1109/TGRS.2006.871234

Bowman, LD and **Horak, RF.** 1972. Continuous Ultraviolet Absorption Ozone Photometer. *Analysis Instrumentation*, 10. Chapman, RL, McNeill, GA and Bartz, AM (eds.), 103–108. Instrument Society of America.

Boxe, CS, Worden, JR, Bowman, KW, Kulawik, SS, Neu, JL, Ford, WC, Osterman, GB, Herman, RL, Eldering, A, Tarasick, DW, Thompson, AM, Doughty, DC, Hoffmann, MR and **Oltmans, SJ.** 2010. Validation of northern latitude Tropospheric Emission Spectrometer stare ozone profiles with ARC-IONS sondes during ARCTAS: sensitivity, bias and error analysis. *Atmos. Chem. Phys.* **10**: 9901–9914. DOI: https://doi.org/10.5194/acp-10-9901-2010

Boynard, A, Clerbaux, C, Coheur, P-F, Hurtmans, D, Turquety, S, George, M, Hadji-Lazaro, J, Keim, C and **MeyerArnek, J.** 2009. Measurements of total and tropospheric ozone from IASI: comparison with correlative satellite, ground-based and ozonesonde observations. *Atmos. Chem. Phys.* **9**: 6255–6271. DOI: https://doi.org/10.5194/acp-9-6255-2009

Boynard, A, Hurtmans, D, Garane, K, Goutail, F, Hadji-Lazaro, J, Koukouli, ME, Wespes, C, Vigouroux, C, Keppens, A, Pommereau, J-P, Pazmino, A, Balis, D, Loyola, D, Valks, P, Sussmann, R, Smale, D, Coheur, P-F and **Clerbaux, C.** 2018. Validation of the IASI FORLI/EUMETSAT ozone products using satellite (GOME-2), ground-based (Brewer–Dobson, SAOZ, FTIR) and ozonesonde measurements. *Atmos. Meas. Tech.* **11**: 5125–5152. DOI: https://doi.org/10.5194/amt-11-5125-2018

Boynard, A, Hurtmans, D, Koukouli, ME, Goutail, F, Bureau, J, Safieddine, S, Lerot, C, Hadji-Lazaro, J, Wespes, C, Pommereau, J-P, Loyola, D, Valks, P, Van Roozendael, M, Coheur, P-F and **Clerbaux, C.** 2016. Seven years of IASI ozone retrievals from FORLI: validation with independent total column and vertical profile measurements. *Atmos. Meas. Tech.* **9**: 4327–4353. DOI: https://doi.org/10.5194/amt-9-4327-2016

Brewer, AW. 1955. Ozone concentration measurements from an aircraft in N. Norway. *Meteorol. Res. Pap. No. 946. Meteorol. Res. Comm. (London).*

Brewer, AW and **Milford, JR.** 1960. The Oxford-Kew ozone sonde. *Proc. R. Soc. London, Ser. A.* **256**: 470–495. DOI: https://doi.org/10.1098/rspa.1960.0120

Browell, EV, Carter, AF, Shipley, ST, Allen, RJ, Butler, CF, Mayo, MN, Siviter, JH, Jr. and **Hall, WM.** 1983. NASA multipurpose airborne DIAL system and measurements of ozone and aerosol profiles. *Appl. Optics.* **22**(4): 522–34. DOI: https://doi.org/10.1364/AO.22.000522

Brunner, D, Staehelin, J, Jeker, D, Wernli, H and **Schumann, U.** 2001. Nitrogen oxides and ozone in the tropopause region of the Northern Hemisphere: Measurements from commercial aircraft in 1995/96 and 1997. *J. Geophys. Res.* **106**: 27673–27699. DOI: https://doi.org/10.1029/2001JD900239

Buchmann, B, Klausen, J and **Zellweger, C.** 2009. Traceability of Long-Term Atmospheric Composition Observations across Global Monitoring Networks: Chemical Metrology Applied to the Measurements of Constituents in Air, Water, and Soil. *Chimia International Journal for Chemistry*. **63**(10): 657–660(4). DOI: https://doi.org/10.2533/chimia.2009.657

Butchart, N. 2014. The Brewer-Dobson circulation. *Rev. Geophys.* **52**. DOI: https://doi.org/10.1002/2013RG000448

Butchart, N, Scaife, AA, Bourqui, M, de Grandpré, J, Hare, SHE, Kettleborough, J, Langematz, U, Manzini, E, Sassi, F, Shibata, K, Shindell, D and **Sigmond, M.** 2006. Simulations of anthropogenic change in the strength of the Brewer-Dobson circulation. *Clim. Dyn.* **27**: 727–741. DOI: https://doi.org/10.1007/s00382-006-0162-4

Byers, DH and **Saltzman, BE.** 1959. Determination of Ozone in Air by Neutral and Alkaline Iodide Procedures. *Advances in Chemistry, ACS Series*. **21**: 93–101. DOI: https://doi.org/10.1021/ba-1959-0021.ch013

Cai, Z, Liu, Y, Liu, X, Chance, K, Nowlan, CR, Lang, R, Munro, R and **Suleiman, R.** 2012. Characterization and Correction of Global Ozone Monitoring Experiment-2 Ultraviolet Measurements and Application to Ozone Profile Retrievals. *J. Geophys. Res.* **117**: D07305. DOI: https://doi.org/10.1029/2011JD017096

Calvert, JG, Orlando, JJ, Stockwell, WR and **Wallington, TJ.** 2015. The Mechanisms of Reactions Influencing Atmospheric Ozone. New York: Oxford University Press. **590**.

Campos, T, Flocke, F and **UCAR/NCAR – Earth Observing Laboratory.** 2006. Nitric Oxide Chemiluminescence Ozone Instrument for HIAPER. *UCAR/NCAR – Earth Observing Laboratory*. (Retrieved 12/07/2019). DOI: https://doi.org/10.5065/D6SN070H

Carbenay, J and **Vassy, A.** 1953. Dosage continu de l'ozone atmosphérique. *Annales de Geophysique*. **9**: 300–308.

Cauer, H. 1935. Bestimmung des Gesamtoxydationswert es des Nitrits, des Ozons und des Gesamtchlorgehalts roher und vergifteter Luft. *Z. anal. Chemie.* **103**: 385–416. DOI: https://doi.org/10.1007/BF01383020

Cauer, H. 1951. *Compendium of Meteorology*. Malone, TF (ed.). Baltimore: Waverly Press, Inc., 1126–1136. DOI: https://doi.org/10.1007/978-1-940033-70-9_91

Central Pollution Control Board, Ministry of Environment & Forests, Govt. of India. 2009. Guidelines for the Measurement of Ambient Air Pollutants, NAAQS Monitoring & Analysis Guidelines Volume-II, Guidelines for Real Time Sampling & Analyses, 47 pp.

Chalonge, D, Götz, F and **Vassy, E.** 1934. Mesures simultanées de la teneur en ozone dans les basses couches de l'atmosphère au Jungfraujoch et a Lauterbrunnen. *Comptes Rendus Acad. Sci.* **198**: 1442.

Chalonge, D and **Vassy, E.** 1934. Recherches sur la transparence de la basse atmosphère et sa teneur en ozone. *J. Phys. Radium*. **5**(7): 309–319. DOI: https://doi.org/10.1051/jphysrad:0193400507030900

Chance, KV, Burrows, JP, Perner, D and **Schneider, W.** 1997. Satellite measurements of atmospheric ozone profiles, including tropospheric ozone, from ultraviolet/visible measurements in the nadir geometry: a potential method to retrieve tropospheric ozone. *J. Quant. Spectrosc. Radiat. Transfer*. **57**: 467–476. DOI: https://doi.org/10.1016/S0022-4073(96)00157-4

Chandra, S, Ziemke, JR and **Martin, RV.** 2003. Tropospheric ozone at tropical and middle latitudes derived from TOMS/MLS residual: Comparison with a global model. *J. Geophys. Res.* **108**: 4291. DOI: https://doi.org/10.1029/2002JD002912

Chang, K-L, Petropavlovskikh, I, Cooper, OR, Schultz, MG and **Wang, T.** 2017. Regional trend analysis of surface ozone observations from monitoring networks in eastern North America, Europe and East Asia. *Elem Sci Anth*. **5**: 50. DOI: https://doi.org/10.1525/elementa.243

Chatfield, R and **Harrison, H.** 1977. Tropospheric ozone: 1. Evidence for higher background values. *J. Geophys. Res,* **82**(37): 5965–5968. DOI: https://doi.org/10.1029/JC082i037p05965

Cherniack, I and **Bryan, RJ.** 1965. A Comparison Study of Various Types of Ozone and Oxidant Detectors Which Are Used for Atmospheric Air Sampling. *Journal of the Air Pollution Control Association*. **15**(8): 351–354. DOI: https://doi.org/10.1080/00022470.1965.10468391

Chung, YS and **Dann, T.** 1985. Observations of stratospheric ozone at the ground level in Regina, Canada. *Atmos. Environ.* **19**: 157–162. DOI: https://doi.org/10.1016/0004-6981(85)90147-7

Claude, H, Hartmannsgruber, R and **Köhler, U.** 1987. Measurement of Atmospheric Profiles using the Brewer-Mast Sonde. *WMO Global Ozone Research and Monitoring Project, Report No. 17*.

Clements, JB. 1975. Summary Report: Workshop on Ozone Measurement by the Potassium Iodide Method. EPA-650/4-75-007 February 1975. *Environmental Monitoring Series*.

Coblentz, WW and **Stair, R.** 1939. Distribution of ozone in the stratosphere. *J. Res. Nat. Bur. Stand.* **22**: 573–606 (R.P. 1207). DOI: https://doi.org/10.6028/jres.022.015

Coblentz, WW and **Stair, R.** 1941. Distribution of ozone in the stratosphere: measurements of 1939 and 1940. *J. Res. Nat. Bur. Stand*, **26**: 161–174 (R.P. 1367). DOI: https://doi.org/10.6028/jres.026.007

Cooper, OR, Parrish, DD, Stohl, A, Trainer, M, Nédélec, P, Thouret, V, Cammas, JP, Oltmans, SJ, Johnson, BJ, Tarasick, D, LeBlanc, T, McDermid, I, Jaffe, D,

Gao, R, Stith, J, Ryerson, T, Aikin, K, Campos, T and **Weinheimer, A.** 2010. Increasing springtime ozone mixing ratios in the free troposphere over western North America. *Nature.* **463**: 344–348. DOI: https://doi.org/10.1038/nature08708

Cooper, OR, Parrish, DD, Ziemke, J, Balashov, NV, Cupeiro, M, Galbally, IE, Gilge, S, Horowitz, L, Jensen, NR, Lamarque, J-F, Naik, V, Oltmans, SJ, Schwab, J, Shindell, DT, Thompson, AM, Thouret, V, Wang, Y and **Zbinden, RM.** 2014. Global distribution and trends of tropospheric ozone: An observation-based review. *Elementa: Science of the Anthropocene.* **2**: 000029. DOI: https://doi.org/10.12952/journal.elementa.000029

Craig, RA. 1950. The observations and photochemistry of atmospheric ozone and their meteorological significance. *Meteorol. Monogr.* Boston, Mass: Am. Meteorol. Soc. **1**(2), 50. DOI: https://doi.org/10.1007/978-1-935704-88-1_1

Crawford, JH and **Pickering, KE.** 2014. DISCOVER-AQ: Advancing Strategies for Air Quality Observations in the Next Decade. *The Magazine for Environmental Managers A&WMA*. September 2014, 4–8.

Cressie, N. 1985. Fitting variogram models by weighted least squares. *J. Int. Assoc. Math. Geol.* **17**(5): 563–586. DOI: https://doi.org/10.1007/BF01032109

Cuesta, J, Eremenko, M, Liu, X, Dufour, G, Cai, Z, Höpfner, M, von Clarmann, T, Sellitto, P, Foret, G, Gaubert, B, Beekmann, M, Orphal, J, Chance, K, Spurr, R and **Flaud, J-M.** 2013. Satellite observation of lowermost tropospheric ozone by multispectral synergism of IASI thermal infrared and GOME-2 ultraviolet measurements over Europe. *Atmos. Chem. Phys.* **13**: 9675–9693. DOI: https://doi.org/10.5194/acp-13-9675-2013

Dantzig, GB and **Cottle, RW.** 1963. Positive (semi-) definite matrices and mathematical programming. No. ORC-63-18-RR. *California Berkeley Operations Research Center*.

Dauvillier, A. 1934. Recherches sur l'ozone atmosphérique effectuées an Scoresby Sund pendant l'anneé polaire. *Journal de Physique et le Radium.* Ser. **7**(5): 455–462. DOI: https://doi.org/10.1051/jphysrad:0193400509045500

Dauvillier, A. 1935. Sur le dosage de l'ozone atmosphérique. Comparaison des méthods spectrographique et chimique. *Comptes Rendus Acad. Sci.* **201**: 679–680.

Davies, TD. 1979. Dissolved sulphur dioxide and sulphate in urban and rural precipitation (Norfolk, U.K.). *Atmos. Environ.* **13**: 1275–1285. DOI: https://doi.org/10.1016/0004-6981(79)90083-0

Del Frate, F, Ortenzi, A, Casadio, S and **Zehner, C.** 2002. Application of neural algorithms for a real-time estimation of ozone profiles from GOME measurements. *IEEE T. Geosci. Remote.* **40**: 2263–2270. DOI: https://doi.org/10.1109/TGRS.2002.803622

De Thierry, M. 1897. Dosage de l'ozone atmosphérique au Mont Blanc. *Comptes Rendus Acad. Sci.* **124**: 460–463.

Dias-Lalcaca, P, Brunner, D, Imfeld, W, Moser, W and **Staehelin, J.** 1998. An automated system for the measurement of nitrogen oxides and ozone concentrations from a passenger aircraft: instrumentation and first results of the project NOXAR. *Env. Sci. Techn.* **32**: 3228–3236. DOI: https://doi.org/10.1021/es980119w

Dietz, RN, Pruzansky, J and **Smith, JD.** 1973. Effect of pH on the Stoichiometry of the ioometric determination of ozone. *Anal. Chem.* **45**: 402–404. DOI: https://doi.org/10.1021/ac60324a059

Di Noia, A, Sellitto, P, Del Frate, F and **De Laat, J.** 2013. Global tropospheric ozone column retrievals from OMI data by means of neural networks. *Atmos. Meas. Tech.* **6**: 895–915. DOI: https://doi.org/10.5194/amt-6-895-2013

Downs, AJ and **Adams, CJ.** 1973. Chlorine, Bromine, Iodine and Astatine. In *Conprehensive Inorganic Chemistry*, Bailar, JC, Jr., Emeléus, HJ, Nyholm, R, Sir and Trotman-Dickenson, AF (eds.), Oxford: Pergammon Press. **2**: 1107–1594. DOI: https://doi.org/10.1016/B978-1-4832-8313-5.50020-6

Draxler, RR and **Hess, GD.** 1998. An overview of the HYSPLIT_4 modeling system for trajectories, dispersion and deposition. *Aust. Met. Mag.* **47**: 295–308.

Dufour, G, Eremenko, M, Cuesta, J, Doche, C, Foret, G, Beekmann, M, Cheiney, A, Wang, Y, Cai, Z, Liu, Y, Takigawa, M, Kanaya, Y and **Flaud, J-M.** 2015. Springtime daily variations in lower-tropospheric ozone over east Asia: the role of cyclonic activity and pollution as observed from space with IASI. *Atmos. Chem. Phys.* **15**: 10839–10856. DOI: https://doi.org/10.5194/acp-15-10839-2015

Dufour, G, Eremenko, M, Griesfeller, A, Barret, B, LeFlochmoën, E, Clerbaux, C, Hadji-Lazaro, J, Coheur, P-F and **Hurtmans, D.** 2012. Validation of three scientific ozone products retrieved from IASI spectra using ozonesondes. *Atmos. Meas. Tech.* **5**: 611–630. DOI: https://doi.org/10.5194/amt-5-611-2012

Dufour, G, Eremenko, M, Orphal, J and **Flaud, J-M.** 2010. IASI observations of seasonal and day-to-day variations of tropospheric ozone over three highly populated areas of China: Beijing, Shanghai, and Hong Kong. *Atmos. Chem. Phys.* **10**: 3787–3801. DOI: https://doi.org/10.5194/acp-10-3787-2010

Eastham, SD and **Jacob, DJ.** 2017. Limits on the ability of global Eulerian models to resolve intercontinental transport of chemical plumes. *Atmos. Chem. Phys.* **17**: 2543–2553. DOI: https://doi.org/10.5194/acp-17-2543-2017

Edgar, JL and **Paneth, FA.** 1941a. The separation of ozone from other gases. *J. Chem. Soc.*, 511–519. DOI: https://doi.org/10.1039/jr9410000511

Edgar, JL and **Paneth, FA.** 1941b. The Determination of Ozone and Nitrogen Dioxide in the Atmosphere. *J. Chem. Soc.*, 519–27. DOI: https://doi.org/10.1039/jr9410000519

Ehmert, A. 1949. Uber das troposphärische Ozon. *Ber. Dtsch. Wetterd, US-Zone.* Nr. **11**: 47.

Ehmert, A. 1951. Ein einfaches Verfahren zur absoluten Messung des Ozongehalts der Luft. *Meteorologische Rundschau.* **4**: 64–68.

Ehmert, A. 1952. Gleichzeitige Messungen des Ozongehaltes bodennaher Luft an mehreren Stationen mit einem einfachen absoluten Verfahren/Simultaneous measurements of the ozone content of air near the earth at several stations by means of a simple absolute method. *J. Atmos. Terr. Phys.* **2**: 189–195. DOI: https://doi.org/10.1016/0021-9169(52)90064-0

Ehmert, A. 1959. Chemical Ozone Measurement. *Advances in Chemistry, ACS Series.* **21**: 128–132. DOI: https://doi.org/10.1021/ba-1959-0021.ch018

Ehmert, A and **Ehmert, H.** 1949. Uber den tagesgang des bodennahen ozons. *Ber. Dtsch. Wetterdienst.* **11**: 58–62.

Eisele, H and **Trickl, T.** 2005. Improvements of the aerosol algorithm in ozone-lidar data processing by use of evolutionary strategies. *Appl. Opt.* **44**: 2638–2651. DOI: https://doi.org/10.1364/AO.44.002638

Elsworth, CM and **Galbally, IE.** 1984. Accurate Surface Ozone Measurements in Clean Air, Fact or Fiction. *Proc. Eighth International Clean Air Conference (Melbourne). Clean Air Society of Australia and New Zealand*, 1093–1112. DOI: https://doi.org/10.1007/978-94-009-5313-0_159

Eremenko, M, Dufour, G, Foret, G, Keim, C, Orphal, J, Beekmann, M, Bergametti, G and **Flaud, J-M.** 2008. Tropospheric ozone distributions over Europe during the heat wave in July 2007 observed from infrared Nadir spectra measured by IASI. *Geophysical Research Letters.* **35**. DOI: https://doi.org/10.1029/2008GL034803

Eriksson, P and **Chen, D.** 2002. Statistical parameters derived from ozonesonde data of importance for passive remote sensing of ozone. *Int. J. Remote Sens.* **23**(22): 4945–4963. DOI: https://doi.org/10.1080/01431160110111036

ESRL. 2019. National Oceanic and Atmospheric Administration, Earth System Research Laboratory. https://www.esrl.noaa.gov/gmd/ozwv/aircraft/data.html. Accessed July 2, 2019.

European Union. 2008. DIRECTIVE 2008/50/EC OF THE EUROPEAN PARLIAMENT AND OF THE COUNCIL on ambient air quality and cleaner air for Europe, O.J. L 152/26, http://eur-lex.europa.eu/LexUriServ/LexUriServ.do?uri=OJ:L:2008:152:0001:0044:en:PDF.

European Union. 2012. DIN EN 14625:2012 2012. Ambient air – Standard method for the measurement of the concentration of ozone by ultraviolet photometry; EN 14625:2012

FAA. 1977. Ozone Irritation During High Altitude Flight, Advisory Circular No. 00-52, July 21, FAA 1977, Federal Aviation Administration.

FAA. 1980. https://www.faa.gov/documentLibrary/media/Advisory_Circular/AC_120-38.pdf.

Fabian, P and **Pruchniewicz, PG.** 1976. Final Report on Project "Troposphärisches Ozon" Contract No Fa 62/1 Deutsche Foraschungagamsinschaft, MPAE-W-100-76-21, 28.

Fabian, P and **Pruchniewicz, PG.** 1977. Meridional distribution of ozone in the troposphere and its seasonal variation. *J. Geophys. Res.* **82**: 2063–2073. DOI: https://doi.org/10.1029/JC082i015p02063

Fabry, C. 1950. *L'ozone atmosphérique.* Centre National de la Recherche Scientifique Paris, 278.

Fabry, C and **Buisson, B.** 1931. Sur l'absorption des radiations dans la basse atmosphère et le dosage de l'ozone. *Comptes Rendus Acad. Sci.* **192**: 457–461.

Falconer, PD and **Holdeman, JD.** 1976. Measurements of atmospheric ozone made from a GASP-equipped 747 airliner Mid-March, 1975. *Geophys. Res. Lett.* **3**: 101–104. DOI: https://doi.org/10.1029/GL003i002p00101

Favaro, G, Jeannet, P and **Stübi, R.** 2002. Re-evaluation and trend analysis of the Payerne ozone soundings. *Veröffentlichung der MeteoSchweiz.* **63**: 99. Zürich, Switzerland: MeteoSchweiz.

Feister, U and **Warmbt, W.** 1987. Long-term measurements of surface ozone in the German Democratic Republic. *J. Atmos. Chem.* **5**: 1–22. DOI: https://doi.org/10.1007/BF00192500

Fishman, J, Brackett, VG, Browell, EV and **Grant, WB.** 1996. Tropospheric ozone derived from TOMS/SBUV measurements during TRACE A. *J. Geophys. Res.* **101**: 24,069–24,082. DOI: https://doi.org/10.1029/95JD03576

Fishman, J, Watson, CE, Larsen, JC and **Logan, JA.** 1990. Distribution of tropospheric ozone determined from satellite data. *J. Geophys. Res.* **95**: 3599–3617. DOI: https://doi.org/10.1029/JD095iD04p03599

Fishman, J, Wozniak, AE and **Creilson, JK.** 2003. Global distribution of tropospheric ozone from satellite measurements using the empirically corrected tropospheric ozone residual technique: Identification of the regional aspects of air pollution. *Atmos. Chem. Phys.* **3**: 893–907. DOI: https://doi.org/10.5194/acp-3-893-2003

Flamm, DL. 1977. Analysis of ozone at low concentrations with boric acid buffered KI. *Environ. Sci. Technol.* **11**: 879–983. DOI: https://doi.org/10.1021/es60133a006

Fleming, ZL, Doherty, RM, von Schneidemesser, E, Malley, CS, Cooper, OR, Pinto, JP, Colette, A, Xu, X, Simpson, D, Schultz, MG, Lefohn, AS, Hamad, S, Moolla, R, Solberg, S and **Feng, Z.** 2018. Tropospheric Ozone Assessment Report: Present-day ozone distribution and trends relevant to human health. *Elem Sci Anth.* **6**(1): 12. DOI: https://doi.org/10.1525/elementa.273

Flemming, J, Stern, R and **Yamartino, RJ.** 2005. A new air quality regime classification scheme for O_3, NO_2, SO_2 and PM10 observations sites. *Atmos. Environ.* **39**: 6121–6129. DOI: https://doi.org/10.1016/j.atmosenv.2005.06.039

Fontijn, A, Sabadell, AJ and **Ronco, RJ.** 1970. Homogeneous chemiluminescent measurement of nitric oxide with ozone. Implications for continuous selective monitoring of gaseous air pollutants.

Analytical Chemistry. **42**(6): 575–579. DOI: https://doi.org/10.1021/ac60288a034

Fox, C. 1873. Ozone and Antozone: Their History and Nature, J. and A. Churchill, London, UK, 329.

Fu, D, Worden, JR, Liu, X, Kulawik, SS, Bowman, KW and **Natraj, V.** 2013. Characterization of ozone profiles derived from Aura TES and OMI radiances. *Atmos. Chem. Phys.* **13**: 3445–3462. DOI: https://doi.org/10.5194/acp-13-3445-2013

Galbally, IE. 1968. Some measurements of ozone variation and destruction in the atmospheric surface layer. *Nature.* **218**(5140): 456–457. DOI: https://doi.org/10.1038/218456a0

Galbally, IE. 1969. An evaluation of the Ehmert technique for measuring ozone profiles in the atmospheric surface layer. *J. Geophys. Res.* **74**(28): 6869–6872. DOI: https://doi.org/10.1029/JC074i028p06869

Galbally, IE. 1971. Ozone profiles and ozone fluxes in the atmospheric surface layer. *Quarterly Journal of the Royal Meteorological Society.* **97**(411): 18–29. DOI: https://doi.org/10.1002/qj.49709741103

Galbally, IE. 1972. Ozone and oxidants in the surface air near Melbourne, Victoria. *Proc. Int. Clean Air Conf. (Melbourne, Australia)*, 192–198.

Galbally, IE. 1979. Section 3.1.3 Surface Ozone, In Baseline Air Monitoring Report 1977, Department of Science, Australian Government Publishing Service. (Canberra, Australia), 3–6.

Galbally, IE, Miller, AJ, Hoy, RD, Ammet, S, Joynt, RC and **Attwood, D.** 1986. Ozone in the surface air over the Latrobe Valley, Victoria and Cape Grim, Tasmania, Australia. *Atmos. Environ.* **20**: 2403–2422. DOI: https://doi.org/10.1016/0004-6981(86)90071-5

Galbally, IE and **Paltridge, G.** 1989. The ozone issue. In: *Disease and Society A Resource Book*, Dircks, R (ed.). Canberra: Australian Academy of Science.

Galbally, IE and **Roy, CR.** 1980. Destruction of ozone at the Earth's surface. *Quarterly Journal of the Royal Meteorological Society.* **106**(449): 599–620. DOI: https://doi.org/10.1256/smsqj.44914

Galbally, IE and **Roy, CR.** 1981. Ozone and nitrogen oxides in the southern hemisphere troposphere. In: *Proceedings in the Quadrennial International Ozone Symposium.* (Boulder, Colorado). 1980, International Ozone Commission, 431–438.

Galbally, IE, Schultz, MG, Buchmann, B, Gilge, S, Guenther, F, Koide, H, Oltmans, S, Patrick, L, Scheel, H-E, Smit, H, Steinbacher, M, Steinbrecht, W, Tarasova, O, Viallon, J, Volz-Thomas, A, Weber, M, Wielgosz, R and **Zellweger, C.** 2013. Guidelines for Continuous Measurement of Ozone in the Troposphere, GAW Report No 209, Publication WMO-No. 1110, ISBN 978-92-63-11110-4, Geneva, Switzerland: World Meteorological Organisation, 76. http://www.wmo.int/pages/prog/arep/gaw/gaw-reports.html.

García, OE, Schneider, M, Redondas, A, González, Y, Hase, F, Blumenstock, T and **Sepúlveda, E.** 2012. Investigating the long-term evolution of subtropical ozone profiles applying ground-based FTIR spectrometry. *Atmos. Meas. Tech.* **5**: 2917–2931. DOI: https://doi.org/10.5194/amt-5-2917-2012

Garland, JA and **Derwent, RG.** 1979. Destruction at the ground and the diurnal cycle of concentration of ozone and other gases. *Q.J.R. Meteorol. Soc.* **105**: 169–183. DOI: https://doi.org/10.1002/qj.49710544311

Gaubert, B, Coman, A, Foret, G, Meleux, F, Ung, A, Rouil, L, Ionescu, A, Candau, Y and **Beekmann, M.** 2014. Regional scale ozone data assimilation using an ensemble Kalman filter and the CHIMERE chemical transport model. *Geosci. Model Dev.* **7**: 283–302. DOI: https://doi.org/10.5194/gmd-7-283-2014

Gaudel, A, Ancellet, G and **Godin-Beekmann, S.** 2015. Analysis of 20 years of tropospheric ozone vertical profiles by lidar and ECC at Observatoire de Haute Provence (OHP) at 44°N, 6.7°E. *Atmos. Environ.* **113**: 78–89. DOI: https://doi.org/10.1039/b205727a

Gaudel, A, Cooper, OR, Ancellet, G, Barret, B, Boynard, A, Burrows, JP, Clerbaux, C, Coheur, P-F, Cuesta, J, Cuevas, E, Doniki, S, Dufour, G, Ebojie, F, Foret, G, Garcia, O, Granados Muños, MJ, Hannigan, JW, Hase, F, Huang, G, Hassler, B, Hurtmans, D, Jaffe, D, Jones, N, Kalabokas, P, Kerridge, B, Kulawik, SS, Latter, B, Leblanc, T, Le Flochmoën, E, Lin, W, Liu, J, Liu, X, Mahieu, E, McClure-Begley, A, Neu, JL, Osman, M, Palm, M, Petetin, H, Petropavlovskikh, I, Querel, R, Rahpoe, N, Rozanov, A, Schultz, MG, Schwab, J, Siddans, R, Smale, D, Steinbacher, M, Tanimoto, H, Tarasick, DW, Thouret, V, Thompson, AM, Trickl, T, Weatherhead, E, Wespes, C, Worden, HM, Vigouroux, C, Xu, X, Zeng, G and **Ziemke, J.** 2018. Tropospheric Ozone Assessment Report: Present-day distribution and trends of tropospheric ozone relevant to climate and global atmospheric chemistry model evaluation. *Elem Sci Anth.* **6**(1): 39. DOI: https://doi.org/10.1525/elementa.291

Glückauf, E. 1944. The ozone content of surface air and its relation to some meteorological conditions. *Quarterly Journal Royal Meteorological Society.* **70**: 13–21. DOI: https://doi.org/10.1002/qj.49707030303

Glückauf, E, Heal, HG,. Martin, GR and **Paneth, FA.** 1944. A method for the continuous measurement of the local concentration of atmospheric ozone. *J. Chem. Soc.* **1944**: 1–4. DOI: https://doi.org/10.1039/jr9440000001

Gonçalves, FLT, Morinobu, WN, Andrade, MF and **Fornaro, A.** 2007. In-cloud and below-cloud scavenging analysis of sulfate in the metropolitan area of São Paulo, Brasil. *Revista Brasileira de Meteorologia*, **22**(1): 94–104. DOI: https://doi.org/10.1590/S0102-77862007000100010

Gorshelev, V, Serdyuchenko, A, Weber, M, Chehade, W and **Burrows, JP.** 2014. High spectral resolution ozone absorption cross-sections – Part 1: Measurements, data analysis and comparison with

previous measurements around 293 K. *Atmos. Meas. Tech.* **7**: 609–624. DOI: https://doi.org/10.5194/amt-7-609-2014

Götz, FWP and **Ladenburg, R.** 1931. Ozongehalt der unteren Atmosphärenschichten. *Die Naturwissenschaften.* **18**: 373–374. DOI: https://doi.org/10.1007/BF01516268

Götz, FWP and **Maier-Leibnitz, H.** 1933. Zur Ultraviolettabsorption bodennaher Luftschichten, Z. *Geophys.* **9**: 253–260.

Götz, FWP, Meetham, AR and **Dobson, GMB.** 1934. The vertical distribution of ozone in the atmosphere. *Proc. Roy. Soc. (London).* **A145**: 416–446. DOI: https://doi.org/10.1098/rspa.1934.0109

Götz, FWP and **Penndorf.** 1941. Weitere Frühjahrswerte des bodennahen Ozons in Arosa. *Meteorol. Zeitschr.* **58**: 409–415.

Götz, FWP, Schein, M and **Stoll, B.** 1935. Messungen des bodennahen Ozons in Zürich, Ger lands Beitr. *Geophys.* **45**: 237–242.

Götz, FWP and **Volz, F.** 1951. Aroser Messungen des Ozongehalts der unteren Troposphäre und sein Jahresgang, Z. *Naturforschg.* **6a**: 634–639.

Granier, C, Bessagnet, B, Bond, T, D'Angiola, A, van der Gon, HD, Frost, GJ, Heil, A, Kaiser, JW, Kinne, S, Klimont, Z, Kloster, S, Lamarque, J-F, Liousse, C, Masui, T, Meleux, F, Mieville, A, Ohara, T, Raut, J-C, Riahi, K, Schultz, MG, Smith, SJ, Thompson, A, van Aardenne, J, van der Werf, GR and **van Vuuren, DP.** 2011. Evolution of anthropogenic and biomass burning emissions of air pollutants at global and regional scales during the 1980–2010 period. *Climatic Change.* **109**: 163–190. DOI: https://doi.org/10.1007/s10584-011-0154-1

Grasso, B. 2011. A Study of Photochemical Pollutants in the Port Phillip Region over 40 years: A Reconstruction of Data from Two Analytical Measurement Techniques. *Science Honours Thesis, School of Applied Sciences.* Melbourne, Australia: RMIT University. 73.

Gudiksen, PH, Hildebrandt, PW and **Kelley, JJ, Jr.** 1966. Comparison of an electrochemical and a colorimetric determination of ozone. *J. Geophys. Res.* **71**(22): 5221–5223. DOI: https://doi.org/10.1029/JZ071i022p05221

Hache, E, Attie, J-L, Tourneur, C, Ricaud, P, Coret, L, Lahoz, WA, El Amraoui, L, Josse, B, Hamer, P, Warner, J, Liu, X, Chance, K, Höpfner, M, Spurr, R, Natraj, V, Kulawik, S, Eldering, A and **Orphal, J.** 2014. The added value of a geostationary thermal infrared and visible instrument to monitor ozone for air quality. *Atmos. Meas. Tech.* **7**: 2185–2201. DOI: https://doi.org/10.5194/amt-7-2185-2014

Hardacre, C, Wild, O and **Emberson, L.** 2015. An evaluation of ozone dry deposition in global scale chemistry climate models. *Atmos. Chem. Phys.* **15**: 6419–6436. DOI: https://doi.org/10.5194/acp-15-6419-2015

Hartley, WN. 1881. On the absorption of solar rays by atmospheric ozone. *Journal of the Chemical Society (London).* **39**: 111–128. DOI: https://doi.org/10.1039/CT8813900111

Hasekamp, OP and **Landgraf, J.** 2001. Ozone profile retrieval from backscattered ultraviolet radiances: The inverse problem solved by regularization. *J. Geophys. Res.* **106**(D8): 8077–8088. DOI: https://doi.org/10.1029/2000JD900692

Hasekamp, OP and **Landgraf, J.** 2002. Tropospheric ozone information from satellite-based polarization measurements. *J. Geophys. Res.* **107**(D17): 4326. DOI: https://doi.org/10.1029/2001JD001346

Hassler, B, Kremser, S, Bodeker, GE, Lewis, J, Nesbit, K, Davis, SM, Chipperfield, MP, Dhomse, SS and **Dameris, M.** 2018. An updated version of a gap-free monthly mean zonal mean ozone database. *Earth Syst. Sci. Data.* **10**: 1473–1490. DOI: https://doi.org/10.5194/essd-10-1473-2018

He, H, Tarasick, DW, Hocking, WK, Carey-Smith, TK, Rochon, Y, Zhang, J, Makar, PA, Osman, M, Brook, J, Moran, M, Jones, D, Mihele, C, Wei, JC, Osterman, G, Argall, PS, McConnell, J and **Bourqui, MS.** 2011. Transport Analysis of Ozone Enhancement in Southern Ontario during BAQS-Met. *Atmos. Chem. Phys.* **11**: 2569–2583. DOI: https://doi.org/10.5194/acp-11-2569-2011

Hearn, AG. 1961. The absorption of ozone in the ultra-violet and visible regions of the spectrum. *Proc. Phys. Soc.* **78**: 932–940. DOI: https://doi.org/10.1088/0370-1328/78/5/340

Heidorn, KC and **Yap, D.** 1986. A synoptic climatology for surface ozone concentrations in Southern Ontario, 1976–1981. *Atmos. Environ.* **20**: 695–703. DOI: https://doi.org/10.1016/0004-6981(86)90184-8

Henne, S, Brunner, D, Folini, D, Solberg, S, Klausen, J and **Buchmann, B.** 2010. Assessment of parameters describing representativeness of air quality in-situ measurement sites. *Atmos. Chem. Phys.* **10**: 3561–3581. DOI: https://doi.org/10.5194/acp-10-3561-2010

Hering, WS. 1964. Ozonesonde Observations Over North America, Volume 1, AFCRL-64-30(I), *Air Force Cambridge Research Labs*, Bedford, MA: Hanscom AFB.

Hering, WS and **Borden, TS.** 1964. Ozonesonde Observations Over North America, Volume 2, AFCRL-64-30(II), *Air Force Cambridge Research Labs*, Bedford, MA: Hanscom AFB. DOI: https://doi.org/10.21236/AD0604880

Hering, WS and **Borden, TS.** 1965. Ozonesonde Observations Over North America, Volume 3, AFCRL-64-30(III), *Air Force Cambridge Research Labs*, Bedford, MA: Hanscom AFB.

Hering, WS and **Borden, TS.** 1967. Ozonesonde Observations Over North America, Volume 4, AFCRL-64-30(IV), *Air Force Cambridge Research Labs*, Bedford, MA: Hanscom AFB.

Hering, WS and **Dütsch, HU.** 1965. Comparison of chemiluminescent and electrochemical ozonesonde

observations. *J. Geophys. Res.* **70**(22): 5483–5490. DOI: https://doi.org/10.1029/JZ070i022p05483

Hess, PG and **Zbinden, R.** 2013. Stratospheric impact on tropospheric ozone variability and trends: 1990–2009. *Atmos. Chem. Phys.* **13**: 649–674. DOI: https://doi.org/10.5194/acp-13-649-2013

Hilboll, A, Richter, A and **Burrows**, **JP.** 2013. Long-term changes of tropospheric NO_2 over megacities derived from multiple satellite instruments. *Atmos. Chem. Phys.* **13**: 4145–4169. DOI: https://doi.org/10.5194/acp-13-4145-2013

Hilsenrath, E, Attmannspacher, W, Bass, A, Evans, W, Hagemeyer, R, Barnes, RA, Komhyr, W, Mauersberger, K, Mentall, J, Proffitt, M, Robbins, D, Taylor, S, Torres, A and **Weinstock**, **E.** 1986. Results from the balloon intercomparison campaign (BOIC). *J. Geophys. Res.* **91**: 13137–13152. DOI: https://doi.org/10.1029/JD091iD12p13137

Hodges, JT, Viallon, J, Brewer, PJ, Drouin, BJ, Gorshelev, V, Janssen, C, Lee, S, Possolo, A, Smith, MAH, Walden, J and **Wielgosz, RI.** 2019. Recommendation of a consensus value of the ozone absorption cross-section at 253.65 nm based on a literature review. *Metrologia.* **56**: 034001. https://iopscience.iop.org/article/10.1088/1681-7575/ab0bdd.

Hodgeson, JA, Baumgardner, RE, Martin, BE and **Rehme, KA.** 1971. Stoichiometry in the neutral iodometric procedure for ozone by gas phase titration with nitric oxide. *Anal. Chem.* **43**(8): 1123–126. DOI: https://doi.org/10.1021/ac60303a026

Hoogen, R, Rozanov, VV and **Burrows, JP.** 1999. Ozone profiles from GOME satellite data: Algorithm description and first validation. *J. Geophys. Res.* **104**(D7): 8263–8280. DOI: https://doi.org/10.1029/1998JD100093

Houzeau, A. 1857. Observations sur la valeur du papier dit ozonométrique et exposition d'une nouvelle méthode analytique pour reconnaitre et doser l'ozone (seance du 10 Mars 1857). *Ann. Soc. Meteorol. Paris.* **5**: 43–53.

Huang, G, Liu, X, Chance, K, Yang, K, Bhartia, PK, Cai, Z, Allaart, M, Ancellet, G, Calpini, B, Coetzee, GJR, Cuevas-Agulló, E, Cupeiro, M, De Backer, H, Dubey, MK, Fuelberg, HE, Fujiwara, M, Godin-Beekmann, S, Hall, TJ, Johnson, B, Joseph, E, Kivi, R, Kois, B, Komala, N, König-Langlo, G, Laneve, G, Leblanc, T, Marchand, M, Minschwaner, KR, Morris, G, Newchurch, MJ, Ogino, S-Y, Ohkawara, N, Piters, AJM, Posny, F, Querel, R, Scheele, R, Schmidlin, FJ, Schnell, RC, Schrems, O, Selkirk, H, Shiotani, M, Skrivánková, P, Stübi, R, Taha, G, Tarasick, DW, Thompson, AM, Thouret, V, Tully, MB, Van Malderen, R, Vömel, H, von der Gathen, P, Witte, JC and **Yela, M.** 2017. Validation of 10-year SAO OMI Ozone Profile (PROFOZ) product using ozonesonde observations. *Atmos. Meas. Tech.* **10**: 2455–2475. DOI: https://doi.org/10.5194/amt-10-2455-2017

Huang, G, Liu, X, Chance, K, Yang, K and **Cai, Z.** 2018. Validation of 10-year SAO OMI ozone profile (PROFOZ) product using Aura MLS measurements. *Atmos. Meas. Tech.* **11**: 17–32. DOI: https://doi.org/10.5194/amt-11-17-2018

Hudson, RD and **Thompson, AM.** 1998. Tropical tropospheric ozone from total ozone mapping spectrometer by a modified residual method. *J. Geophys. Res.* **103**(D17): 22129–22145. DOI: https://doi.org/10.1029/98JD00729

Inn, ECY and **Tanaka, Y.** 1953. Absorption Coefficient of Ozone in the Ultraviolet and Visible Regions. *J. Opt. Soc. Am.* **43**: 870. DOI: https://doi.org/10.1364/JOSA.43.000870

Ionescu, A, Lefevre, RA, Brimblecombe, P and **Grossi, CM.** 2012. Long-term damage to glass in Paris in a changing environment. *Science of the Total Environment.* **431**: 151–156. DOI: https://doi.org/10.1016/j.scitotenv.2012.05.028

IPCC. 2001. Climate Change 2001, The Physical Science Basis, Working Group I, Chapter 6, Section 6.5.2.1, Ozone radiative forcing: process studies. https://www.ipcc.ch/report/ar3/wg1/.

IPCC. 2013. The Physical Science Basis Working Group I Contribution to the Fifth Assessment Report of the Intergovernmental Panel on Climate Change, Edition: 2014. https://www.ipcc.ch/assessment-report/ar5/.

ISO. 2017. ISO 13964 1998 Ambient Air—Determination of Ozone—Ultraviolet Photometric Method. Geneva: International Organization for Standardization. https://www.iso.org/standard/23528.html.

Janssen, S, Dumont, G, Fierens, F, Deutsch, F, Maiheu, B, Celis, D, Trimpeneers, E and **Mensink, C.** 2012. Land use to characterize spatial representativeness of air quality monitoring stations and its relevance for model validation. *Atmos. Environ.* **59**: 492–500. DOI: https://doi.org/10.1016/j.atmosenv.2012.05.028

JCGM. 2008. JCGM-100: Evaluation of measurement data – Guide to the expression of uncertainty in measurement (JCGM-100), http://www.bipm.org/utils/common/documents/jcgm/JCGM_100_2008_E.pdf.

Jiang, Y and **Yung, YL.** 1996. Concentrations of tropospheric ozone from 1979 to 1992 over tropical Pacific South America from TOMS data. *Science.* **272**: 714–716. DOI: https://doi.org/10.1126/science.272.5262.714

Jing, P, Cunnold, D, Choi, Y and **Wang, Y.** 2006. Summertime tropospheric ozone columns from Aura OMI/MLS measurements versus regional model results over the United States. *Geophys. Res. Lett.* **33**: L17817. DOI: https://doi.org/10.1029/2006GL026473

Johnson, BJ, Oltmans, SJ, Voemel, H, Smit, HGJ, Deshler, T and **Kroeger, C.** 2002. ECC Ozonesonde pump efficiency measurements and tests on the sensitivity to ozone of buffered and unbuffered ECC sensor cathode solutions. *J. Geophys. Res.* **107**: D19. DOI: https://doi.org/10.1029/2001JD000557

Joly, M and **Peuch, VH.** 2012. Objective Classification of air quality monitoring sites over Europe.

Atmos. Environ. **47**: 111–123. DOI: https://doi.org/10.1016/j.atmosenv.2011.11.025

Kawamura, K and **Sakurai, S.** 1966. The concentrations of nitrogen dioxide and ozone in the air at inland and seashore in Japan. *Pap. Met. Geophys*, **17**: 200–209. DOI: https://doi.org/10.2467/mripapers1950.17.3_200

Kay, RH. 1953. An interim report on the measurement of the vertical distribution of atmospheric ozone by a chemical method, to heights of 12 km, from aircraft. *Meteorol. Res. Pap. No.* **817**: 1–15. Meteorol. Res. Comm. (London).

Kelley, JJ. 1970. Atmospheric ozone investigations at Barrow, Alaska, during 1966, 1967: Report No. 2. *Scientific Report, Office of Naval Research* [Contract N00014-67-A-0103-0007 NR 307-252]; 5 Seattle, WA: Department of Atmospheric Sciences, University of Washington, 110.

Kelley, JJ. 1973. Surface ozone in the Arctic atmosphere. *PAGEOPH* **106**: 1106. DOI: https://doi.org/10.1007/BF00881064

Kerr, JB, Fast, H, McElroy, CT, Oltmans, SJ, Lathrop, JA, Kyro, E, Paukkunen, A, Claude, H, Köhler, U, Sreedharan, CR, Takao, T and **Tsukagoshi, Y.** 1994. The 1991 WMO international ozonesonde intercomparison at Vanscoy, Canada. *Atmosphere-Ocean.* **32**: 685–716. DOI: https://doi.org/10.1080/07055900.1994.9649518

Kesztembaum, L and **Rosenthal, JL.** 2014. Income versus Sanitation: Mortality decline in Paris 1880–1914. *PSE Working Papers no 2014-26 2014 <halshs-01018594>* https://halshs.archives-ouvertes.fr/halshs-01018594.

Kim, E and **Barles, S.** 2012. The energy consumption of Paris and its supply areas from the eighteenth century to the present. *Reg. Environ. Change.* **12**: 295–310. DOI: https://doi.org/10.1007/s10113-011-0275-0

Kim, JH, Hudson, RD and **Thompson, AM.** 1996. A new method of deriving time-averaged tropospheric column ozone over the tropics using total ozone mapping spectrometer (TOMS) radiances: Intercomparison and analysis using TRACE A data. *J. Geophys. Res.* **101**(D19): 24317–24330. DOI: https://doi.org/10.1029/96JD01223

Kim, JH, Newchurch, MJ and **Lee, K.** 2001. Distribution of Tropical Tropospheric Ozone Determined by the Scan-Angle Method Applied to TOMS Measurements. *J. Atmos. Sci.* **58**(18): 2699–2708. DOI: https://doi.org/10.1175/1520-0469(2001)058<2699:DOTTOD>2.0.CO;2

Kley, D, Volz, A and **Mulheims, F.** 1988. Ozone measurements in historic perspective. In: *Tropospheric Ozone.* **227**: 63–72. Norwell, Mass: D. Reidel. DOI: https://doi.org/10.1007/978-94-009-2913-5_4

Kobayashi, J and **Toyama, Y.** 1966a. On various methods of measuring the vertical distribution of atmospheric ozone (II)—titration type chemical ozone sonde. *Pap. Met. Geophys.* **17**: 97–112. DOI: https://doi.org/10.2467/mripapers1950.17.2_97

Kobayashi, J and **Toyama, Y.** 1966b. On various methods of measuring the vertical distribution of atmospheric ozone (III)—Cabon-iodine type chemical ozone sonde. *Pap. Met. Geophys.* **17**: 113–126. DOI: https://doi.org/10.2467/mripapers1950.17.2_113

Kolbig, J and **Warmbt, W.** 1978. Messungen des bodennahen Ozons in Mirny – Antarktika. *Zeitschrift für Meteorologie Band 28 Heft* **5**: 274–277.

Komhyr, WD. 1964. A carbon-iodide ozone sensor for atmospheric sounding. *Proceedings of the Ozone Symposium, Alburquerque, NM*, Dutsch, HV (ed.). Geneva, Switzerland: Secretariat of the World Meteorological Organization, 26.

Komhyr, WD. 1969. Electrochemical concentration cells for gas analysis. *Ann. Geoph.* **25**: 203–210.

Komhyr, WD, Barnes, RA, Brothers, GB, Lathrop, JA and **Opperman, DP.** 1995. Electrochemical concentration cell ozonesonde performance evaluation during STOIC 1989. *J. Geophys. Res.* **100**(D5): 9231–9244. DOI: https://doi.org/10.1029/94JD02175

Komhyr, WD, Grass, RD and **Proulx, RA.** 1968. Ozonesonde intercomparison tests, ESSA Tech. Rep. ERL 85-APCL 4, ESSA Research Laboratories, U.S. Dept. of Commerce, U.S. G.P.O. Washington, DC, 74.

Komhyr, WD and **Sticksel, DR.** 1967. Ozonesonde Observations 1962–1966 (Volume 1), ESSA Technical Report, IER 5I-IAS I, August 1967, Boulder, CO.

Komhyr, WD and **Sticksel, DR.** 1968. Ozonesonde Observations 1962–1966 (Volume 2), ESSA Technical Report, ERL 80-APCL 3, August 1968, Boulder, CO.

Kopczynski, SL and **Bufalini, JJ.** 1971. Some Observations on Stoichiometry of Iodometric Analyses of Ozone at pH 7.0. *Analytical Chemistry* **43**: 1126–1127. DOI: https://doi.org/10.1021/ac60303a024

Kroon, M, de Haan, JF, Veefkind, JP, Froidevaux, L, Wang, R, Kivi, R and **Hakkarainen, JJ.** 2011. Validation of operational ozone profiles from the Ozone Monitoring Instrument. *J. Geophys. Res.* **116**: D18305. DOI: https://doi.org/10.1029/2010JD015100

Krzyścin, JW and **Rajewska-Więch, B.** 2007. Preliminary comparison of the ozone vertical profiles from Umkehr and ozonesonde measurements over Poland with EOS-MLS Aura spacecraft overpasses, 2004–2005. *International Journal of Remote Sensing.* **28**(6): 1089–1100. DOI: https://doi.org/10.1080/01431160600887748

Kuang, S, Burris, JF, Newchurch, MJ, Johnson, S and **Long, S.** 2011. Differential Absorption Lidar to Measure Subhourly Variation of Tropospheric Ozone Profiles. *Geoscience and Remote Sensing, IEEE Transactions on Geoscience and Remote Sensing.* **49**: 557–571. DOI: https://doi.org/10.1109/TGRS.2010.2054834

Kulkarni, RN and **Pittock, AB.** 1970. Results of a comparison between Umkehr and ozone-sonde data. *Q.J.R. Meteorol. Soc.* **96**: 739–743. DOI: https://doi.org/10.1002/qj.49709641015

Ladureau, A. 1883. L'acide sulphureux dans l'atmosphere de Lille. *Annales de chimie.* **29**: 427–432.

Lamarque, JF, Hess, P, Emmons, L, Buja, Washington, W and **Granier, C.** 2005. Tropospheric ozone evolution between 1890 and 1990. *J. Geophys. Res.* **110**: D08304. DOI: https://doi.org/10.1029/2004JD005537

Landgraf, J and **Hasekamp, OO.** 2007. Retrieval of tropospheric ozone: the synergistic use of thermal infrared emission and ultraviolet reflectivity measurements from space. *J. Geophys. Res.* **112**: D08310. DOI: https://doi.org/10.1029/2006JD008097

Langford, AO, Senff, CJ, Alvarez, RJ, Brioude, J, Cooper, OR, Holloway, JS, Lin, MY, Marchbanks, RD, Pierce, RB, Sandberg, SP, Weickmann, AM and **Williams, EJ.** 2015. An overview of the 2013 Las Vegas Ozone Study (LVOS): Impact of stratospheric intrusions and long-range transport on surface air quality. *Atmos. Environ.* DOI: https://doi.org/10.1016/j.atmosenv.2014.08.040

Lanting, RW. 1979. Modification of the potassium iodide procedure for improved stoichiometry. *Atmos. Environ.* **13**: 553–554. DOI: https://doi.org/10.1016/0004-6981(79)90150-1

LARC. 2019. NASA LaRC Airborne Science Data for Atmospheric Composition, https://www-air.larc.nasa.gov/data.htm. Accessed July 2, 2019.

Läuchli, A. 1928. Über die Absorption des ultravioletten Lichts in Ozon. *Helv. Phys. Acta.* **1**: 208–236.

Leblanc, T, Brewer, MA, Wang, PS, Granados-Muñoz, MJ, Strawbridge, KB, Travis, M, Firanski, B, Sullivan, JT, McGee, TJ, Sumnicht, GK and **Twigg, LW.** 2018. Validation of the TOLNet lidars: the Southern California Ozone Observation Project (SCOOP). *Atmos. Meas. Tech.* **11**(11): 6137–6162. DOI: https://doi.org/10.5194/amt-11-6137-2018

Leblanc, T, Sica, RJ, van Gijsel, JAE, Godin-Beekmann, S, Haefele, A, Trickl, T, Payen, G and **Gabarrot, F.** 2016a. Proposed standardized definitions for vertical resolution and uncertainty in the NDACC lidar ozone and temperature algorithms – Part 1: Vertical resolution. *Atmos. Meas. Tech.* **9**: 4029–4049. DOI: https://doi.org/10.5194/amt-9-4029-2016

Leblanc, T, Sica, RJ, van Gijsel, JAE, Godin-Beekmann, S, Haefele, A, Trickl, T, Payen, G and **Liberti, G.** 2016b. Proposed standardized definitions for vertical resolution and uncertainty in the NDACC lidar ozone and temperature algorithms – Part 2: Ozone DIAL uncertainty budget. *Atmos. Meas. Tech.* **9**: 4051–4078. DOI: https://doi.org/10.5194/amt-9-4051-2016

Lefohn, A, Emery, C, Shadwick, D, Wernli, H, Jung, J and **Oltmans, S.** 2014. Estimates of background surface ozone concentrations in the United States based on model-derived source apportionment. *Atmos. Environ.* **84**: 275–288. DOI: https://doi.org/10.1016/j.atmosenv.2013.11.033

Lefohn, AS, Malley, CS, Smith, L, Wells, B, Hazucha, M, Simon, H, Naik, V, Mills, G, Schultz, MG, Paoletti, E, De Marco, A, Xu, X, Zhang, L, Wang, T, Neufeld, HS, Musselman, RC, Tarasick, D, Brauer, M, Feng, Z, Tang, H, Kobayashi, K, Sicard, P, Solberg, S and **Gerosa, G.** 2018. Tropospheric ozone assessment report: Global ozone metrics for climate change, human health, and crop/ecosystem research. *Elem Sci Anth.* **6**(1): 28. DOI: https://doi.org/10.1525/elementa.279

Lehman, J, Swinton, K, Bortnick, S, Hamilton, C, Baldridge, E, Eder, B and **Cox, B.** 2004. Spatio-temporal characterization of tropospheric ozone across the eastern United States. *Atmos. Environ.* **38**(26): 4357–4369. DOI: https://doi.org/10.1016/j.atmosenv.2004.03.069

Lehmann, P. 2005. An Estimate of the Vertical Ozone Profile Discrepancy between the Australian Brewer–Mast and Electrochemical Concentration Cell Ozonesondes. *J. Atmos. Oceanic Technol.* **22**: 1864–1874. DOI: https://doi.org/10.1175/JTECH1821.1

Lelieveld, J, Berresheim, H, Borrmann, S, Crutzen, PJ, Dentener, FJ, Fischer, H, Feichter, J, Flatau, PJ, Heland, J, Holzinger, R, Korrmann, R, Lawrence, MG, Levin, Z, Markowicz, KM, Mihalopoulos, N, Minikin, A, Ramanathan, V, De Reus, M, Roelofs, GJ, Scheeren, HA, Sciare, J, Schlager, H, Schultz, M, Siegmund, P, Steil, B, Stephanou, EG, Stier, P, Traub, M, Warneke, C, Williams, J and **Ziereis, H.** 2002. Global air pollution crossroads over the Mediterranean. *Science.* Oct 25. **298**(5594): 794–9. DOI: https://doi.org/10.1126/science.1075457

Lenschow, DH, Delany, AC, Stankov, BB and **Stedman, DH.** 1980. Airborne measurements of the vertical flux of ozone in the boundary layer. *Boundary-Layer Meteorology.* **19**: 249–265. DOI: https://doi.org/10.1007/BF00117223

Lespieau, R. 1906. Étude du pouvoir oxydant de l'air sur un mélange d'iodure et d'arsénite de potassium en divers points du Mont-Blanc. *Bull. Soc. Chim. France.* **35**: 616–619.

Leventidou, E, Eichmann, KU, Weber, M and **Burrows, JP.** 2016. Tropical tropospheric ozone columns from nadir retrievals of GOME-1/ERS-2, SCIAMACHY/Envisat, and GOME-2/MetOp-A (1996–2012). *Atmos. Meas. Tech.* **9**: 3407–3427. DOI: https://doi.org/10.5194/amt-9-3407-2016

Lin, M, Fiore, AM, Horowitz, LW, Langford, AO, Oltmans, SJ, Tarasick, D and **Reider, HE.** 2015a. Climate variability modulates western US ozone air quality in spring via deep stratospheric intrusions. *Nature Communications.* **6**: 7105. DOI: https://doi.org/10.1038/ncomms8105

Lin, M, Horowitz, LW, Cooper, OR, Tarasick, DW, Conley, S, Iraci, LT, Johnson, B, Leblanc, T, Petropavlovskikh, I and **Yates, EL.** 2015b. Revisiting the evidence of increasing springtime ozone mixing ratios in the free troposphere over western North America. *Geophys. Res. Lett.* **42**. DOI: https://doi.org/10.1002/2015GL065311

Lin, MAM, Fiore, OR, Cooper, LW, Horowitz, AO, Langford, H, Levy, II, Johnson, BJ, Naik, V, Oltmans, SJ and **Senff, CJ.** 2012a. Springtime high surface ozone events over the western United States: Quantifying the role of stratospheric intrusions. *J. Geophys. Res.* **117**: D00V22. DOI: https://doi.org/10.1029/2012JD018151

Lin, W, Xu, X, Ma, Z, Zhao, H, Liu, X and **Wang, Y.** 2012b. Characteristics and recent trends of sulfur dioxide at urban, rural, and background sites in North China: Effectiveness of control measures. *J. Environ. Sci.* **24**: 34–49. DOI: https://doi.org/10.1016/S1001-0742(11)60727-4

Linvill, DE, Hooker, WJ and **Olson, B.** 1980. Ozone in Michigan's environment. *Monthly Weather Review.* **180**: 1883–1891. DOI: https://doi.org/10.1175/1520-0493(1980)108<1883:OIME>2.0.CO;2

Lisac, I and **Grubišić, V.** 1991. An analysis of surface ozone data measured at the end of the 19th Century in Zagreb, Yugoslavia. *Atmos. Environ.* **25A**(2): 481–486. DOI: https://doi.org/10.1016/0960-1686(91)90319-3

Liu, G, Liu, J, Tarasick, DW, Fioletov, VE, Jin, JJ, Moeini, O, Liu, X, Sioris, CE and **Osman, M.** 2013. A global tropospheric ozone climatology from trajectory-mapped ozone soundings. *Atmos. Chem. Phys.* **13**: 10659–10675. DOI: https://doi.org/10.5194/acp-13-10659-2013

Liu, G, Tarasick, DW, Fioletov, VE, Sioris, CE and **Rochon, YJ.** 2009. Ozone correlation lengths and measurement uncertainties from analysis of historical ozonesonde data in North America and Europe. *J. Geophys. Res.* **114**: D04112. DOI: https://doi.org/10.1029/2008JD010576

Liu, J, Tarasick, DW, Fioletov, VE, McLinden, C, Zhao, T, Gong, S, Sioris, C, Jin, J, Liu, G and **Moeini, O.** 2013. A Global Ozone Climatology from Ozone Soundings via Trajectory Mapping: A Stratospheric Perspective. *Atmos. Chem. Phys.* **13**: 11441–11464. DOI: https://doi.org/10.5194/acp-13-11441-2013

Liu, X, Bhartia, PK, Chance, K, Froidevaux, L, Spurr, RJD and **Kurosu, TP.** 2010b. Validation of Ozone Monitoring Instrument (OMI) ozone profiles and stratospheric ozone columns with Microwave Limb Sounder (MLS) measurements. *Atmos. Chem. Phys.* **10**: 2539–2549. DOI: https://doi.org/10.5194/acp-10-2539-2010

Liu, X, Bhartia, PK, Chance, K, Spurr, RJD and **Kurosu, TP.** 2010a. Ozone profile retrievals from the Ozone Monitoring Instrument. *Atmos. Chem. Phys.* **10**: 2521–2537. DOI: https://doi.org/10.5194/acp-10-2521-2010

Liu, X, Chance, K, Sioris, CE, Spurr, RJD, Kurosu, TP, Martin, RV and **Newchurch, MJ.** 2005. Ozone profile and tropospheric ozone retrievals from the Global Ozone Monitoring Experiment: Algorithm description and validation. *J. Geophys. Res.* **110**: D20307. DOI: https://doi.org/10.1029/2005JD006240

Logan, JA. 1999. An analysis of ozonesonde data for the troposphere: Recommendations for testing 3-D models and development of a gridded climatology for tropospheric ozone. *J. Geophys. Res.* **104**: 16115–16149. DOI: https://doi.org/10.1029/1998JD100096

Logan, JA, Staehelin, J, Megretskaia, IA, Cammas, JP, Thouret, V, Claude, H, De Backer, H, Steinbacher, M, Scheel, HE, Stübi, R, Fröhlich, M and **Derwent, R.** 2012. Changes in ozone over Europe: Analysis of ozone measurements from sondes, regular aircraft (MOZAIC) and alpine surface sites. *J. Geophys. Res.* **117**: D09301. DOI: https://doi.org/10.1029/2011JD016952

Low, PS, Davies, TD, Kelly, PM and **Farmer, G.** 1990. Trends in surface ozone at Hohenpeissenberg and Arkona. *J. Geophys. Res.* **95**(D13): 22441–22453. DOI: https://doi.org/10.1029/JD095iD13p22441

Low, PS, Davies, TD, Kelly, PM and **Reiter, R.** 1991. Uncertainties in surface ozone trend at Hohenpeissenberg. *Atmos. Environ. 25A.* **2**: 511–515. DOI: https://doi.org/10.1016/0960-1686(91)90323-Y

Luhar, AK, Galbally, IE, Woodhouse, MT and **Thatcher, M.** 2017. An improved parameterisation of ozone dry deposition to the ocean and its impact in a global climate-chemistry model. *Atmos. Chem. Phys.* **17**: 3749–3767. DOI: https://doi.org/10.5194/acp-17-3749-2017

Luhar, AK, Woodhouse, MT and **Galbally, IE.** 2018. A revised global ozone dry deposition estimate based on a new two-layer parameterisation for air-sea exchange and the multi-year MACC composition reanalysis. *Atmos. Chem. Phys.* **18**: 4329–4348. DOI: https://doi.org/10.5194/acp-18-4329-2018

Lyapina, O, Schultz, MG and **Hense, A.** 2016. Cluster analysis of European surface ozone observations for evaluation of MACC reanalysis data. *Atmos. Chem. Phys.* **16**: 6863–6881. DOI: https://doi.org/10.5194/acp-16-6863-2016

MacDonald, AE. 2005. A global profiling system for improved weather and climate prediction. *Bull. Am. Met. Soc.* **86**: 174. DOI: https://doi.org/10.1175/BAMS-86-12-1747

Macdowall, FDH, Mukammal, EI and **Cole, AFW.** 1964. Direct correlation of air-polluting ozone and tobacco weather fleck. *Canadian Journal of Plant Science.* **44**(5): 410–417. DOI: https://doi.org/10.4141/cjps64-081

MacDowall, J. 1962. The Royal Society I.G.Y. Antarctic Expedition 1955–1959. **3**. London: The Royal Society.

Malicet, J, Daumont, D, Charbonnier, J, Raisse, C, Chakir, A and **Brion, J.** 1995. Ozone UV Spectroscopy. II. Absorption Cross-Sections and Temperature Dependence. *J. Atmos. Chem.* **21**: 263–273. DOI: https://doi.org/10.1007/BF00696758

Mann, HB and **Whitney, DR.** 1947. On a test of whether one of two random variables is stochastically larger than the other. *Annals of Mathematical Statistics.* **18**(1): 50–60. DOI: https://doi.org/10.1214/aoms/1177730491

Marécal, V, Peuch, V-H, Andersson, C, Andersson, S, Arteta, J, Beekmann, M, Benedictow, A, Bergström, R, Bessagnet, B, Cansado, A, Chéroux, F, Colette, A, Coman, A, Curier, RL, Denier van der Gon, HAC, Drouin, A, Elbern, H, Emili, E, Engelen, RJ, Eskes, HJ, Foret, G,

Friese, E, Gauss, M, Giannaros, C, Guth, J, Joly, M, Jaumouillé, E, Josse, B, Kadygrov, N, Kaiser, JW, Krajsek, K, Kuenen, J, Kumar, U, Liora, N, Lopez, E, Malherbe, L, Martinez, I, Melas, D, Meleux, F, Menut, L, Moinat, P, Morales, T, Parmentier, J, Piacentini, A, Plu, M, Poupkou, A, Queguiner, S, Robertson, L, Rouïl, L, Schaap, M, Segers, A, Sofiev, M, Tarasson, L, Thomas, M, Timmermans, R, Valdebenito, Á, van Velthoven, P, van Versendaal, R, Vira, J and **Ung, A.** 2015. A regional air quality forecasting system over Europe: the MACC-II daily ensemble production. *Geosci. Model Dev.* **8**: 2777–2813. DOI: https://doi.org/10.5194/gmd-8-2777-2015

Marenco, A, Gouget, H, Nedelec, P, Pages, JP and **Karcher, J.** 1994. Evidence of a Long-term Increase in Tropospheric ozone from Pic du Midi Data Series: Consequences: Positive Radiative Forcing. *J. Geophys. Res.* **99**: 16617–16632. DOI: https://doi.org/10.1029/94JD00021

Marenco, A, Thouret, V, Nédélec, P, Smit, H, Helten, M, Kley, D, Karcher, F, Simon, P, Law, K, Pyle, J, Poschmann, G, Von Wrede, R, Hume, C and **Cook, T.** 1998. Measurement of ozone and water vapor by Airbus in-service aircraft: The MOZAIC airborne program, an overview. *J. Geophys. Res.* **103**: DOI: https://doi.org/10.1029/98JD00977

Martins, DK, Stauffer, RM, Thompson, AM, Halliday, HS, Kollonige, D, Joseph, E and **Weinheimer, AJ.** 2015. *J. Atmos Chem* **72**: 373. DOI: https://doi.org/10.1007/s10874-013-9259-4

Mast, GM and **Saunders, HE.** 1962. Research and development of the instrumentation of ozone sensing. *I.S.A. Trans. 1*. **4**: 325–328.

Mauersberger, K, Barnes, J, Hanson, D and **Morton, J.** 1986. Measurement of the Ozone Absorption Cross Section at the 253.7 nm Mercury Line. *Geophys. Res. Lett.* **13**: 671–673. DOI: https://doi.org/10.1029/GL013i007p00671

McBratney, A, Webster, BR and **Burgess, TM.** 1981. The design of optimal sampling schemes for local estimation and mapping of regionalized variables—I: Theory and method. *Comput. Geosci.* **7**(4): 331–334. DOI: https://doi.org/10.1016/0098-3004(81)90077-7

McPeters, RD and **Labow, GJ.** 2012. Climatology 2011: An MLS and sonde derived ozone climatology forsatellite retrieval algorithms. *J. Geophys. Res.* **117**: D10303. DOI: https://doi.org/10.1029/2011JD017006

McPeters, RD, Labow, GJ and **Logan, JA.** 2007. Ozone climatological profiles for satellite retrieval algorithms. *J. Geophys. Res.* **112**: D05308. DOI: https://doi.org/10.1029/2005JD006823

Meijer, YJ, Swart, DPJ, Baier, F, Bhartia, PK, Bodeker, GE, Casadio, S, Chance, K, Del Frate, F, Erbertseder, T, Felder, MD, Flynn, LE, Godin-Beekmann, S, Hansen, G, Hasekamp, OP, Kaifel, AK, Kelder, HM, Kerridge, BJ, Lambert, JC, Landgraf, J, Latter, B, Liu, X, McDermid, IS, Pachepsky, Y, Rozanov, V, Siddans, R, Tellmann, S, van der A, RJ, van Oss, RF, Weber, M and **Zehner, C.** 2006. Evaluation of Global Ozone Monitoring Experiment (GOME) ozone profiles from nine different algorithms. *J. Geophys. Res.* **111**: D21306. DOI: https://doi.org/10.1029/2005JD006778

Mickley, LJ, Jacob, DJ and **Rind, D.** 2001. Uncertainty in preindustrial abundance of tropospheric ozone: Implications for radiative forcing calculations. *J. Geophys. Res.* **106**: 3389–3399. DOI: https://doi.org/10.1029/2000JD900594

Mielonen, T, de Haan, JF, van Peet, JCA, Eremenko, M and **Veefkind, JP.** 2015. Towards the retrieval of tropospheric ozone with the Ozone Monitoring Instrument (OMI). *Atmos. Meas. Tech.* **8**: 671–687. DOI: https://doi.org/10.5194/amt-8-671-2015

Miles, GM, Siddans, R, Kerridge, BJ, Latter, BG and **Richards, NAD**. 2015**.** Tropospheric ozone and ozone profiles retrieved from GOME-2 and their validation. *Atmos. Meas. Tech.* **8**: 385–398. DOI: https://doi.org/10.5194/amt-8-385-2015

Mills, G, Pleijel, H, Malley, CS, Sinha, B, Cooper, OR, Schultz, MG, Neufeld, HS, Simpson, D, Sharps, K, Feng, Z, Gerosa, G, Harmens, H, Kobayashi, K, Saxena, P, Paoletti, E, Sinha, V and **Xu, X.** 2018. Tropospheric Ozone Assessment Report: Present-day tropospheric ozone distribution and trends relevant to vegetation. *Elem Sci Anth.* **6**(1): 47. DOI: https://doi.org/10.1525/elementa.302

Miyake, Y, Kawamura, K and **Sakurai, S.** 1962. Atmospheric ozone and nitrogen dioxide observed at Mt. Norikura. *Pap. Met. Geophys.* **12**: 310–317. DOI: https://doi.org/10.2467/mripapers1950.12.3-4_310

Monks, PS, Archibald, AT, Colette, A, Cooper, O, Coyle, M, Derwent, R, Fowler, D, Granier, C, Law, KS, Mills, GE, Stevenson, DS, Tarasova, O, Thouret, V, von Schneidemesser, E, Sommariva, R, Wild, O and **Williams, ML.** 2015. Tropospheric ozone and its precursors from the urban to the global scale from air quality to short-lived climate forcer. *Atmos. Chem. Phys.* **15**: 8889–8973. DOI: https://doi.org/10.5194/acp-15-8889-2015

Mukammal, EI. 1965. Ozone as a cause of tobacco injury. *Agr. Meteorol.* **2**: 145–165. DOI: https://doi.org/10.1016/0002-1571(65)90016-6

Müller, MD, Kaifel, AK, Weber, M, Tellmann, S, Burrows, JP and **Loyola, D.** 2003. Ozone profile retrieval from Global Ozone Monitoring Experiment (GOME) data using a neural network approach (Neural Network Ozone Retrieval System (NNORSY). *J. Geophys. Res.* **108**(D16): 4497. DOI: https://doi.org/10.1029/2002JD002784

Munro, R, Siddans, R, Reburn, WJ and **Kerridge, B.** 1998. Direct measurement of tropospheric ozone from space. *Nature.* **392**: 168–171. DOI: https://doi.org/10.1038/32392

Mylona, S. 1996. Sulphur dioxide emissions in Europe 1880–1991 and their effect of sulphur concentrations and depositions. *Tellus.* **48B**: 662–689. DOI: https://doi.org/10.3402/tellusb.v48i5.15939

Naja, M and **Lal, S.** 1996. Changes in surface ozone amount and its diurnal and seasonal patterns, from 1954–55 to 1991–93, measured at Ahmedabad (23 N), India. *Geophys. Res. Lett.* **23**: 81–84. DOI: https://doi.org/10.1029/95GL03589

Nassar, R, Logan, JA, Worden, HM, Megretskaia, IA, Bowman, KW, Osterman, GB, Thompson, AM, Tarasick, DW, Austin, S, Claude, H, Dubey, MK, Hocking, WK, Johnson, BJ, Joseph, E, Merrill, J, Morris, GA, Newchurch, M, Oltmans, SJ, Posny, F, Schmidlin, FJ, Whiteman, DN and **Witte, JC.** 2008. Validation of Tropospheric Emission Spectrometer (TES) Nadir Ozone Profiles Using Ozonesonde Measurements. *J. Geophys. Res.* **113**: D15S17. DOI: https://doi.org/10.1029/2007JD008819

Nastrom, GD. 1977. Vertical and horizontal fluxes of ozone at the tropopause from the first year of GASP data. *J. Appl. Meteor.* **16**: 740–744. DOI: https://doi.org/10.1175/1520-0450(1977)016<0740:VAHFOO>2.0.CO;2

NCAR. 2019. National Center for Atmospheric Research, Earth Observing Laboratory, https://www.eol.ucar.edu/all-field-projects-and-deployments. Accessed July 2, 2019.

Nédélec, P, Blot, R, Boulanger, D, Athier, G, Cousin, JM, Gautron, B, Petzold, A, Volz-Thomas, A and **Thouret, V.** 2015. Instrumentation on commercial aircraft for monitoring the atmospheric composition on a global scale: The IAGOS system, technical overview of ozone and carbon monoxide measurements. *Tellus B* **67**: 1–16. DOI: https://doi.org/10.3402/tellusb.v67.27791

Newchurch, MJ, Liu, X and **Kim, JH.** 2001. Lower tropospheric ozone derived from TOMS near mountainous regions. *J. Geophys. Res.* **106**(D17): 20403–20412. DOI: https://doi.org/10.1029/2000JD000162

Newchurch, MJ, Sun, D, Kim, JH and **Liu, X.** 2003. Tropical tropospheric ozone derived using Clear-Cloudy Pairs (CCP) of TOMS measurements. *Atmos. Chem. and Phys.* **3**: 683–695. DOI: https://doi.org/10.5194/acp-3-683-2003

NOAA. 2018. The NOAA Annual Greenhouse Gas Index (AGGI). https://www.esrl.noaa.gov/gmd/aggi/aggi.html. Accessed July 2, 2019.

Nolle, M, Ellul, R, Ventura, F and **Güsten, H.** 2005. A study of historical surface ozone measurements (1884–1900) on the island of Gozo in the central Mediterranean. *Atmos. Environ.* **39**: 5608–5618. DOI: https://doi.org/10.1016/j.atmosenv.2005.06.017

Ny, TZ and **Choong, SP.** 1933. *Chinese J. Phys.* **1**: 38.

Nychka, D and **Saltzman, N.** 1998. Design of air-quality monitoring networks, *In Case studies in environmental statistics*, 51–76. Springer, US. DOI: https://doi.org/10.1007/978-1-4612-2226-2_4

O'Brien, B, Stewart, HS and **Mohler, FL.** 1936. Vertical distribution of ozone in the atmosphere. *Nat. Geogr. Soc. Cont. Tech. Pap, Stratosphere Series.* **2**: 49–93.

Oltmans, SJ. 1981. Surface ozone measurements in clean air. *J. Geophys. Res.* **86**(C2): 1174–1180. DOI: https://doi.org/10.1029/JC086iC02p01174

Oltmans, SJ and **Komhyr, WD.** 1976. Surface ozone in Antarctica. *J. Geophys. Res.* **81**(30): 5359–55364. DOI: https://doi.org/10.1029/JC081i030p05359

Oltmans, SJ, Lefohn, AS, Harris, JM, Galbally, I, Scheel, HE, Bodeker, G, Brunke, E, Claude, H, Tarasick, D, Johnson, BJ, Simmonds, P, Shadwick, D, Anlauf, K, Hayden, K, Schmidlin, F, Fujimoto, T, Akagi, K, Meyer, C, Nichol, S, Davies, J, Redondas, A and **Cuevas, E.** 2006. Long-term Changes in Tropospheric Ozone. *Atmos. Environ.* **40**: 3156–3173. DOI: https://doi.org/10.1016/j.atmosenv.2006.01.029

Oltmans, SJ, Lefohn, AS, Shadwick, D, Harris, JM, Scheel, HE, Galbally, I, Tarasick, DW, Johnson, BJ, Brunke, EG, Claude, H, Zeng, G, Nichol, S, Schmidlin, F, Davies, J, Cuevas, E, Redondas, A, Naoe, H, Nakano, T and **Kawasato, T.** 2013. Recent Tropospheric Ozone Changes – A Pattern Dominated by Slow or No Growth. *Atmos. Environ.* **67**: 331–351. DOI: https://doi.org/10.1016/j.atmosenv.2012.10.057

Orphal, J, Staehelin, J, Tamminen, J, Braathen, G, De Backer, MR, Bais, A, Balis, D, Barbe, A, Bhartia, PK, Birk, M, Burkholder, JW, Chance, KV, von Clarmann, T, Cox, A, Degenstein, D, Evans, R, Flaud, JM, Flittner, D, Godin-Beekmann, S, Gorshelev, V, Gratien, A, Hare, E, Janssen, C, Kyrölä, E, McElroy, T, McPeters, R, Pastel, M, Petersen, M, Petropavlovskikh, I, Picquet-Varrault, B, Pitts, M, Labow, G, Rotger-Languereau, M, Leblanc, T, Lerot, C, Liu, X, Moussay, P, Redondas, A, Van Roozendael, M, Sander, SP, Schneider, M, Serdyuchenko, A, Veefkind, P, Viallon, J, Viatte, C, Wagner, G, Weber, M, Wielgosz, RI and **Zehner, C.** 2016. Absorption Cross-Sections of Ozone in the Ultraviolet and Visible Spectral Regions – Status Report 2015. *J. Mol. Spectroscopy.* **327**: 105–121. DOI: https://doi.org/10.1016/j.jms.2016.07.007

Osman, MK, Hocking, W and **Tarasick, DW.** 2016. Parameterization of large-scale turbulent diffusion in the presence of both well-mixed and weakly mixed patchy layers. *Journal of Atmospheric and Solar-Terrestrial Physics.* **143–144**: 14–36. DOI: https://doi.org/10.1016/j.jastp.2016.02.025

Paetzold, HK. 1955a. New experimental and theoretical investigations on the atmospheric ozone layer. *J. Atmosph. Terrestr. Physics.* **7**: 128–140. DOI: https://doi.org/10.1016/0021-9169(55)90120-3

Paetzold, HK. 1955b. Die vertikale verteilung des atmosphärischen ozons nach ballonaufstiegen. *Z. Naturforsch* **10a**: 33–41. DOI: https://doi.org/10.1515/zna-1955-0106

Paetzold, HK. 1959. Vertical Atmospheric Ozone Distributions. *Advances in Chemistry, ACS Series* **21**: 209–220. DOI: https://doi.org/10.1021/ba-1959-0021.ch033

Paneth, FA and **Glückauf, E.** 1941. Measurement of atmospheric ozone by a quick electrochemical

method. *Nature* **147**: 614–615. DOI: https://doi.org/10.1038/147614a0

Parrish, DD, Lamarque, JF, Naik, V, Horowitz, L, Shindell, DT, Staehelin, J, Derwent, R, Cooper, OR, Tanimoto, H, Volz-Thomas, A, Gilge, S, Scheel, HE, Steinbacher, M and **Fröhlich, M.** 2014. Long-term changes in lower tropospheric baseline ozone concentrations: comparing chemistry-climate models and observations at northern midlatitudes. *J. Geophys. Res.* **119**: 719–5736. DOI: https://doi.org/10.1002/2013JD021435

Parrish, DD, Law, KS, Staehelin, J, Derwent, R, Cooper, OR, Tanimoto, H, Volz-Thomas, A, Gilge, S, Scheel, HE, Steinbacher, M and **Chan, E.** 2012. Long-term changes in lower tropospheric baseline ozone concentrations at northern mid-latitudes. *Atmos. Chem. Phys* **12**: 11,485–11,504. DOI: https://doi.org/10.5194/acp-12-11485-2012

Paur, RJ, Bass, AM, Norris, JE and **Buckley, TJ.** 2003. Standard reference photometer for the assay of ozone in calibration atmospheres. *NISTIR* 6369.

Pavelin, EG, Johnson, CE, Rughooputh, S and **Toumi, R.** 1999. Evaluation of pre-industrial surface ozone measurements made using the Schönbein method. *Atmos. Environ.* **33**: 919–929. DOI: https://doi.org/10.1016/S1352-2310(98)00257-X

Pelon, J and **Mégie, G.** 1982. Ozone monitoring in the troposphere and lower stratosphere: Evaluation and operation of a ground-based lidar station. *J. Geophys. Res* **87**(C7): 4947–4955. DOI: https://doi.org/10.1029/JC087iC07p04947

Perl, G. 1965. Das bodennahe ozon in Arosa, seine regelmäßigen und un regelmäßigen schwankungen. Archive für Meteorologie. *Geophysik und Bioklimatologie Band* **14**(4): 449–458. DOI: https://doi.org/10.1007/BF02253490

Peterson, JT (ed.). 1978. Summary Report 1977. *Geophysical Monitoring for Climatic Change*. Boulder, Colorado: NOAA Environmental Research Laboratories.

Petetin, H, Jeoffrion, M, Sauvage, B, Athier, G, Blot, R, Boulanger, D, Clark, H, Cousin, JM, Gheusi, F, Nedelec, P, Steinbacher, M and **Thouret, V.** 2018. Representativeness of the IAGOS airborne measurements in the lower troposphere. *Elementa – Science of the Anthropocene* **6**(1): 23. DOI: https://doi.org/10.1525/elementa.280

Petetin, H, Thouret, V, Fontaine, A, Sauvage, B, Athier, G, Blot, R, Boulanger, D, Cousin, JM and **Nedelec, P.** 2016. Characterising tropospheric O_3 and CO around Frankfurt over the period 1994–2012 based on MOZAIC-IAGOS aircraft measurements. *Atmos. Chem. Phys.* **16**(23): 15147–15163. 2016. DOI: https://doi.org/10.5194/acp-16-15147-2016

Petzold, A, Thouret, V, Gerbig, C, Zahn, A, Brenninkmeijer, CAM, Gallagher, M, Hermann, M, Pontaud, M, Ziereis, H, Boulanger, D, Marshall, J, Nédélec, P, Smit, HGJ, Friess, U, Flaud, J-M, Wahner, A, Cammas, J-P, Volz-Thomas, A and **IAGOS TEAM.** 2015. Global-scale atmosphere monitoring by in-service aircraft – current achievements and future prospects of the European Research Infrastructure IAGOS. *Tellus B* **67**: 1–24. DOI: https://doi.org/10.3402/tellusb.v67.28452

Pitts, JN, McAfee, JM, Long, WD and **Winer, AM.** 1976a. Long-path infrared spectroscopic investigation at ambient concentrations of 2 percent neutral buffered potassium iodide method for determination of ozone. *Environmental Science and Technology* **10**(8): 787–793. DOI: https://doi.org/10.1021/es60119a008

Pitts, JN, Sprung, JL, Poe, M, Carpelan, MC and **Lloyd, AC.** 1976b. Corrected south coast air basin oxidant data: some conclusions and implications. *Environmental Science & Technology* **10**(8): 794–801. DOI: https://doi.org/10.1021/es60119a011

Platt, U, Perner, D and **Pätz, HW.** 1979. Simultaneous measurements of atmospheric CH_2O, O_3 and NO_2 by differential optical absorption. *J. Geophys. Res.* **84**: 6329–6335. DOI: https://doi.org/10.1029/JC084iC10p06329

Potter, L and **Duckworth, S.** 1965. Field Experience with the Mast Ozone Recorder. *Journal of the Air Pollution Control Association.* **15**(5): 207–209. DOI: https://doi.org/10.1080/00022470.1965.10468364

Price, S and **Pales, JC.** 1963. Mauna Loa Observatory: The First Five Years. *Monthly Weather Review, October–December 1963*, 665–680. DOI: https://doi.org/10.1175/1520-0493(1963)091<0665:MLOTFF>2.3.CO;2

Pruchniewicz, PG. 1970. Über ein Ozonregistriergerät und Untersuehung der zeitliehen und räumliehen Variationen des troposphärischen Ozons auf der Nordhalbkugel der Erde. *Mitt. Max-Planck-Inst. f. Aeronomie* **42**: 70. DOI: https://doi.org/10.1007/978-3-642-47849-9

Pruchniewicz, PG. 1973. A new automatic ozone recorder for near surface measurements working at 19 stations on a meridional chain between Norway and South Africa. *Pure and Applied Geophysics (PAGEOPH)* **106–108**: 1074–1084. DOI: https://doi.org/10.1007/BF00881060

Rasool, I and **Vassy, A.** 1956. Comparaison des méthodes chimique et spectrographique de dosage de l'ozone au voisinage du sol. *Annales de Geophysique* **12**: 239–244.

Regener, E and **Regener, VH.** 1934. Aufnahmen des ultravioletten Sonnenspektrums in der Stratosphäre und die vertikale Ozonverteilung. *Phys. Z.* **35**: 788–793.

Regener, VH. 1938a. Neue Messungen der vertikalen Verteilung des ozons in der atmosphere. *Zeitschrift für Physik.* **109**: 642–670. DOI: https://doi.org/10.1007/BF01341590

Regener, VH. 1938b. Messungen des ozongehalts der luft in Bodennähe. *Meteor. Z.* **55**: 459–462.

Regener, VH. 1959. Automatic chemical determination of atmospheric ozone. *Advan. Chem. Ser.* **21**: 124—127. DOI: https://doi.org/10.1021/ba-1959-0021.ch017

Regener, VH. 1960. On a sensitive method for the recording of atmospheric ozone. *J. Geophys. Res.* **12**: 3975–3977. DOI: https://doi.org/10.1029/JZ065i012p03975

Regener, VH. 1964. Measurement of atmospheric ozone with the chemiluminescent method. *J. Geophys. Res.* **69**(18): 3795–3800. DOI: https://doi.org/10.1029/JZ069i018p03795

Renzetti, NA. 1959. Ozone in Los Angeles atmosphere. *Advances in Chemistry, ACS Series.* **21**: 230–262. DOI: https://doi.org/10.1021/ba-1959-0021.ch036

Reynolds, WC. 1930. Notes on London and suburban air. *J. Soc. Chem. Ind. (London).* **49**(168): T-172.

Richter, A, Burrows, JP, Nuss, H, Granier, C and **Niemeier, U.** 2005. Increase in tropospheric nitrogen dioxide over China observed from space. *Nature.* **437**(7055): 129–132. DOI: https://doi.org/10.1038/nature04092

Rodgers, C. 2000. Inverse Methods for Atmospheric Sounding: Theory and Practise. *World Sci.* Hackensack, N.J. DOI: https://doi.org/10.1142/9789812813718

Roscoe, HK and **Roscoe, J.** 2006. Polar tropospheric ozone depletion events observed in the International Geophysical Year of 1958. *Atmos. Chem. Phys.* **6**: 3303–3314. DOI: https://doi.org/10.5194/acp-6-3303-2006

Royal Society. 1908. National Antarctic Expedition, 1901–1904. *Meteorology, Part 1*. London: Royal Society.

Rubin, MB. 2001. The history of ozone. The Schönbein period, 1839–1868. *Bull. Hist. Chem.* **26**: 40–56.

Russell, AR, Valin, LC and **Cohen, RC.** 2012. Trends in OMI NO_2 observations over the United States: effects of emission control technology and the economic recession. *Atmos. Chem. Phys.* **12**(24): 12197–12209. DOI: https://doi.org/10.5194/acp-12-12197-2012

Safieddine, S, Boynard, A, Hao, N, Huang, F, Wang, L, Ji, D, Barret, B, Ghude, SD, Coheur, P-F, Hurtmans, D and **Clerbaux, C.** 2016. Tropospheric ozone variability during the East Asian summer monsoon as observed by satellite (IASI), aircraft (MOZAIC) and ground stations. *Atmos. Chem. Phys.* **16**: 10489–10500. DOI: https://doi.org/10.5194/acp-16-10489-2016

Saltzman, BE and **Gilbert, N.** 1959a. Iodometric microdetermination of organic oxidants and ozone: Resolution of mixtures by kinetic colourimetry. *Anal. Chem.* **31**: 1914–1920. DOI: https://doi.org/10.1021/ac60155a078

Sandroni, S and **Anfossi, D.** 1994. Historical data of surface ozone at tropical latitudes. *Science of The Total Environment.* **148**: 1–97. DOI: https://doi.org/10.1016/0048-9697(94)90369-7

Sandroni, S, Anfossi, D and **Viarengo, S.** 1992. Surface ozone levels at the end of the nineteenth century in South America. *J. Geophys. Res.* **97**(D2): 2535–2539. DOI: https://doi.org/10.1029/91JD02660

Saunois, M, Emmons, L, Lamarque, JF, Tilmes, S, Wespes, C, Thouret, V and **Schultz, M.** 2012. Impact of sampling frequency in the analysis of tropospheric ozone observations. *Atmos. Chem. Phys.* **12**: 6757–6773. DOI: https://doi.org/10.5194/acp-12-6757-2012

Schenkel, A and **Broder, B.** 1982. Interference of some trace gases with ozone measurements by the KI method. *Atmos. Environ.* **16**: 2187–2190. DOI: https://doi.org/10.1016/0004-6981(82)90289-X

Schnadt Poberaj, C, Staehelin, J, Brunner, D, Thouret, V, De Backer, H and **Stübi, R.** 2009. Long-term changes in UT/LS ozone between the late 1970s and the 1990s deduced from the GASP and MOZAIC aircraft programs and from ozonesondes. *Atm. Chem. Phys.* **9**: 5343–5369. DOI: https://doi.org/10.5194/acp-9-5343-2009

Schnadt Poberaj, C, Staehelin, J, Brunner, D, Thouret, V and **Mohnen, V.** 2007. A UT/LS ozone climatology of the nineteen seventies deduced from the GASP aircraft measurement program. *Atmos. Chem. Phy.* **7**: 5917–5936. DOI: https://doi.org/10.5194/acp-7-5917-2007

Schneider, M and **Hase, F.** 2008. Technical Note: Recipe for monitoring of total ozone with a precision of around 1 DU applying mid-infrared solar absorption spectra. *Atmos. Chem. Phys.* **8**: 63–71. DOI: https://doi.org/10.5194/acp-8-63-2008

Schneider, M, Hase, F, Blumenstock, T, Redondas, A and **Cuevas, E.** 2008. Quality assessment of O_3 profiles measured by a state-of-the-art ground-based FTIR observing system. *Atmos. Chem. Phys.* **8**: 5579–5588. DOI: https://doi.org/10.5194/acp-8-5579-2008

Schoeberl, MR, Ziemke, JR, Bojkov, B, Livesey, N, Duncan, B, Strahan, S, Froidevaux, L, Kulawik, S, Bhartia, PK, Chandra, S, Levelt, PF, Witte, JC, Thompson, AM, Cuevas, E, Redondas, A, Tarasick, DW, Davies, J, Bodeker, G, Hansen, G, Johnson, BJ, Oltmans, SJ, Vömel, H, Allaart, M, Kelder, H, Newchurch, M, Godin-Beekmann, S, Ancellet, G, Claude, H, Andersen, SB, Kyrö, E, Parrondos, M, Yela, M, Zablocki, G, Moore, D, Dier, H, von der Gathen, P, Viatte, P, Stübi, R, Calpini, B, Skrivankova, P, Dorokhov, V, de Backer, H, Schmidlin, FJ, Coetzee, G, Fujiwara, M, Thouret, V, Posny, F, Morris, G, Merrill, J, Leong, CP, Koenig-Langlo, G and **Joseph, E.** 2007. A trajectory-based estimate of the tropospheric ozone column using the residual method. *J. Geophys. Res.* **112**: D24S49. DOI: https://doi.org/10.1029/2007JD008773

Schönbein, CF. 1840. On the odour accompanying electricity and on the probability of its dependency on the presence of a new substance. *Philos. Mag.* **17**: 293–294. also Roy. Soc. Proc. IV, 1840, 226.

Schönbein, CF. 1845. Einige Bemerkungen uber die Anwesenheit des Ozons in der atmosphärischen Luft und die Rolle welcher dieser bei langsamen Oxydationen spielen durfte. *Ann. Phys. Chim. (Poggendorf's Annalen).* **65**: 161–172. DOI: https://doi.org/10.1002/andp.18451410602

Schultz, MG, Akimoto, H, Bottenheim, J, Buchmann, B, Galbally, IE, Gilge, S, Helmig, D, Koide, H, Lewis, AC, Novelli, PC, Plass-Dülmer, C, Ryerson, TB, Steinbacher, M, Steinbrecher, R, Tarasova, O, Tørseth, K, Thouret, V and **Zellweger, C.**

2015. The Global Atmosphere Watch reactive gases measurement network. *Elem Sci Anth.* **3**: 000067. DOI: https://doi.org/10.12952/journal.elementa.000067

Schultz, MG, Schröder, S, Lyapina, O, Cooper, O, Galbally, I, Petropavlovskikh, I, von Schneidemesser, E, Tanimoto, H, Elshorbany, Y, Naja, M, Seguel, R, Dauert, U, Eckhardt, P, Feigenspahn, S, Fiebig, M, Hjellbrekke, A-G, Hong, Y-D, Christian Kjeld, P, Koide, H, Lear, G, Tarasick, D, Ueno, M, Wallasch, M, Baumgardner, D, Chuang, M-T, Gillett, R, Lee, M, Molloy, S, Moolla, R, Wang, T, Sharps, K, Adame, JA, Ancellet, G, Apadula, F, Artaxo, P, Barlasina, M, Bogucka, M, Bonasoni, P, Chang, L, Colomb, A, Cuevas, E, Cupeiro, M, Degorska, A, Ding, A, Fröhlich, M, Frolova, M, Gadhavi, H, Gheusi, F, Gilge, S, Gonzalez, MY, Gros, V, Hamad, SH, Helmig, D, Henriques, D, Hermansen, O, Holla, R, Huber, J, Im, U, Jaffe, DA, Komala, N, Kubistin, D, Lam, K-S, Laurila, T, Lee, H, Levy, I, Mazzoleni, C, Mazzoleni, L, McClure-Begley, A, Mohamad, M, Murovic, M, Navarro-Comas, M, Nicodim, F, Parrish, D, Read, KA, Reid, N, Ries, L, Saxena, P, Schwab, JJ, Scorgie, Y, Senik, I, Simmonds, P, Sinha, V, Skorokhod, A, Spain, G, Spangl, W, Spoor, R, Springston, SR, Steer, K, Steinbacher, M, Suharguniyawan, E, Torre, P, Trickl, T, Weili, L, Weller, R, Xu, X, Xue, L and **Zhiqiang, M.** 2017. Tropospheric Ozone Assessment Report: Database and Metrics Data of Global Surface Ozone Observations. *Elem Sci Anth.* **5**: 58. DOI: https://doi.org/10.1525/elementa.244

Schutgens, NA, Gryspeerdt, E, Weigum, N, Tsyro, S, Goto, D, Schulz, M and **Stier, P.** 2016. Will a perfect model agree with perfect observations? The impact of spatial sampling. *Atmos. Chem. Phys.* **16**(10): 6335–6353. DOI: https://doi.org/10.5194/acp-16-6335-2016

Sellitto, P, Bojkov, BR, Liu, X, Chance, K and **Del Frate, F.** 2011. Tropospheric ozone column retrieval from the Ozone Monitoring Instrument by means of a neural network algorithm. *Atmos. Meas. Tech.* **4**: 2375–2388. DOI: https://doi.org/10.5194/amt-4-2375-2011

Sellitto, P, Del Frate, F, Solimini, D and **Casadio, S.** 2012b. Tropospheric ozone column retrieval from ESA EnviSat SCIAMACHY nadir UV/VIS radiance measurements by means of a neural network algorithm. *IEEE Transaction on Geoscience and Remote Sensing.* **50**(3): 998–1011. DOI: https://doi.org/10.1109/TGRS.2011.2163198

Sellitto, P, Di Noia, A, Del Frate, F, Burini, A, Casadio, S and **Solimini, D.** 2012a. On the role of visible radiation in ozone profile retrieval from nadir UV/VIS satellite measurements: an experiment with neural network algorithms inverting SCIAMACHY data. *J. Quant. Spectro. Radiat. Transfer.* **113**(3): 1429–1436. DOI: https://doi.org/10.1016/j.jqsrt.2012.04.007

Simpson, WR, von Glasow, R, Riedel, K, Anderson, P, Ariya, P, Bottenheim, J, Burrows, J, Carpenter, LJ, Frieß, U, Good-site, ME, Heard, D, Hutterli, M, Jacobi, HW, Kaleschke, L, Neff, B, Plane, J, Platt, U, Richter, A, Roscoe, H, Sander, R, Shepson, P, Sodeau, J, Steffen, A, Wagner, T and **Wolff, E.** 2007. Halogens and their role in polar boundary-layer ozone depletion. *Atmos. Chem. Phys.* **7**: 4375–4418. DOI: https://doi.org/10.5194/acp-7-4375-2007

Smit, HGJ. 2002. Ozonesondes. In *Encyclopedia of Atmospheric Sciences.* Holton, J, Pyle, J and Curry, J (eds.), 1469–1476. London: Academic Press.

Smit, HGJ and **ASOPOS-panel.** 2011. Quality assurance and quality control for ozonesonde measurements in GAW, WMO Global Atmosphere Watch report series, No. 121, 100 pp, World Meteorological Organization, GAW Report No. 201. 100 pp, Geneva. [Available online at http://www.wmo.int/pages/prog/arep/gaw/documents/GAW_201.pdf].

Smit, HGJ and **Kley, D.** 1998. JOSIE: The 1996 WMO International intercomparison of ozonesondes under quasi flight conditions in the environmental simulation chamber at Jülich. *WMO Global Atmosphere Watch Report No. 130, WMO TD No. 926.* Geneva: World Meteorological Organization.

Smit, HGJ and **Straeter, W.** 2004. JOSIE-2000. Jülich Ozone Sonde Intercomparison Experiment 2000. The 2000 WMO international intercomparison of operating procedures for ECC-ozonesondes at the environmental simulation facility at Jülich. *WMO Global Atmosphere Watch report series, No. 158 (Technical Document No. 1225).* Geneva: World Meteorological Organization.

Smit, HGJ, Straeter, W, Johnson, B, Oltmans, S, Davies, J, Tarasick, DW, Hoegger, B, Stubi, R, Schmidlin, F, Northam, T, Thompson, A, Witte, J, Boyd, I and **Posny, F.** 2007. Assessment of the performance of ECC-ozonesondes under quasi-flight conditions in the environmental simulation chamber: Insights from the Juelich Ozone Sonde Intercomparison Experiment (JOSIE). *J. Geophys Res.* **112**: D19306. DOI: https://doi.org/10.1029/2006JD007308

Smit, HGJ, Tarasick, DW, Thompson, AM, Morris, GA, Witte, J and **Davies, J.** 2017. How Well Can We Assess Atmospheric Ozone Changes? The Ozone-Sonde Data Quality Assessment (O3S-DQA). *AGU Fall Meeting.* Abstract 269391. New Orleans.

Smith, SJ, van Aardenne, J, Klimont, Z, Andres, RJ, Volke, A and **Delgado Arias, S.** 2011. Anthropogenic sulfur dioxide emissions: 1850–2005. *Atmos. Chem. Phys.* **11**: 1101–1116. DOI: https://doi.org/10.5194/acp-11-1101-2011

Smyth, RB. 1858. Meteorological report with diagram of barometric pressure, etc 3rd: 1857/58 by Flagstaff Observatory (Melbourne, Vic.). Melbourne: Victorian Government Printer.

Sofen, ED, Bowdalo, D and **Evans, MJ.** 2016. How to most effectively expand the global surface ozone observing network. *Atmos. Chem. Phys.* **16**: 1445–1457. DOI: https://doi.org/10.5194/acp-16-1445-2016

Sofieva, VF, Tamminen, J, Haario, H, Kyrölä, E and **Lehtinen, M.** 2004. Ozone profile smoothness

as a priori information of limb measurements. *Ann. Geophys.* **22**: 3411–3420. DOI: https://doi.org/10.5194/angeo-22-3411-2004

Solazzo, E and **Galmarini, S.** 2015. Comparing apples with apples: Using spatially distributed time series of monitoring data for model evaluation. *Atmos. Environ.* **112**: 234–245. DOI: https://doi.org/10.1016/j.atmosenv.2015.04.037

Spangl, W, Schneider, J, Moosmann, L and **Nagl, C.** 2007. Representativeness and Classification of Air Quality Monitoring Stations, Final Report, REP–0121, Vienna, 216.

Staehelin, J, Thudium, J, Buehler, R, Volz-Thomas, A and **Graber, W.** 1994. Trends in surface ozone concentrations at Arosa (Switzerland). *Atmos. Environ.* **28**: 75–87. DOI: https://doi.org/10.1016/1352-2310(94)90024-8

Staehelin, J, Tummon, F, Revell, L, Stenke, A and **Peter, T.** 2017. Tropospheric Ozone at Northern Mid-Latitudes: Modeled and Measured Long-Term Changes. *Atmosphere.* **8**(9): 163. DOI: https://doi.org/10.3390/atmos8090163

Staehelin, J, Viatte, P, Stübi, R, Tummon, F and **Peter, T.** 2018. Stratospheric ozone measurements at Arosa (Switzerland): history and scientific relevance. *Atmos. Chem. Phys.* **18**(9): 6567–6584. DOI: https://doi.org/10.5194/acp-18-6567-2018

Staufer, J, Staehelin, J, Stübi, R, Peter, T, Tummon, F and **Thouret, V.** 2013. Trajectory matching of ozonesondes and MOZAIC measurements in the UTLS – Part 1: Method description and application at Payerne, Switzerland. *Atmos. Meas. Tech.* **6**: 3393–3406. DOI: https://doi.org/10.5194/amt-6-3393-2013

Staufer, J, Staehelin, J, Stübi, R, Peter, T, Tummon, F and **Thouret, V.** 2014. Trajectory matching of ozonesondes and MOZAIC measurements in the UTLS – Part 2: Application to the global ozonesonde network. *Atmos. Meas. Tech.* **7**: 241–266. DOI: https://doi.org/10.5194/amt-7-241-2014

Stauffer, RM, Thompson, AM and **Young, GS.** 2016. Tropospheric ozonesonde profiles at long-term U.S. monitoring sites: 1. A climatology based on self-organizing maps. *J. Geophys. Res. Atmos.* **121**: 1320–1339. DOI: https://doi.org/10.1002/2015JD023641

Stedman, DH, Daby, EE, Stuhl, F and **Niki, H.** 1972. Analysis of Ozone and Nitric Oxide by a Chemiluminescent Method in Laboratory and Atmospheric Studies of Photochemical Smog. *Journal of the Air Pollution Control Association.* **22**(4): 260–263. DOI: https://doi.org/10.1080/00022470.1972.10469635

Sterling, CW, Johnson, BJ, Oltmans, SJ, Smit, HGJ, Jordan, AF, Cullis, PD, Hall, EG, Thompson, AM and **Witte, JC.** 2018. Homogenizing and estimating the uncertainty in NOAA's long term vertical ozone profile records measured with the electrochemical concentration cell ozonesonde. *Atmos. Meas. Tech.* DOI: https://doi.org/10.5194/amt-2017-397

Stevenson, DS, Young, PJ, Naik, V, Lamarque, JF, Shindell, DT, Voulgarakis, A, Skeie, RB, Dalsoren, SB, Myhre, G, Berntsen, TK, Folberth, GA, Rumbold, ST, Collins, WJ, MacKenzie, IA, Doherty, RM, Zeng, G, van Noije, TPC, Strunk, A, Bergmann, D, Cameron-Smith, P, Plummer, DA, Strode, SA, Horowitz, L, Lee, YH, Szopa, S, Sudo, K, Nagashima, T, Josse, B, Cionni, I, Righi, M, Eyring, V, Conley, A, Bowman, KW and **Wild, O.** 2013. Tropospheric ozone changes, radiative forcing and attribution to emissions in the Atmospheric Chemistry and Climate Model Intercomparison Project (ACCMIP). *Atmos. Chem. Phys.* **13**: 3063–3085. DOI: https://doi.org/10.5194/acp-13-3063-2013

Stohl, A and **Trickl, T.** 1999. A textbook example of long-range transport: Simultaneous observation of ozone maxima of stratospheric and North American origin in the free troposphere over Europe. *J. Geophys. Res.* **104**(D23): 30,445–30,462. DOI: https://doi.org/10.1029/1999JD900803

Stohl, A, Wernli, H, James, P, Bourqui, M, Forster, C, Liniger, MA, Seibert, P and **Sprenger, M.** 2003b. A New Perspective of Stratosphere–Troposphere Exchange. *Bull. Amer. Meteor. Soc.* **84**: 1565–1573. DOI: https://doi.org/10.1175/BAMS-84-11-1565

Stohl, A, Bonasoni, P, Cristofanelli, P, Collins, W, Feichter, J, Frank, A, Forster, C, Gerasopoulos, E, Gäggeler, H, James, P, Kentarchos, T, Kromp-Kolb, H, Krüger, B, Land, C, Meloen, J, Papayannis, A, Priller, A, Seibert, P, Sprenger, M, Roelofs, GJ, Scheel, HE, Schnabel, C, Siegmund, P, Tobler, L, Trickl, T, Wernli, H, Wirth, V, Zanis, P and **Zerefos, C.** 2003a. Stratosphere-troposphere exchange: A review and what we have learned from STACCATO. *J. Geophys. Res.* **108**(D12): 8516. DOI: https://doi.org/10.1029/2002JD002490

Stone, K, Tully, MB, Rhodes, SK and **Schofield, R.** 2015. A new Dobson Umkehr ozone profile retrieval method optimising information content and resolution. *Atmos. Meas. Tech.* **8**: 1043–1053. DOI: https://doi.org/10.5194/amt-8-1043-2015

Strawbridge, KB, Travis, MS, Firanski, BJ, Brook, JR, Staebler, R and **Leblanc, T.** 2018. A fully autonomous ozone, aerosol and night time water vapor LIDAR: a synergistic approach to profiling the atmosphere in the Canadian oil sands region. *Atmos. Meas. Tech.* **11**: 6735–6759. DOI: https://doi.org/10.5194/amt-11-6735-2018

Stutz, J and **Platt, U.** 1996. Numerical analysis and estimation of the statistical error of differential optical absorption spectroscopy measurements with least-squares methods. *Appl. Opt.* **35**: 6041–6053. DOI: https://doi.org/10.1364/AO.35.006041

Tanimoto, H, Mukai, H, Hashimoto, S and **Norris, JE.** 2006. Intercomparison of ultraviolet photometry and gas-phasetitration techniques for ozone reference standards at ambient levels. *J. Geophys. Res.-Atmos.* **111**(D16313). DOI: https://doi.org/10.1029/2005JD006983

Tanimoto, H, Mukai, H, Sawa, Y, Matsueda, H, Yonemura, S, Wang, T, Poon, S, Wong, A, Lee, G,

Jung, JY, Kim, KR, Lee, MH, Lin, NH, Wang, JL, Ou-Yang, CF, Wu, CF, Akimoto, H, Pochanart, P, Tsuboi, K, Doi, H, Zellweger, C and **Klausen, J.** 2007. Direct assessment of international consistency of standards for ground-level ozone: Strategy and implementation toward metrological traceability network in Asia. *J. Environ. Monit.* **9**: 1183–1193. DOI: https://doi.org/10.1039/b701230f

Tanimoto, H, Zbinden, RM, Thouret, V and **Nédélec, P.** 2015. Consistency of tropospheric ozone observations made by different platforms and techniques in the global databases. *Tellus A.* **67**(0): 1–20. DOI: https://doi.org/10.3402/tellusb.v67.27073

Tarasick, DW, Davies, J, Anlauf, K and **Watt, M.** 2000. Response of ECC and Brewer-Mast ozonesondes to sulfur dioxide interference, Proc. Quadrennial Ozone Symposium 2000, Sapporo, Japan, pp. 675–676. Natl. Space Dev. Agency of Jpn, Tokyo, 2000.

Tarasick, DW, Davies, J, Anlauf, K, Watt, M, Steinbrecht, W and **Claude, HJ.** 2002. Laboratory investigations of the response of Brewer-Mast sondes to tropospheric ozone. *J. Geophys. Res.* **107**(D16): 4308. DOI: https://doi.org/10.1029/2001JD001167

Tarasick, DW, Davies, J, Smit, HGJ and **Oltmans, SJ.** 2016. A re-evaluated Canadian ozonesonde record: measurements of the vertical distribution of ozone over Canada from 1966 to 2013. *Atmos. Meas. Tech.* **9**: 195–214. DOI: https://doi.org/10.5194/amt-9-195-2016

Tarasick, DW, Fioletov, VE, Wardle, DI, Kerr, JB and **Davies, J.** 2005. Changes in the vertical distribution of ozone over Canada from ozonesondes: 1980–2001. *J. Geophys. Res.* **110**(D02304). DOI: https://doi.org/10.1029/2004JD004643

Tarasick, DW, Jin, JJ, Fioletov, VE, Liu, G, Thompson, AM, Oltmans, SJ, Liu, J, Sioris, CE, Liu, X, Cooper, OR, Dann, T and **Thouret, V.** 2010. High-resolution tropospheric ozone fields for INTEX and ARCTAS from IONS ozonesondes. *J. Geophys. Res.* **115**(D20301). DOI: https://doi.org/10.1029/2009JD012918

Tarasick, DW, Lukovich, J, Moeini, O, Osman, M and **Liu, JJ.** 2014. Arctic surface ozone depletions from ozone soundings. *13th Quadrennial iCACGP Symposium & 13th IGAC Science Conference.* **56**(P1): 22–26. September 2014, Natal, Brazil.

Tarasova, OA, Brenninkmeijer, CAM, Jockel, P, Zvyagintsev, AM and **Kuznetsov, GI.** 2007. A climatology of surface ozone in the extra tropics: cluster analysis of observations and model results. *Atmos. Chem. Phys.* **7**: 6099–6117. DOI: https://doi.org/10.5194/acp-7-6099-2007

Teichert, F. 1955. Vergleichende Messung des Ozongehaltes der Luft am Erdboden und in 80 m Höhe. *Z. Meteorol.* **9**: 21–27.

Thompson, AM, Balashov, NV, Witte, JC, Coetzee, JGR, Thouret, V and **Posny, F.** 2014. Tropospheric ozone increases over the southern Africa region: bellwether for rapid growth in Southern Hemisphere pollution? *Atmos. Chem. Phys.* **14**: 9855–9869. DOI: https://doi.org/10.5194/acp-14-9855-2014

Thompson, AM, Oltmans, SJ, Tarasick, DW, von der Gathen, P, Smit, HGJ and **Witte, JC.** 2011. Strategic Ozone Sounding Networks: Review Of Design And Accomplishments. *Atmos. Environ.* ISSN 1352-2310. DOI: https://doi.org/10.1016/j.atmosenv.2010.05.002

Thompson, AM, Witte, JC, Sterling, C, Jordan, A, Johnson, BJ, Oltmans, SJ, Fujiwara, M, Vömel, H, Allaart, M, Piters, A, Coetzee, GJR, Posny, F, Corrales, E, Diaz, JA, Félix, C, Komala, N, Lai, N, Nguyen, HTA, Maata, M, Mani, F, Zainal, A, Ogino, S, Paredes, F, Penha, TLB, da Silva, FR, Sallons-Mitro, S, Selkirk, HB, Schmidlin, FJ, Stübi, R and **Thiongo, K.** 2018. First Reprocessing of Southern Hemisphere Additional Ozonesondes (SHADOZ) Ozone Profiles (1998–2016): 2. Comparisons With Satellites and Ground-Based Instruments. *J. Geophys. Res.* **122**(23): 13000–13025. DOI: https://doi.org/10.1002/2017JD027406

Thouret, V, Marenco, A, Logan, JA, Nédélec, P and **Grouhel, C.** 1998. Comparisons of ozone measurements from the MOZAIC airborne program and the ozone sounding network at eight locations. *J. Geophys. Res.* **103**(D19): 25695–25720. DOI: https://doi.org/10.1029/98JD02243

Tilmes, S, Lamarque, JF, Emmons, LK, Conley, A, Schultz, MG, Saunois, M, Thouret, V, Thompson, AM, Oltmans, SJ, Johnson, B and **Tarasick, D.** 2012. Technical Note: Ozonesonde climatology between 1995 and 2011: description, evaluation and applications. *Atmos. Chem. Phys.* **12**: 7475–7497. DOI: https://doi.org/10.5194/acp-12-7475-2012

Tiwari, VS and **Sreedharan, CR.** 1973. Ozone concentration studies and ozone flux measurements near the ground at Poona. *PAGEOPH.* **106**: 1124. DOI: https://doi.org/10.1007/BF00881066

Torres, AL and **Bandy, AR.** 1978. Performance characteristics of the electrochemical concentration cell ozonesonde. *J. Geophys. Res.* **83**(C11): 5501–5504. DOI: https://doi.org/10.1029/JC083iC11p05501

Trickl, T. 2019. Three Decades of Tropospheric Ozone-Lidar Development at Garmisch-Partenkirchen, in preparation.

Trickl, T, Bärtsch-Ritter, N, Eisele, H, Furger, M, Mücke, R, Sprenger, M and **Stohl, A.** 2011. High-ozone layers in the middle and upper troposphere above Central Europe: potential import from the stratosphere along the subtropical jet stream. *Atmos. Chem. Phys.* **11**: 9343–9366. DOI: https://doi.org/10.5194/acp-11-9343-2011

Trickl, T, Feldmann, H, Kanter, HJ, Scheel, HE, Sprenger, M, Stohl, A and **Wernli, H.** 2010. Forecasted deep stratospheric intrusions over Central Europe: case studies and climatologies. *Atmos. Chem. Phys.* **10**: 499–524. DOI: https://doi.org/10.5194/acp-10-499-2010

Trickl, T, Vogelmann, H, Giehl, H, Scheel, HE, Sprenger, M and **Stohl, A.** 2014. How stratospheric are

deep stratospheric intrusions? *Atmos. Chem. Phys.* **14**(18): 9941–9961. DOI: https://doi.org/10.5194/acp-14-9941-2014

Trickl, T, Vogelmann, H, Fix, A, Schäfler, A, Wirth, M, Calpini, B, Levrat, G, Romanens, G, Apituley, A, Wilson, KM, Begbie, R, Reichardt, J, Vömel, H and **Sprenger, M.** 2016. How Stratospheric Are Deep Stratospheric Intrusions into the Troposphere? LUAMI 2008. *Atmos. Chem. Phys.* **16**: 8791–8815. DOI: https://doi.org/10.5194/acp-16-8791-2016

Uchino, O, Sakai, T, Nagai, T, Morino, I, Maki, T, Deushi, M, Shibata, K, Kajino, M, Kawasaki, T, Akaho, T, Takubo, S, Okumura, H, Arai, K, Nakazato, M, Matsunaga, T, Yokota, T, Kawakami, S, Kita, K and **Sasano, Y.** 2014. DIAL measurement of lower tropospheric ozone over Saga (33.24°N, 130.29°E), Japan, and comparison with a chemistry–climate model. *Atmos. Meas. Tech.* **7**: 1385–1394. DOI: https://doi.org/10.5194/amt-7-1385-2014

US EPA. 2013. *Transfer Standards For Calibration of Air Monitoring Analyzers for Ozone: Technical Assistance Document*. United States Environmental Protection Agency, Office of Air Quality Planning and Standards, Air Quality Assessment Division, Research Triangle Park, NC. Publication No. EPA-454/B-13-004, October, 2013.

Valks, P, Hao, N, Gimeno Garcia, S, Loyola, D, Dameris, M, Jöckel, P and **Delcloo, A.** 2014. Tropical tropospheric ozone column retrieval for GOME-2. *Atmos. Meas. Tech.* **7**: 2513–2530. DOI: https://doi.org/10.5194/amt-7-2513-2014

van der A, RJ, van Oss, RF, Piters, AJM, Fortuin, JPF, Meijer, YJ and **Kelder, HM.** 2002. Ozone profile retrieval from recalibrated GOME data. *J. Geophys. Res.* **107**: 4239. DOI: https://doi.org/10.1029/2001JD000696

Van Malderen, R, Allaart, MAF, De Backer, H, Smit, HGJ and **De Muer, D.** 2016. On instrumental errors and related correction strategies of ozonesondes: possible effect on calculated ozone trends for the nearby sites Uccle and De Bilt. *Atmos. Meas. Tech.* **9**: 3793–3816. DOI: https://doi.org/10.5194/amt-9-3793-2016

van Peet, JCA, van der A, RJ, Tuinder, ONE, Wolfram, E, Salvador, J, Levelt, PF and **Kelder, HM.** 2014. Ozone ProfilE Retrieval Algorithm (OPERA) for nadir-looking satellite instruments in the UV–VIS. *Atmos. Meas. Tech.* **7**: 859–876. DOI: https://doi.org/10.5194/amt-7-859-2014

van Oss, R, de Haan, J, Tuinder, O and **Delcloo, A.** 2015. O3MSAF Algorithm Theoretical Basis Document, NRT and Offline Vertical Ozone Profile and Tropospheric Ozone Column Products, available at: https://acsaf.org/docs/atbd/Algorithm_Theoretical_Basis_Document_NOP_NHP_OOP_OHP_O3Tropo_Jul_2015.pdf.

Vassy, A. 1958. Appareil enregistreur donnant la concentration de l'ozone dans l'air Geofisica Pura e Applicata. **39**(164). DOI: https://doi.org/10.1007/BF02001142

Viallon, J, Moussay, P, Esler, M, Wielgosz, R, Bremser, W, Novák, J, Vokoun, M, Botha, A, Janse Van Rensburg, M, Zell-weger, C, Goldthorp, S, Borowiak, A, Lagler, F, Walden, J, Malgeri, E, Sassi, MP, Morillo Gomez, P, Fernandez Patier, R, Galan Madruga, D, Woo, J-C, Doo Kim, Y, Macé, T, Sutour, C, Surget, A, Niederhauser, B, Schwaller, D, Frigy, B, Györgyné Váraljai, I, Hashimoto, S, Mukai, H, Tani-moto, H, Ahleson, HP, Egeløv, A, Ladegard, N, Marsteen, L, Tørnkvist, K, Guenther, FR, Norris, JE, Hafkenscheid, TL, Van Rijn, MM, Quincey, P, Sweeney, B, Langer, S, Mag-nusson, B, Bastian, J, Stummer, V, Fröhlich, M, Wolf, A, Konopelko, LA, Kustikov, YA and **Rumyanstev, DV.** 2006b. Pilot study: International comparison CCQM-P28: ozone at ambient level. *Metrologia, Tech. Suppl.* **43**: 08010. DOI: https://doi.org/10.1088/0026-1394/43/1A/08010

Viallon, J, Lee, S, Moussay, P, Tworek, K, Petersen, M and **Wielgosz, RI.** 2015. Accurate measurements of ozone absorption cross-sections in the Hartley band. *Atmos. Meas. Tech.* **8**: 1245–1257. DOI: https://doi.org/10.5194/amt-8-1245-2015

Viallon, J, Moussay, P, Flores, E and **Wielgosz, RI.** 2016. Ozone Cross-Section Measurement by Gas Phase Titration. *Anal. Chem.* **88**(21): 10720–10727. DOI: https://doi.org/10.1021/acs.analchem.6b03299

Viallon, J, Moussay, P, Norris, JE, Guenther, FR and **Wielgosz, RI.** 2006a. A study of systematic biases and measurement uncertainties in ozone mole fraction measurements with the NIST Standard Reference Photometer. *Metrologia.* **43**: 441–450. DOI: https://doi.org/10.1088/0026-1394/43/5/016

Vigouroux, C, Blumenstock, T, Coffey, M, Errera, Q, García, O, Jones, NB, Hannigan, JW, Hase, F, Liley, B, Mahieu, E, Mellqvist, J, Notholt, J, Palm, M, Persson, G, Schneider, M, Servais, C, Smale, D, Thölix, L and **De Mazière, M.** 2015. Trends of ozone total columns and vertical distribution from FTIR observations at eight NDACC stations around the globe. *Atmos. Chem. Phys.* **15**(6): 2915–2933. DOI: https://doi.org/10.5194/acp-15-2915-2015

Vigroux, E. 1953. Contribution à l'étude expérimentale de l'absorption de l'ozone. *Ann. Phys.* **12**(8): 709–762. DOI: https://doi.org/10.1051/anphys/195312080709

Volz, A and **Kley, D.** 1988. Evaluation of the Montsouris series of ozone measurements made in the 19th century. *Nature.* **332**(6161): 240–242. DOI: https://doi.org/10.1038/332240a0

Walshaw, CD and **Goody, RM.** 1956. An experimental investigation of the 9.6 μ band of ozone in the solar spectrum. *Q.J.R. Meteorol. Soc.* **82**: 177–186. DOI: https://doi.org/10.1002/qj.49708235204

Wang, Y and **Jacob, DJ.** 1998. Anthropogenic forcing on tropospheric ozone and OH since preindustrial times. *J. Geophys. Res.* **103**: 31,123–31,135. DOI: https://doi.org/10.1029/1998JD100004

Wargan, K, Pawson, S, Olsen, MA, Witte, JC, Douglass, AR, Ziemke, JR, Strahan, SE and **Nielsen, JE.** 2015. The global structure of upper

troposphere-lower stratosphere ozone in GEOS-5: A multiyear assimilation of EOS Aura data. *J. Geophys. Res. Atmos.* **120**: 2013–2036. DOI: https://doi.org/10.1002/2014JD022493

Warmbt, W. 1964. Luftchemische Untersuchungen des bodennahen Ozons 1952–61 Methoden und Ergebnisse. *Abh. Meteorol. Dienst DDR* **X**(72): 95.

Warren, GJ and **Babcock, G.** 1970. Portable ethylene chemiluminescence ozone monitor. *Review of Scientific Instruments.* **41**(2): 280–282. DOI: https://doi.org/10.1063/1.1684493

Watanabe, I and **Stephens, ER.** 1979. Pressure-Volume Technique for the Calibration of Ozone Analyzers. *Analytical Chemistry.* **51**(2): 313–315. DOI: https://doi.org/10.1021/ac50038a043

Weatherhead, EC, Wielicki, BA, Ramaswamy, V, Abbott, M, Ackerman, TP, Atlas, R, Brasseur, G, Bruhwiler, L, Busalacchi, AJ, Butler, JH, Clack, CTM, Cooke, R, Cucurull, L, Davis, SM, English, JM, Fahey, DW, Fine, SS, Lazo, JK, Liang, S, Loeb, NG, Rignot, E, Soden, B, Stanitski, D, Stephens, G, Tapley, BD, Thompson, AM, Trenberth, KE and **Wuebbles, D.** 2017. Designing the Climate Observing System of the Future. *Earth's Future.* **5**. DOI: https://doi.org/10.1002/2017EF000627

Weidinger, T, Baranka, G, Balázs, R and **Tóth, K**. 2011. Comparison of 19th century and present concentrations and depositions of ozone in Central Europe. *Acta Silvatica et Lignaria Hungarica.* **7**: 23–28.

Welch, BL. 1947. The generalization of "Student's" problem when several different population variances are involved. *Biometrika.* **34**(1–2): 28–35. DOI: https://doi.org/10.1093/biomet/34.1-2.28

Wesely, M. 1989. Parameterization of surface resistances to gaseous dry deposition in regional-scale numerical models. *Atmos. Environ.* **23**: 1293–1304. DOI: https://doi.org/10.1016/0004-6981(89)90153-4

Wespes, C, Emmons, L, Edwards, DP, Hannigan, J, Hurtmans, D, Saunois, M, Coheur, PF, Clerbaux, C, Coffey, MT, Batchelor, RL, Lindenmaier, R, Strong, K, Weinheimer, AJ, Nowak, JB, Ryerson, TB, Crounse, JD and **Wennberg, PO.** 2012. Analysis of Ozone and Nitric Acid in spring and summer Arctic pollution using aircraft, ground-based, satellite observations and MOZART-4 model: source attribution and partitioning. *Atmos. Chem. Phys.* **12**(1): 237–259. DOI: https://doi.org/10.5194/acp-12-237-2012

Wexler, H, Moreland, W and **Weyant, W.** 1960. A preliminary report on ozone observations at Little America. *Antarctica Monthly Weather Review.* **88**(2): 43–54. DOI: https://doi.org/10.1175/1520-0493(1960)088<0043:APROOO>2.0.CO;2

Wilcox, RW. 1978. Comments [on "Tropospheric ozone, 1, Evidence for higher background values" by R. Chatfield and H. Harrison]. *J. Geophys. Res.* **83**(C12): 6263–6264. DOI: https://doi.org/10.1029/JC083iC12p06263

Williams, EJ, Fehsenfeld, FC, Jobson, BT, Kuster, WC, Goldan, PD, Stutz, J and **McClenny, WA.** 2006. Comparison of ultraviolet absorbance, chemiluminescence, and DOAS instruments for ambient ozone monitoring. *Environ. Sci. Technol.* **40**(18): 5755–62. DOI: https://doi.org/10.1021/es0523542

Wilson, WS, Guenther, WB, Lowrey, RD and **Cain, JC.** 1952. Surface ozone at College, Alaska, for the year 1950. *Trans. Am. Geophys. Union.* **33**: 361–364. DOI: https://doi.org/10.1029/TR033i003p00361

Wisse, JA and **Meerburg, AJ.** 1969. Ozone observations at Base King Baudouin in 1965 and 1966. *Arch. Met. Geoph. Biokl. A.* **18**: 41. DOI: https://doi.org/10.1007/BF02247863

Witte, JC, Thompson, AM, Schmidlin, FJ, Northam, ET, Wolf, KR and **Brothers, GB.** 2019. The NASA Wallops Flight Facility Digital Ozonesonde Record: Reprocessing, Uncertainties, and Dual Launches. *J. Geophys. Res,* accepted. DOI: https://doi.org/10.1029/2018JD030098

Witte, JC, Thompson, AM, Smit, HGJ, Fujiwara, M, Posny, F, Coetzee, GJR, Northam, ET, Johnson, BJ, Sterling, C, Mohamad, M, Ogino, S, Jordan, A and **da Silva, FR.** 2017. First reprocessing of Southern Hemisphere ADditional OZonesondes (SHADOZ) profile records (1998–2015): 1. Methodology and evaluation. *J. Geophys. Res.* **122**(12): 6611–6636. DOI: https://doi.org/10.1002/2016JD026403

Witz, M. 1885. Sur la présence de l'acide sulfureux dans l'atmosphère des villes. *C. R. Acad. Sci.* **100**: 1385–8. Paris.

WMO. 1972. Report of the first session of the RA V Working Group on Atmospheric Ozone, Aspendale, Australia, 28 February to 4 March 1972. *World Meteorological Organisation, Document no R/OZO/2.* Geneva: Switzerland 9pp plus 5 Appendices.

WMO. October 2018. *Reactive Gases Bulletin, No. 2.* Geneva, Switzerland: rld Meteorological Organization, Atmospheric Environment Research Division, Research Department. https://library.wmo.int/doc_num.php?explnum_id=5244.

Worden, HM, Logan, JA, Worden, JR, Beer, R, Bowman, K, Clough, SA, Eldering, A, Fisher, BM, Gunson, MR, Herman, RL, Kulawik, SS, Lampel, MC, Luo, M, Megretskaia, IA, Osterman, GB and **Shephard, MW.** 2007a. Comparisons of Tropospheric Emissions Spectrometer (TES) ozone profiles to ozonesondes: Methods and initial results. *J. Geophys. Res.* **112**(D03309). DOI: https://doi.org/10.1029/2006JD007258

Worden, J, Liu, X, Bowman, K, Chance, K, Beer, R, Eldering, A, Gunson, M and **Worden, H.** 2007b. Improved tropospheric ozone profile retrievals using OMI and TES radiances. *Geophys. Res. Lett.* **34**(L01809): 1. DOI: https://doi.org/10.1029/2006GL027806

World Climate Research Programme. 1998. SPARC/IOC/GAW Assessment of Trends in the Vertical Distribution of Ozone, Stratospheric Processes and Their Role in Climate, World Meteorol. *Organ. Global Ozone Res. Monit. Proj. Rep.* **43**. Geneva, Switzerland.

Yang, Q, Cunnold, DM, Wang, HJ, Froidevaux, L, Claude, H, Merrill, J, Newchurch, M and **Oltmans, SJ.** 2007. Midlatitude tropospheric ozone columns derived from the Aura Ozone Monitoring Instrument and Microwave Limb Sounder measurements. *J. Geophys. Res.* **112**(D20305). DOI: https://doi.org/10.1029/2007JD008528

Yeung, LY, Murray, LT, Martinerie, P, Witrant, E, Hu, H, Banerjee, A, Orsi, A and **Chappellaz, J.** 2019. Isotopic constraint on the twentieth-century increase in tropospheric ozone. *Nature.* **570**: 224–227. DOI: https://doi.org/10.1038/s41586-019-1277-1

Yost, RS, Uehara, G and **Fox, RL.** 1982. Geostatistical analysis of soil chemical properties of large land areas. I. Semi-variograms. *Soil Science Society of Am. J.* **46**(5): 1028–1032. DOI: https://doi.org/10.2136/sssaj1982.03615995004600050028x

Young, PJ, Archibald, AT, Bowman, KW, Lamarque, JF, Naik, V, Stevenson, DS, Tilmes, S, Voulgarakis, A, Wild, O, Bergmann, D, Cameron-Smith, P, Cionni, I, Collins, WJ, Dalsøren, SB, Doherty, RM, Eyring, V, Faluvegi, G, Horowitz, LW, Josse, B, Lee, YH, MacKenzie, IA, Nagashima, T, Plummer, DA, Righi, M, Rumbold, ST, Skeie, RB, Shindell, DT, Strode, SA, Sudo, K, Szopa, S and **Zeng, G.** 2013. Pre-industrial to end 21st century projections of tropospheric ozone from the Atmospheric Chemistry and Climate Model Intercomparison Project (ACCMIP). *Atmos. Chem. Phys.* **13**: 2063–2090. DOI: https://doi.org/10.5194/acp-13-2063-2013

Young, PJ, Naik, V, Fiore, AM, Gaudel, A, Guo, J, Lin, MY, Neu, JL, Parrish, DD, Rieder, HE, Schnell, JL, Tilmes, S, Wild, O, Zhang, L, Ziemke, JR, Brandt, J, Delcloo, A, Doherty, RM, Geels, C, Hegglin, MI, Hu, L, Im, U, Kumar, R, Luhar, A, Murray, L, Plummer, D, Rodriguez, J, Saiz-Lopez, A, Schultz, MG, Woodhouse, MT and **Zeng, G.** 2018. Tropospheric Ozone Assessment Report: Assessment of global-scale model performance for global and regional ozone distributions, variability, and trends. *Elem Sci Anth.* **6**(1): 10. DOI: https://doi.org/10.1525/elementa.265

Zanis, P, Hadjinicolaou, P, Pozzer, A, Tyrlis, E, Dafka, S, Mihalopoulos, N and **Lelieveld, J.** 2014. Summertime free-tropospheric ozone pool over the eastern Mediterranean/Middle East. *Atmos. Chem. Phys.* **14**: 115–132. DOI: https://doi.org/10.5194/acp-14-115-2014

Zhang, L, Jacob, DJ, Downey, NV, Wood, DA, Blewitt, D, Carouge, CC, van Donkelaar, A, Jones, DBA, Murray, LT and **Wang, Y.** 2011. Improved estimate of the policy-relevant background ozone in the United States using the GEOS-Chem global model with 1/2° × 2/3° horizontal resolution over North America. *Atmos. Environ.* **45**(37): 6769–6776. DOI: https://doi.org/10.1016/j.atmosenv.2011.07.054

Ziemke, JR, Chandra, S and **Bhartia, PK.** 1998. Two new methods for deriving tropospheric column ozone from TOMS measurements: Assimilated UARS MLS/HALOE and convective-cloud differential techniques. *J. Geophys. Res.* **103**(D17): 22115–22128. DOI: https://doi.org/10.1029/98JD01567

Ziemke, JR, Chandra, S and **Bhartia, PK.** 2001. "Cloud slicing": A new technique to derive upper tropospheric ozone from satellite measurements. *J. Geophys. Res.* **106**(D9): 9853–9867. DOI: https://doi.org/10.1029/2000JD900768

Ziemke, JR, Chandra, S and **Bhartia, PK.** 2003. Upper tropospheric ozone derived from the cloud slicing technique: Implications for large-scale convection. *J. Geophys. Res.* **108**(D13): 4390. DOI: https://doi.org/10.1029/2002JD002919

Ziemke, JR, Chandra, S and **Bhartia, PK.** 2005. A 25-year data record of atmospheric ozone in the Pacific from Total Ozone Mapping Spectrometer (TOMS) cloud slicing: Implications for ozone trends in the stratosphere and troposphere. *J. Geophys. Res.* **110**(D15105). DOI: https://doi.org/10.1029/2004JD005687

Ziemke, JR, Chandra, S, Duncan, BN, Froidevaux, L, Bhartia, PK, Levelt, PF and **Waters, JW.** 2006. Tropospheric ozone determined from Aura OMI and MLS: Evaluation of measurements and comparison with the Global Modeling Initiative's Chemical Transport Model. *J. Geophys. Res.* **111**(D19303). DOI: https://doi.org/10.1029/2006JD007089

Ziemke, JR, Joiner, J, Chandra, S, Bhartia, PK, Vasilkov, A, Haffner, DP, Yang, K, Schoeberl, MR, Froidevaux, L and **Levelt, PF.** 2009. Ozone mixing ratios inside tropical deep convective clouds from OMI satellite measurements. *Atmos. Chem. Phys.* **9**: 573–583. DOI: https://doi.org/10.5194/acp-9-573-2009

Ziemke, JR, Strode, SA, Douglass, AR, Joiner, J, Vasilkov, A, Oman, LD, Liu, J, Strahan, SE, Bhartia, PK and **Haffner, DP.** 2017. A cloud-ozone data product from Aura OMI and MLS satellite measurements. *Atmos. Meas. Tech.* **10**: 4067–4078. DOI: https://doi.org/10.5194/amt-10-4067-2017

How to cite this article: Tarasick, D, Galbally, IE, Cooper, OR, Schultz, MG, Ancellet, G, Leblanc, T, Wallington, TJ, Ziemke, J, Liu, X, Steinbacher, M, Staehelin, J, Vigouroux, C, Hannigan, JW, García, O, Foret, G, Zanis, P, Weatherhead, E, Petropavlovskikh, I, Worden, H, Osman, M, Liu, J, Chang, K-L, Gaudel, A, Lin, M, Granados-Muñoz, M, Thompson, AM, Oltmans, SJ, Cuesta, J, Dufour, G, Thouret, V, Hassler, B, Trickl, T and Neu, JL. 2019. Tropospheric Ozone Assessment Report: Tropospheric ozone from 1877 to 2016, observed levels, trends and uncertainties. *Elem Sci Anth,* 7: 39. DOI: https://doi.org/10.1525/elementa.376

Domain Editor-in-Chief: Detlev Helmig, Institute of Alpine and Arctic Research, University of Colorado Boulder, US

Associate Editor: Alastair Lewis, National Centre for Atmospheric Science, University of York, US

Knowledge Domain: Atmospheric Science

Part of an *Elementa* Special Feature: Tropospheric Ozone Assessment Report (TOAR): GLOBAL METRICS FOR CLIMATE CHANGE, HUMAN HEALTH AND CROP/ECOSYSTEM RESEARCH

Submitted: 26 February 2019 **Accepted:** 29 August 2019 **Published:** 11 October 2019

ELEMENTA Science of the Anthropocene

Elem Sci Anth is a peer-reviewed open access journal published by University of California Press.

OPEN ACCESS